

# **Membrane Processes for the Dehydration of Organic Compounds**

Vom Fachbereich Maschinenbau  
der Universität Hannover  
zur Erlangung des akademischen Grades

Doktor-Ingenieur

genehmigte  
Dissertation

von

M. Eng. Alaa Fahmy

geboren am 2. Dezember 1972 in Kairo

2002

1. Referent: Prof. Dr.-Ing. Dieter Mewes  
2. Referent: Prof. Dr. Rolf-Dieter Behling  
Mitprüfer: Prof. Dr.-Ing. Günter-Peter Merker  
Gutachter: Dipl.-Ing. Klaus Ohlrogge  
Vorsitz der Prüfungskommission: Prof. Dr.-Ing. Jörg Seume  
Tag der Promotion: 24. Juni 2002

## Vorwort

Die vorliegende Arbeit entstand während meiner Tätigkeit als wissenschaftlicher Mitarbeiter am Institut für Verfahrenstechnik der Universität Hannover. Mein besonderer Dank gilt dem Institutsleiter, Herrn Prof. Dr.-Ing. D. Mewes, für die Anregung und die großzügige Förderung der Arbeit. Herrn Dipl.-Ing. K. Ohlrogge danke ich für die Mitbetreuung des Forschungsprojektes und für sein Gutachten zu dieser Arbeit.

Herrn Dr. R.-D. Behling danke ich für die Übernahme des Korreferats und das freundliche Interesse, welches er der Arbeit entgegenbrachte. Herrn Prof. Dr.-Ing. G.-P. Merker danke ich für seine Tätigkeit als Mitprüfer und Herrn Prof. Dr.-Ing. J. Seume für die Übernahme des Vorsitzes der Prüfungskommission.

Meinen Kollegen danke ich für die Unterstützung und für die angenehme Zeit, die ich am Institut verbracht habe. Weiterhin danke ich Herrn Streichert für die Administration der Rechner und für die freundlichen Diskussionen. Frau Sladek und Frau Greiser danke ich für die organisatorische Hilfestellung. Ebenso möchte ich mich bei meinen Studenten M. Dahlberg, T. Larsen, S. Tajouri und T. Lippe bedanken, ohne die die Durchführung der Arbeit nicht möglich gewesen wäre.

Ein besonderer Dank an Euch, Samia, Ola, Susanne und Omar für Eure Unterstützung und Geduld während der letzten Jahre.

Dem Deutschen Akademischen Austauschdienst und der GKSS danke ich für die finanzielle Unterstützung.

Hannover, im Juni 2002

Alaa Fahmy



# Contents

<b>Nomenclature</b>	<b>VII</b>
<b>Abstract</b>	<b>IX</b>
<b>Kurzfassung</b>	<b>X</b>
<b>1 Introduction</b>	<b>1</b>
<b>2 Pervaporation and vapor permeation</b>	<b>3</b>
2.1 Historical development	3
2.2 Technical realization	4
2.3 Membranes	7
2.3.1 Organic membranes	7
2.3.2 Inorganic membranes	9
2.4 Membrane modules	11
2.5 Dehydration of organic compounds	14
2.5.1 Dehydration of bio-ethanol	14
2.5.2 Dehydration of spent solvents	14
2.5.3 Different hybrid combinations to distillation	15
2.5.4 Dehydration of reaction mixtures	17
<b>3 Objectives</b>	<b>19</b>
<b>4 Mass transport mechanisms and models</b>	<b>21</b>
4.1 Feed-side mass transport	22
4.2 Modeling the sorption process	23
4.2.1 Sorption in organic membranes	24
4.2.2 Adsorption in inorganic membranes	27
4.3 Modeling the diffusion process	28
4.3.1 Diffusion in dense organic membranes	28
4.3.2 Diffusion in microporous inorganic membranes	31
4.4 Flow through the support layer	32

4.5	Empirical and semi-empirical modeling	34
4.6	Simulation of the membrane process in Aspen Plus	35
4.7	Calculation of pervaporation stages	41
<b>5</b>	<b>Optimizing membrane dehydration processes</b>	<b>43</b>
5.1	Effect of the membrane selectivity	43
5.2	Optimization calculations	50
5.3	Heat integration in multistage-separations	58
<b>6</b>	<b>Steam jet ejectors within hybrid processes</b>	<b>60</b>
6.1	Suggested process scheme	61
6.2	Operating principle of jet ejectors	62
6.3	Motive steam requirements	63
6.4	Process control	65
6.5	Economic evaluation	65
6.6	Other potential applications for steam jet ejectors	68
<b>7</b>	<b>Absorption assisted pervaporation</b>	<b>71</b>
7.1	Limitations of the condensation technology	71
7.2	Suggested absorption technology	73
7.3	Application to dehydration processes	74
7.3.1	Integration into absorption refrigeration cycles	75
7.3.2	Effect of lower membrane selectivity	77
7.3.3	Process simulation and economic evaluation	78
7.4	Technical evaluation	81
<b>8</b>	<b>Conclusion</b>	<b>83</b>
<b>Appendix A: Fixed and variable cost functions</b>		<b>85</b>
<b>Appendix B: Material and energy balance for the dehydration process</b>		<b>87</b>
<b>References</b>		<b>92</b>

## Nomenclature

$a$	[-]	activity
$A$	[m <sup>2</sup> ]	membrane Area
$c$	[kmole/m <sup>3</sup> ]	molar concentration
$d$	[m]	diamter
$D$	[m <sup>2</sup> /s]	diffusion coefficient
$h$	[J/kmole[	specific enthalpy
$J$	[kg/(m <sup>2</sup> h)]	total permeation flux across the membrane
$\bar{J}$	[kg/(m <sup>2</sup> h)]	average total permeation flux
$k$	[kg/(m <sup>2</sup> h)]	mass transfer coefficient
$L$	[kg/(m <sup>2</sup> h bar)]	permeability or permeation coefficient
$n$	[kmole/h]	molar flow rate
$R$	[J/kmol K]	universal gas constant
$p$	[bar]	pressure
$S$	[kg/m <sup>3</sup> ]	sorption coefficient
$V$	[m <sup>3</sup> ]	volume
$x$	[-]	mole fraction
$z$	[m]	Path perpendicular to membrane surface
$\alpha_L$	[-]	membrane selectivity
$\alpha_x$	[-]	separation factor
$\bar{\alpha}_x$	[-]	average separation factor
$\delta$	[m]	thickness
$\eta$	[Pa s]	dynamic viscosity

## VIII

$f_o$	[bar]	standard (reference) fugacity
$\theta$	[-]	module cut rate
$\phi$	[-]	volume fraction
$\gamma$	[-]	activity coefficient

### Subscripts

A	most permeable component
b	boundary layer
B	less permeable component
F	feed stream
K	Knudsen diffusion
M	membrane
i	component i
P	permeate stream
R	retentate stream

### Superscripts

F	locally on the feed side
P	locally on the permeate side
*	at the membrane interface

## Abstract

Fahmy, Alaa

### Membrane Processes for the Dehydration of Organic Compounds

Pervaporation and vapor permeation processes are investigated within the present work in terms of process design improvements and technical optimization. Special emphasis is placed thereby on the dehydration processes of organic solvents. On that account a simulation program is developed for such membrane processes and is integrated into the commercial process simulation software “Aspen Plus”. The program is extended by functions for fixed and variable costs of all components of the membrane separation unit. Thus, process parameters of the membranes and of the peripheral equipment can be optimized and areas for process development and improvement can be determined. The results of the optimization calculations encourage the development and the use of low selectivity membranes, especially if a retentate of high purity is required. Though the resulting permeate stream is of lower purity, it is, in many cases, recycled to a distillation step. For membrane units not coupled to a distillation column, a second separation step for the purification of the permeate is required. Heat integration measures for such two stage processes are investigated using the pinch technology.

The condensation technology, which is the most established method for vacuum production on the permeate side, is reviewed for improvements and refinements. The use of steam jet ejectors is suggested as an alternative technology in the case of solvent dehydration processes. High pressure steam is mixed with the permeate vapor and the resulting low pressure steam can be used for heating tasks inside the process. Thus, applications within the scope of hybrid combinations to distillation and chemical reactors are suggested and investigated for implementing this technique. In another suggested process the driving force for permeation is enabled by the absorption of the permeate vapors by a suitable solvent with a low vapor pressure so that refrigeration could be overcome. Technical and economic advantages over the conventional condensation can be achieved by integrating the membranes into commercial scale absorption refrigerators with little modification. Process simulations and feasibility investigations for the suggested process are presented and discussed.

**Keywords:** Pervaporation, Vapor Permeation, Process Design

## Kurzfassung

Fahmy, Alaa

### Membranprozesse für die Entwässerung von organischen Lösungen

In der vorliegenden Arbeit werden der Entwurf von Pervaporations- und Dampfpermeationsprozessen sowie deren Optimierung mit den Zielen untersucht, die Entwässerung von organischen Lösungsmitteln kostengünstig zu gestalten. Dazu wird ein Computerprogramm entwickelt und in die kommerzielle Prozesssimulationssoftware „Aspen Plus“ integriert. Das Programm wird um Funktionen für die festen und die variablen Kosten aller Komponenten der Membrantrennanlage erweitert. Damit können Prozessparameter optimiert und potentielle Gebiete für die Prozessentwicklung festgestellt werden. Die Ergebnisse der Optimierung fördern die Entwicklung und den Einsatz von Membranen niedriger Selektivität, insbesondere wenn ein Retentat mit hoher Reinheit gefordert wird. Hierdurch sinkt die Reinheit des Permeats, jedoch wird es in vielen Fällen zu einer Destillationskolonne zurückgeführt. Für die Membrananlagen, die nicht mit einer Destillationskolonne verbunden sind, wird eine zweite Trennstufe für die Reinigung des Permeats benötigt. Maßnahmen für die Wärmeintegration innerhalb solcher zweistufigen Prozesse werden mit Hilfe der Pinch Methode entwickelt.

Ferner wird die für die permeatseitige Vakuumproduktion eingesetzte Kondensationstechnik untersucht. Der Einsatz von Dampfstrahlpumpen wird als alternative Technologie innerhalb des Entwässerungsprozesses vorgeschlagen. Der Treibdampf wird mit dem Permeatdampf vermischt und der resultierende Niederdruckdampf kann als Heizmittel innerhalb des Prozesses benutzt werden. Es werden Anwendungen in Verbindung mit hybriden Kombinationen zu Destillationskolonnen und chemischen Reaktoren für das Anwenden dieser Technik vorgeschlagen. Des weiteren wird die Absorption als mögliche Senke für den permeierenden Stoffstrom vorgeschlagen. Wenn das Lösungsmittel einen niedrigen Dampfdruck besitzt, kann auf die Wärmeabfuhr vollständig verzichtet werden. Für die Entwässerung stehen kommerzielle Absorptionskälteanlagen zur Verfügung, die nur in geringem Maß modifiziert werden müssen. Die Prozesssimulation und die wirtschaftliche Evaluation dieser Technik werden im Rahmen der vorliegenden Arbeit durchgeführt.

**Stichwörter:** Pervaporation, Dampfpermeation, Prozessdesign

## 1 Introduction

Considering that the first membrane experiments might have already been carried out in the 18<sup>th</sup> century using membranes of animal origin, industrial membrane separation is a rather young technology. The seminal innovation that transformed membrane separation from a laboratory to an industrial process was the development of the Loeb-Sourirajan technique [1] for making defect-free, high flux, asymmetric reverse osmosis membranes in the early 1960s. With following developments in the last four decades membranes have evolved from a laboratory tool to industrial products with significant technical and commercial impact. During that period, the expectation for their technical and commercial relevance was very high. A multitude of potential applications were identified and a several billion dollar market was predicted for the membrane-based industry by the turn of the last century [2].

Today, membranes are used for desalination of sea and brackish water and for treating industrial effluents. They are efficient tools for the concentration and purification of food and pharmaceutical products and the production of base chemicals. Furthermore, membranes are key components in artificial organs, drug delivery devices, and energy conversion systems. In combination with conventional techniques membranes often provide cleaner and more energy-efficient production routes for high-quality products. Despite these wide application fields the overall success of the membrane technology is lagging behind former expectations [3]. In some applications, indeed, membranes have established themselves as an indispensable technology. The success was mainly in novel implementations such as in medical applications and fuel cells, or in high-flux applications as in reverse osmosis and in micro- and ultrafiltration. Other applications concerning the separation of liquid mixtures (pervaporation), vapor mixtures (vapor permeation) and gas mixtures (gas separation) are still a niche technology with a limited number of industrial applications. These membrane processes are characterized by low permeation fluxes as the mass transport is determined by solution and diffusion through dense membranes. Although they offer potential solutions in a wide range of applications, they find it difficult to compete with conventional well established thermal separation processes. The relatively high capital cost of the membrane units and the lack of long time industrial experience build thereby the main obstacles.

However, in the last decade pervaporation and vapor permeation have experienced much development towards its industrial realization. Great efforts are being undertaken to improve the membrane properties. Many research groups are working on the development of modified membrane materials and improved membrane-making technologies to achieve higher fluxes, proper selectivities and stable membrane materials. Many new types of pervaporation membranes have been emerged in recent years. Ceramic membranes with improved separation properties, even still at higher prices compared to polymeric membranes, are owning a growing share in the pervaporation and vapor permeation membrane market.

Process design improvements and proper integration of the membrane units within the overall process bring additional savings to the effective cost of the membrane unit. With increasing membrane fluxes and decreasing membrane prices, the share of the membrane in the total cost of the unit is decreasing. Thus efforts to optimize, modify and improve the periphery equipment would also be worth while.

The vision of the present work is to contribute to the development of pervaporation and vapor permeation assisting in accelerating the steps towards a wide industrial realization.

The studies within the scope of the present thesis are substantially theoretical. However, they rely on and are accompanied by experimental developments of dehydration membranes at the institute of chemistry of the GKSS research center. The general scopes of the study are:

- modeling and simulation of pervaporation and vapor permeation processes in order to optimize the process parameters including those of the membranes and of the peripheral equipment,
- and the investigation of feasible areas for process development and modification for achieving technical and economic refinements.

In the next chapter the state of the art and technology of pervaporation and vapor permeation will be presented with emphasis on dehydration of organics. The limitations and the areas for potential improvements will be extensively reviewed. In Chapter 3 the areas subject to investigation within the scope of the present thesis will be highlighted, and the procedural approach will be introduced.

## 2 Pervaporation and vapor permeation

### 2.1 Historical development

Liquid mixtures can be separated by partial vaporization through *a nonporous perm-selective membrane*. This technique, which was originally called ‘liquid permeation’ has subsequently been termed ‘pervaporation’ in order to emphasize the fact that the permeate undergoes a phase change, from liquid to vapor, during its transport through the barrier.

As early as 1906, Kahlenberg [4] reported some quantitative observations concerning the selective transport of hydrocarbon/alcohol mixtures through a thin rubber sheet. The term of pervaporation was first introduced in 1917 by Kober [5], whereby he made a distinction between pervaporation (vaporization through a membrane at room temperature) and perstillation, according to which the feed mixture is heated in order to increase its transport rate through the barrier. Following these preliminary studies, mention is to be made of the work done by Schwob [6] in 1949, who presented dehydration of water/alcohol mixtures by means of a thin (20 µm) regenerated cellulose film (CELLOPHANE), where the water-rich permeate is swept away by a stream of dry air.

For a long period, pervaporation was only considered as a laboratory tool as the low fluxes through homogeneous dense films seemed likely to prevent any large-scale industrial application. This situation changed in the sixties when the phase inversion procedure was developed by Loeb and Sourirajan [1] to manufacture high-flux, asymmetric, reverse osmosis cellulose acetate membranes. Systematic studies on pervaporation started in France by Neel and his coworkers [7,8], who clearly demonstrated that pervaporation and distillation could be associated to fractionate mixtures of close boiling-temperature liquids, or mixtures leading to azeotropes.

With regard to the commercial application, it seems that the earliest mention of an operating pilot-plant dates back to 1982 [9] as a demonstration unit for ethanol dehydration was designed to produce 1,300 liters of ethanol 99.2 wt% per day using spiral-wound membrane modules. This experiment fully corroborated the previsions [10] concerning the low energy-

cost of the membrane process compared with that of conventional dehydration by ternary azeotropic distillation after addition of benzene. Following studies [11-13] confirmed the economic advantage of the membrane process over extractive distillation for the separation of azeotropic and closely boiling mixtures.

Already during the 1980s, about 20 more plants with larger productive capacities (ranging from 2,000 to 15,000 liters per day) were installed for the dehydration of ethanol and other organic solvents [14-16]. In the late 1980s the vapor permeation was introduced as a logical outgrowth of the pervaporation, with the membrane feed in the vapor state [17,18]. Vapor permeation has proven to be especially suitable for the purification of top streams of fractionation columns that can be used as feed directly. Further substantial growth in both processes was observed in the 1990s with more than 100 installations worldwide for solvent dehydration [19]. Today, effort is made to the improve of membrane materials, module concepts, process design and process integration methods in order to bear up pervaporation and vapor permeation as attractive and reliable basic unit operations.

## 2.2 Technical realization

In pervaporation and vapor permeation processes the feed mixture is contacted with a nonporous membrane. One or more components selectively permeate through the barrier and evolve in the vapor state from its opposite side.

According to the solution-diffusion model the transport of the permeate takes place in three successive steps:

- Selective sorption of the components at the feed side
- Diffusion of the components through the membrane
- Desorption of the components at the permeate side

The driving force is a chemical potential gradient across the membrane. This is normally achieved by creating a lower partial pressure at the permeate side compared to the feed side.

The most common technique is vacuum generation by condensing the permeate stream prior a vacuum pump as shown in Figure 2-1(a). The vacuum pump removes the non-condensed compounds and the leakage air. In another technique a sweep gas or vapor is used to lower the

partial pressure of the permeating components and carrying them out at the permeate side as shown in Figure 2-1(b). Large flow rates of sweep gases are required to achieve the same effect of condensation. It is also possible to combine both the condensation and the sweep gas technology [20].

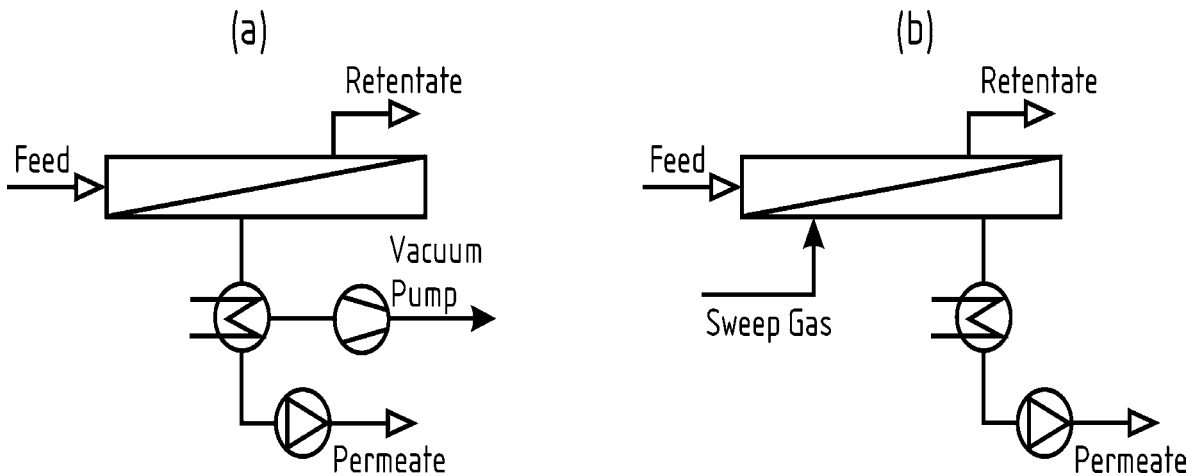


*Figure 2-1: Principal configuration of pervaporation and vapor permeation*

For pervaporation the feed is liquid and the permeate evaporates through the membrane. The latent heat of vaporization is usually supplied to the feed stream by intermediate heat-exchangers, installed between a number of pervaporation modules in series as shown in Figure 2-2(a). This configuration is necessary to keep the temperature of the feed at the highest possible level along the whole membrane area to guarantee a high transport rate. Integrating the membrane modules into a vacuum condenser has the advantage of low pressure drop on the permeate side, and is suitable for permeate-side open modules.

For vapor permeation the feed is vapor and no phase change occurs during the permeation, which makes the process less complex as shown in Figure 2-2(b). Vapor permeation has proven to be especially suitable for the purification of top streams of fractionation columns that can be used as feed directly. Although vapor permeation is less sensitive to concentration polarization at the feed side of the membrane, the mass transport is sensitive to the degree of superheating and to friction losses in the feed side. Little superheating lowers the transmembrane flux in the case of polymeric membranes as a result of decreased sorption and swelling. Brüschke and Schneider have invented a process [21], which combines both vapor permeation and pervaporation, whereby the feed is introduced as a liquid-vapor mixture that flows upwards a vertically mounted membrane module. The mass transport could be improved by insuring saturation conditions throughout the feed side of the membrane.

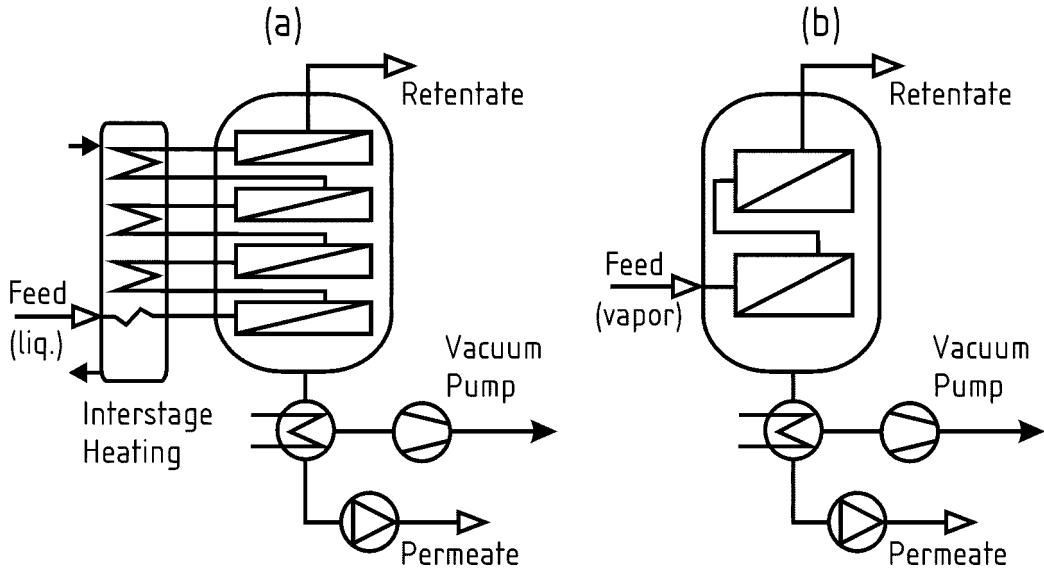


*Figure 2-2: Technical features of pervaporation and vapor permeation*

As stated above, vapor permeation is used when the feed is already available in the vapor phase. However, the evaporation of liquid in order to employ vapor permeation is accepted for small flow rates and large concentration range, which otherwise would request too many small pervaporation stages. The same is practiced when dissolved or undissolved solids are present in the feed, and an additional purification step by evaporation has to be performed anyway.

The membrane plants can be either batch or continuous. The continuous plants as shown in Figure 2-2 are optimized for a specific separation and capacity, and consumes the minimum of energy. If a different stream has to be treated, the plant will be operated outside optimal conditions, and compromises with respect to capacity or final product quality will have to be accepted. In batch plants there is usually one stage and preheater, and the retentate stream is recycled back to the feed storage tank and passes over the membrane several times until the whole content of the tank has reached the final specification. Due to lower efficiency caused by the continuous dilution of the feed and the fact that not all the sensible heat of the circulating stream can be recovered, such plant consumes more energy and requires more membrane area than the straight forward plant. However, it offers more flexibility with respect to the final product quality by additional passes of the feed. Capacity can be adapted by the same means, and streams of different nature and composition can be treated with the same plant.

## 2.3 Membranes

First experiments with pervaporation that were performed using reverse osmosis phase inversion membranes showed that, despite the similarities, both processes require different membranes. In both processes mass transport takes place through a dense membrane layer that must be as thin as possible. In desalination high pressures are applied, up to 100 bar at ambient temperatures, whereas in pervaporation pressure differences across the membrane are in the range of a few bar only. On the other hand pervaporation membranes have to be stable against aggressive components at elevated temperatures. In reverse osmosis both sides of the membrane are in contact with a liquid phase and the degree of swelling between the two sides does not differ too much. In pervaporation the feed side of the membrane is highly swollen as contacted with the hot liquid (or saturated vapor), whereas the permeate side is “dry” and almost non-swollen. A high gradient of swelling thus exists over the separating layer of the membrane, demanding additional resistance and stability.

Membranes used so far in industrial pervaporation plants are generally of composite type. They are prepared by coating a porous support of definite structure with a thin, dense permselective layer. In the composite configuration thus obtained, the structure of the porous support exert a significant influence on the performance of the membrane. Pores must be wide enough to avoid undesirable pressure drop in the permeate stream but not too large to prevent any deep penetration of the coating material during the formation of the membrane.

### 2.3.1 Organic membranes

The structure of a composite pervaporation polymeric membrane is shown in Figure 2-3. By the manufacture of this type a porous support membrane with an asymmetric pore structure is laid onto a carrier layer of a textile fabric and a basic ultrafiltration membrane is formed. On the free side of this asymmetric porous substructure the pores have diameters in the order of 20 to 50 nanometers which widen up to the fabric side to the micrometer range. Polyester, polyethylene, polypropylene, polyphenylene sulfide, polytetrafluor ethylene, and similar fibers are used for the textile carrier layer. Structural polymers with high chemical resistance and good thermal and mechanical properties like polyacrylonitrile, polyetherimide, polysulfone, polyethersulfone, and polyvinylidene flouride form the porous support.

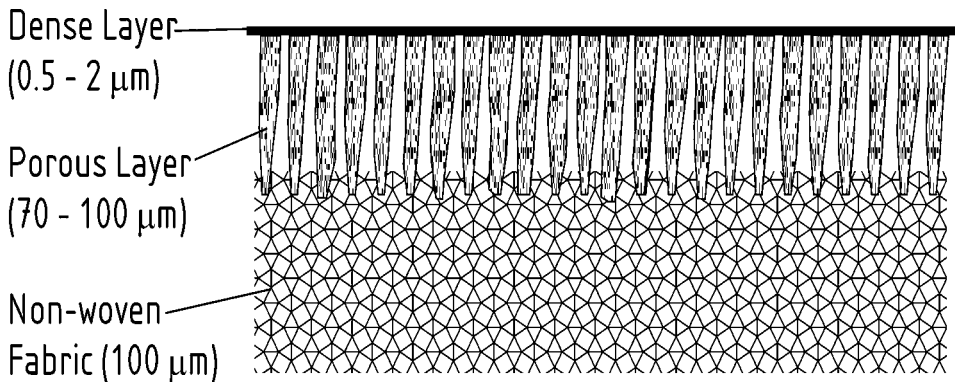


*Figure 2-3: Cross section of a composite polymeric membrane*

This substructure is coated with a thin dense layer of appropriate separation capability. The most common coating technique is spreading a solution of the respective polymer onto the porous substructure [22]. The solvent is evaporated, followed by further treatment to effect cross-linking of the polymer. Another technique is the deposition of thin layers from a vapor by means of nonthermal plasmas. They are generated by electrical glow-discharge under reduced pressure of gas (approximately 5 mbar) and application of a high-frequency electrical field. [23]. With a precise control of the operating conditions a very thin ( $<1\mu\text{m}$ ) but uniform cross-linked active layer can be achieved. Plasma membranes are generally as selective as those produced by solution coating and, in most cases, are more permeable.

*Hydrophilic membranes* have dense separating layers made from different polymers like poly-vinyl-alcohol (PVA) [22,24], polyimides [25,26], natural polymers like chitosan blended with other polymers [27,28], or cellulose acetate (CA) [29], or alginates [30,31], which are cross-linked by various chemical reactions. Pervaporation tests using ion exchange polymers [32], Polyelectrolytes [33-35], and recently with other types of polymers [36-41] are also found in literature.

*Organophilic membranes* have dense separating layers of cross-linked silicones, mostly polydimethyl siloxane (PDMS) or polymethyl octyl siloxane (POMS). Successful applications of separating organics from water have been rarely reported, as in most cases the selectivity of pervaporation does not significantly exceed that of the liquid vapor equilibrium. A number of experimental works in that field are recently reviewed in [42]. Yet, hydrophilic membranes have found industrial applications in the separation of light alcohols from their mixtures with other organics [43,44].

Polymeric pervaporation membranes are generally manufactured as flat sheets, which can be tailored for different module configurations (summarized in section 2.4). Hollow fibers are less used for pervaporation as it is difficult to coat them with a dense, defect free, but very thin layer. However, surface modified ultrafiltration hollow fibers were tested successfully on a pilot scale [45]. Detailed reviews on pervaporation membranes, yet with emphasis on polymeric ones are found in literature [46-48].

### 2.3.2 Inorganic membranes

Despite the material variability and the highly developed module technology of organic membranes, an increasing interest in membranes made of inorganic materials has been realized in recent years. Their specific features like: stability at high temperatures, resistance to swelling, resistance to harsh environments, mechanical stability, and ease of catalytic activation argue for this increased interest. Porous ceramic membranes with a mean pore diameter down to 1 nm are already commercialized for water treatment applications. For effective liquid and gas separations a thin additional layer of a mean pore diameter well below 1 nm has to be applied onto these membranes. The structure of such a configuration is shown schematically in Figure 2-4. The active separating layer can be applied by crystallization of zeolites [49,50], by deposition of amorphous silica by sol-gel techniques [51,52], by chemical vapor deposition (CVD) [53], by chemical vapor infiltration (CVI) [54], or by surface area modification [57]. Separation through these membranes is based on selective adsorption and diffusion through the micropores. Molecular sieving effects, caused by shape and size of molecules, and shape and size of the pores assess the feasibility of the separation. Preferential sorption on the membrane and inside the pores and surface diffusion in the adsorbed layer play an important role.

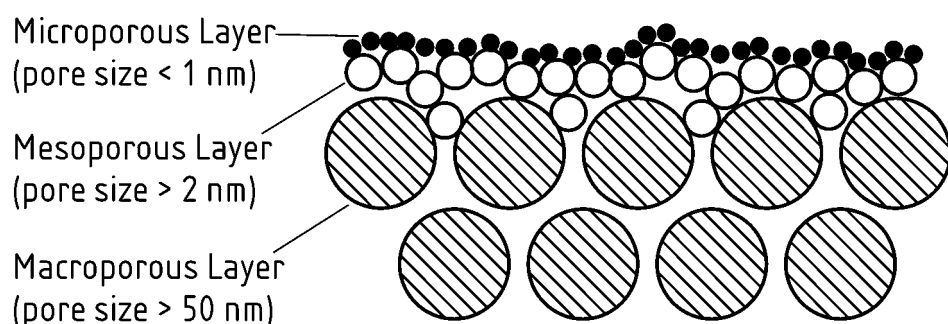


*Figure 2-4: Schematic structure of inorganic pervaporation membranes*

Zeolites are aluminosilicates having crystalline structures with well defined pores in the range of several Angstroms. Zeolites can be classified into several groups based on channel size: large-pore zeolites of 12 membered oxygen rings, such as ‘X’ and ‘Y’, intermediate-pore zeolites of ten membered rings, such as ‘ZSM-5’ , small-pore zeolites of eight-membered rings, such as ‘A’, ‘erionite’, and ‘chabazite’; and six-membered rings such as ‘sodalite’. Zeolites are generally hydrophilic at high alumina to silica ratios and organophilic at low alumina content.

Especially NaA-type zeolites are extremely hydrophilic and the pore of the crystal is accessible for water molecules only. Only the NaA-type has been used for the dehydration of organic liquids on a large commercial scale [49]. The more hydrophobic the zeolite, however, the higher is its sensitivity against acidic conditions. More acid stable zeolites are less hydrophilic, thus the selectivity and the flux of the respective membrane is substantially lower when used in dehydration applications. Meanwhile attempts are carried out to produce membranes with acid resistance down to pH=0 [56]. Organophilic zeolite membranes have been tested in the laboratory and applications for the removal of methanol and ethanol from larger organic molecules like ethers and esters are expected [44]. Recent reviews on zeolite membranes are found in literature [56-61].

Other hydrophilic membranes are those coated with amorphous silica [51,52]. They can be produced either by a sol-gel technique or by interfacial precipitation. Amorphous silica is stable against acid conditions. It is, however, difficult to obtain a uniform pore size by simple coating, therefore a multi-layer structure is found in this type of membranes as well. Selectivity and flux of silica membranes is comparable to that of a zeolite membrane, but they are not yet available on the commercial scale.

Inorganic membranes are so far mostly manufactured as tubes, with the separating layer on the inside or outside surface of the tube. They are resistant against temperatures up to 250°C, and against all neutral organic solvents. As the separating layer does not swell, they are less sensitive against fast concentration and temperature changes than the polymeric membranes. In contrast they are brittle, they have a lower surface-to-volume ratio, and they are more expensive due to the multi-stage coating and firing procedure. Module assembly with connections between ceramic tubes and other stainless steel module components is complicated and expensive, too. However, when high temperature operation is feasible they can compete with polymeric ones, as the increased fluxes overbalance the high costs. It is

therefore assumed that, like in other membrane processes, polymeric and inorganic membranes will find their respective areas of applications [44].

## 2.4 Membrane modules

Membrane modules for pervaporation and vapor permeation are based on those used for water treatment. However, they are modified and adapted to some specific requirements. For pervaporation and vapor permeation high permeate side pressure losses are not allowed to hold up the driving force. For vapor permeation feed side pressure losses have also to be avoided, otherwise the feed side vapors will deviate from the saturation condition reducing the separation efficiency. In pervaporation feed side pressure losses are not that important, but in multistage arrangements will eventually limit the number of applicable stages. As any feed mixture contains organic components at high concentrations and elevated temperatures, chemical and mechanical stability of all module components are essential. So far plate, spiral wound, envelope and tubular modules are the main types in use on an industrial scale.

The design of *plate modules* shown in Figure 2-5(a) is close to that of a filter press. The flat membranes are placed in a sandwich-like fashion with their feed sides facing each other. In each feed and permeate compartment thus obtained a suitable spacer is placed. The number of sets needed for a given membrane area furnished with sealing rings and two end plates builds up the plate and frame stack. The membranes are in most cases arranged for parallel flow of the feed. Serial flow would result in higher flow velocities and higher Reynolds numbers, but then feed side pressure losses would become too high. The plate modules are mainly used for dehydration processes, with permeate channels as open as possible. In the *envelope module* shown in Figure 2-5(b) developed by the research institute GKSS in Germany every two membrane sheets are welded together to a sandwich structure with a permeate spacer between the two membranes. A multitude of these sandwiches, each with a central hole are arranged on a central perforated tube which removes the permeate. Feed spacers keep the membrane sandwiches from each other, and feed side baffles can direct the flow in parallel or serial flow. The main advantage of this module is its flexibility towards different separation tasks, for instance, changing feed spacers for viscous media or where high turbulence is needed. These modules are used for organophilic as well as for hydrophilic separations.

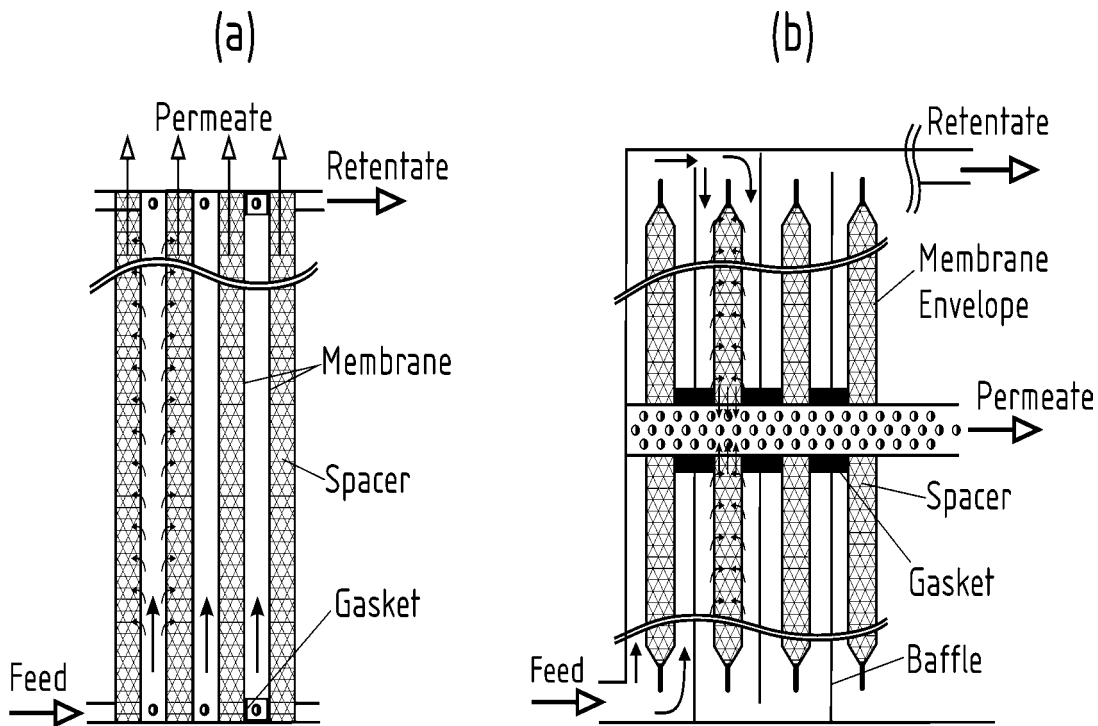


Figure 2-5: Schematic drawing of a plate module (a) and of an envelope module (b)

The *spiral wound module* shown in Figure 2-6 is more compact and cheaper than the plate and envelope modules, but characterized by higher permeate side pressure losses. Thus it is mainly used for the organophilic separations, as the permeate components have large molecular weights and hence lower volumetric flow causing smaller pressure drop compared to dehydration applications, for which the plate module is principally preferred.

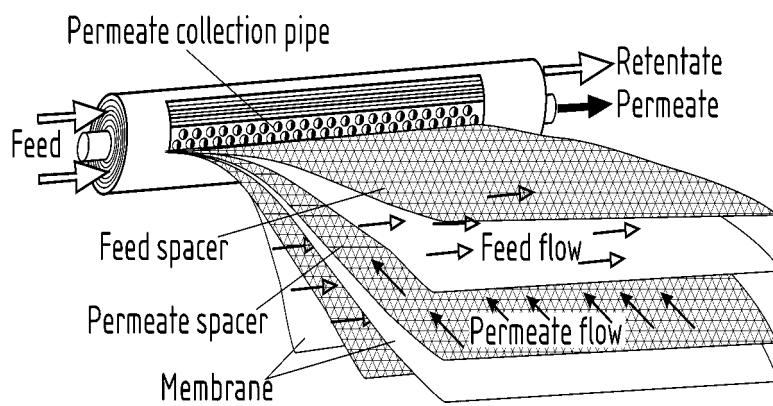


Figure 2-6: Schematic drawing of a spiral wound module

The *tubular modules* shown in Figure 2-7(a) are the first industrial realization of ceramic membranes. Their design is similar to a shell and tub heat exchanger. If the separating layer is

on the inside of the tube, high Reynolds numbers can be obtained for the feed side. The permeate vapor can be condensed inside the module shell which has to be kept under vacuum. If the separating layer is on the outside of the tube, the feed flow is directed by baffles to achieve a good flow distribution and high Reynolds numbers, and the length of the tubes is limited to avoid an increased pressure drop of the permeate flowing inside the tubes. In this case the feed can be heated in the module through additional heat exchanger tubes or through the shell of the module.

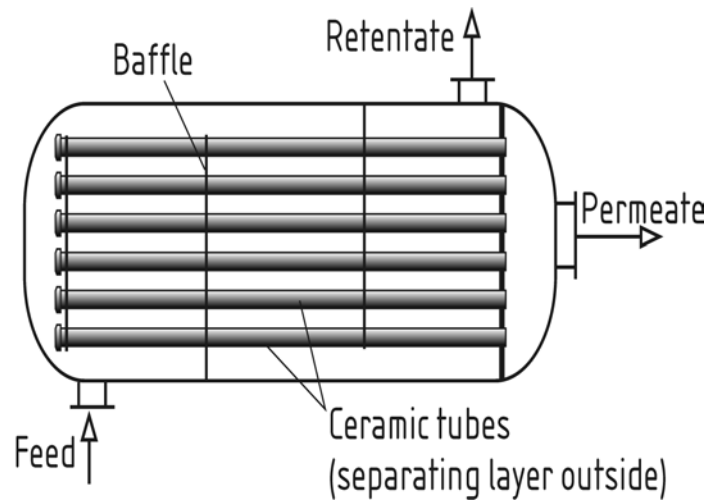


Figure 2-7: Tubular module (a) and hollow fiber module (b)

Although *hollow fibers* or *capillary modules* shown in Figure 2-7(b) are offered for pervaporation, no industrial application with these membranes have been yet reported [44]. As stated in section 2.3.1 the surface treatment and the coating of such membranes is difficult, especially at the inner side. However, this type of membranes is successfully developed and tested in a pilot scale [45]. When coating the outer surface of the capillaries, the permeate pressure losses inside the fibers limits the process.

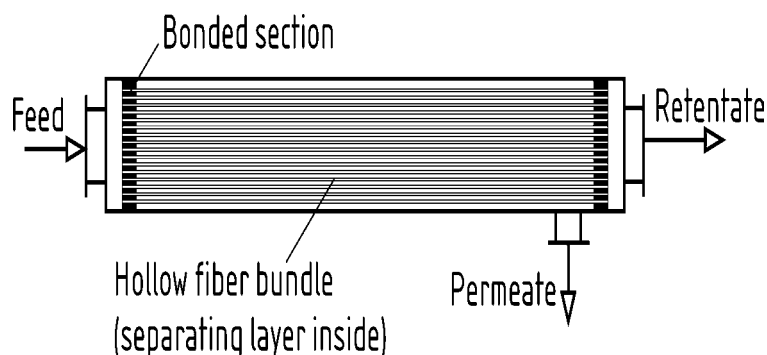


Figure 2-8: Hollow fiber module with the separating layer inside the fibers

## 2.5 Dehydration of organic compounds

One of the classical challenges to distillation was the dehydration of organic compounds that form azeotropes in their aqueous solutions. This separation problem was solved by the azeotropic or extractive distillation using an additional entrainer or by using pressure swing adsorption. However, many economic studies and industrial experiences have presented the pervaporation and vapor permeation as a favorable low-cost alternative to these processes. The first dehydration units operated with feed and product storage tanks -even by continuous operation- to be easily bypassed in case of trouble. With increasing experience and confidence in the new technology, solvent dehydration by means of pervaporation and vapor permeation became an essential step in the production, and are directly combined to distillation columns and chemical reactors in hybrid configurations.

### 2.5.1 Dehydration of bio-ethanol

When ethanol is used as gasoline extender and octane enhancer or as a solvent or intermediate, its water content must be as low as 1wt% down to 0.1 wt %. Atmospheric distillation of the fermentation beer is limited by the azeotrope at about 4.4 wt.% water. Overcoming this azeotrope and final dehydration by pervaporation and vapor permeation is state-of-the-art and large-scale plants have been installed and run in the last two decades. The combination of the membrane unit to the pre-distillation column as shown in Figure 2-9(a) has caught much interest as a novel hybrid separation technique. Membranes were optimized for this process for high fluxes, and even at the cost of the selectivity as the permeate stream can be recycled back to the distillation column. Especially vapor permeation is interesting for this application if it is installed near to the distillation unit as its feed can be won in the vapor phase as the top stream of the column, which saves a great deal of energy compared to the pervaporation alternative.

### 2.5.2 Dehydration of spent solvents

Organic solvents are commonly used in many branches in the chemical and pharmaceutical industries. Well known applications are in the synthesis of pharmaceuticals, to precipitate materials from aqueous solutions, for cleaning purposes and for drying of final products. Spent solvents nearly always contain some water and have to be purified and recycled.

Dehydration is an essential step in their recovery but difficult since most of the more common solvents form azeotropes with water.

In the pharmaceutical and fine chemical industries other factors in addition to the economical ones argue for the implementation of such membrane processes. The contamination of the products with the entrainer, or at least the monitoring of its concentration is avoided. Furthermore, the amount of solvent to be treated at a single location is often below the economic capacity of extractive distillation. The modular nature of pervaporation makes it economical even at small capacities. An in-situ recovery of the solvents using pervaporation or vapor permeation thus reduces storage and shipping of hazardous goods and is becoming standard practice in the pharmaceutical and chemical industries.

The most important solvents to be treated are the light alcohols, ethanol, the propanols, and butanol. Methanol is rarely treated by pervaporation as it does not form an azeotrope with water and can easily be purified by distillation. Other solvents are esters like ethyl- and butylacetate, ketones like acetone, butanone, methyl ethyl ketone, methyl isobutyl ketone, ethers like tetrahydrofuran (THF) or methyl tertiary butyl ether, or acetonitrile, or mixtures of these solvents. The final water concentrations to be reached vary between 1% to below 500 ppm for the alcohol to below 100 ppm for THF.

### 2.5.3 Different hybrid combinations to distillation

The coupling of the membrane units to a distillation column in the so called ‘hybrid separation processes’ has gained much attention in recent years. This coupling benefits from the special advantages of each process: the low cost of distillation in the regions of high difference of relative volatility, and the independency of the membrane separation process on the vapor-liquid equilibrium of the mixture to be separated. Thus the membrane process is implemented to overcome azeotropes and in the regions with close relative volatility, as it was proven that it is more economic than azeotropic and extractive distillation as stated in section 2.1.

This type of hybrid processes has been extensively studied in recent years. Pressly and Ng [62] presented a review on the economical aspects of these processes and presented a break-even analysis for investigating the feasibility of various types of distillation-membrane hybrids. Lipnizki, Field and Ten [48] reviewed process design and economic aspects of pervaporation based hybrid processes. Pettersen and Lien [63] presented parametric studies

illustrating some of the trade-offs in a hybrid distillation/membrane process for ethanol dehydration. Their calculations are based on an algebraic model for describing the mass transport through the membrane. Pettersen, Arg, Noble and Koval [64] analyzed an olefin purification by a distillation/membrane hybrid process. They studied different process configurations for determining the optimal operating conditions for each configuration. Rautenbach, Knauf, Struck and Vier [65] optimized a hybrid process separating methanol from dimethylcarbonate by calculating the processing cost. Hömmerich and Rautenbach [66] designed and optimized pervaporation–distillation processes within the production process of methyl tertiary butyl ether (MTBE). The membranes are considered for the separation of methanol from the reaction mixture, and a substantial economic advantage of the hybrid combination over the conventional azeotropic distillation process has been shown.

Different configurations for the coupling of membrane units and distillation columns for the purpose of dehydration of organics are shown in Figure 2-9. In the first scheme (a) the membrane feed is at the water side of the azeotrope and the membrane is used for overcoming the azeotrope and for the final dehydration. Examples are the dehydration of ethanol and acetone. In the second configuration (b) the membrane is used only to overcome the azeotrope and the final dehydration is done by the second column. An example for this process is the dehydration of isopropanol or aceonitrile. The arrangement (c) is used when the original feed composition is on the organic side of the azeotrope. The column separates the feed into the high boiling organic at the bottom and a low boiling mixture close to the azeotrope at the top. The vapor from the top is passed through a vapor permeation unit which removes water. The retentate has a residual concentration close to that of the original feed.

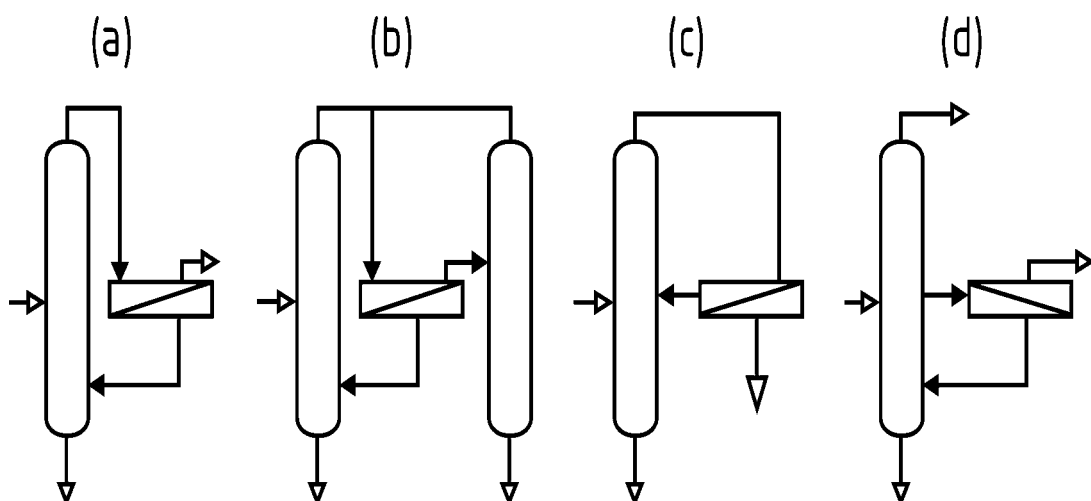
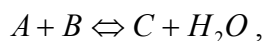


*Figure 2-9: Membrane dehydration processes coupled to distillation*

The configuration (d) is used for a three component separation like that of the system methanol-isopropanol-water [67]. In this system a minimum azeotrope that exists between water and isopropanol. The simplest way to separate this mixture through distillation is by using a fourth component and at least three distillation columns. In the alternative hybrid process, a side stream is drawn from the column and water is removed continuously by a pervaporation unit. Pure methanol can be obtained at the top and pure isopropanol at the bottom of the column.

#### 2.5.4 Dehydration of reaction mixtures

In many chemical reactions like esterification, etherification, acetalisation and poly-condensation water is produced as an unwanted by-product. As these are equilibrium reactions of the form



high yields can be obtained by adding an excess of one reactant or by constant removal of the produced water from the reaction mixture in order to shift the reaction to the product side. Application of pervaporation and vapor permeation processes to selectively separate water from reaction mixture forms an interesting alternative to distillation, especially in the case of azeotropic formation and low boiling reactants. Waldburger and Widmer [68] have reviewed and tabulated a number of membrane-assisted esterification reactions. More recent reviews are conducted by Lipnizki, Field, and Ten [48] and by Kemmere and Keurentjes [69].

There are generally two basic configurations of membrane-assisted reactors: both reaction and separation take place in the same piece of equipment as shown in Figure 2-10(a), or the reactor is equipped externally with the membrane unit as shown in Figure 2-10(b). The first configuration (a), which is known as ‘membrane reactor’, requires membrane modules with high surface to volume ratio and is characterized by low flexibility against variable operating conditions. The variance (b) can be used for different processes or adjusted to the process conditions by varying the membrane area used. It is also easier to operate and maintain. During the membrane replacements and in trouble cases the reactor can be operated independently.

Thus the type (b) is often used for pervaporation assisted reactors operating in batch or continuous modes. The flexibility is an important factor by designing the batch units, which

are often used as multi-product units in the chemical plants. For continuous operations a multistage reactor-membrane cascade is necessary to achieve the desired high yield. Brüsck and Schneider [70] reported on one of the first industrial plants, combining pervaporation and an esterification reaction, operating continuously with a cascade scheme.

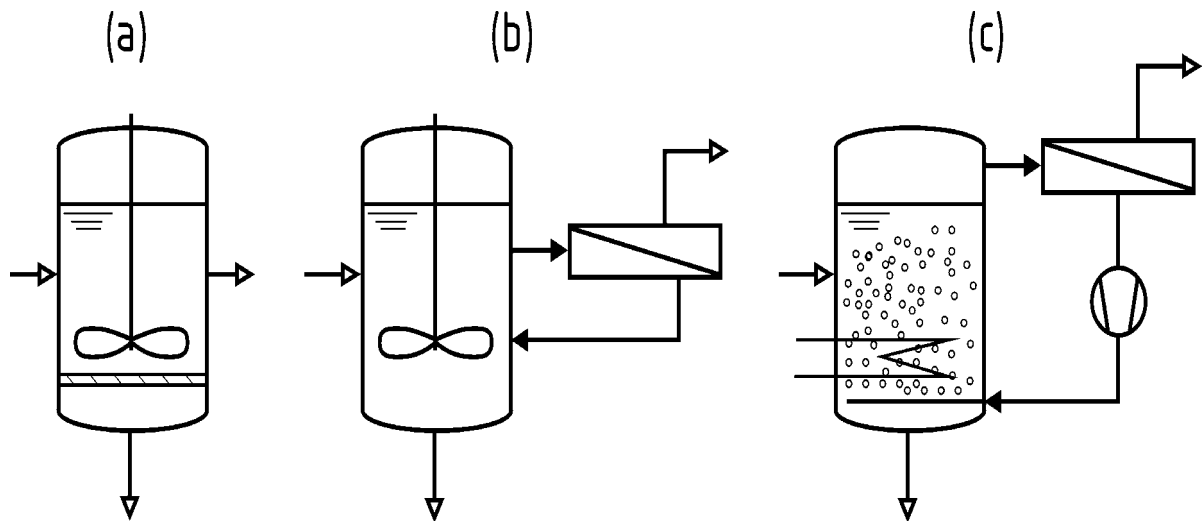


*Figure 2-10: Membrane-assisted chemical reactors*

The implementation of vapor permeation is recommended in the cases of heterogeneous catalysis, in which the flow of a liquid reaction mixture through the membrane modules would cause mechanical damage to the membrane material. Also when aggressive low volatility components are present in the reaction mixture, the water can be won in the vapor phase by partial evaporation and removed by vapor permeation. Though in the case of vapor permeation the evaporation of the membrane feed is necessary, yet the energy consumption of this process is reduced by the recycle of the vaporous retentate as shown in Figure 2-10 (c) [71]. The energy input will be reduced to the latent heat of the vaporization of the permeate stream. The recycled vapor stream also assists the stripping of water out of the reaction mixture .

### 3 Objectives

As stated in chapter 1, the studies within this work are substantially theoretical. The aim is achieving technical and economic improvements in pervaporation and vapor permeation through systematic process design investigations. The modeling and simulation of the membrane process is implemented in a subroutine integrated in the standard flow-sheeting software ‘Aspen Plus’. The model can then be used in conjunction with the existing ‘Aspen Plus’ unit operation models to simulate the whole membrane unit with its periphery equipment and as a hybrid process combined with distillation.

Using the developed simulation program, it is possible to carry out different parametric studies and to optimize the membrane unit on an economic basis. In addition to the permeate side parameters of temperature and pressure, the transport parameters of the membrane are included in the optimization calculations. The experimental work that is carried out in parallel to this theoretical work gives guidelines and basis for the transport parameters assumed and optimized in the process simulation. The target is to be able to tailor the transport properties of the used membranes for each specific application, and for each stage within one application. With a good information exchange between the process simulation and the membrane-making experimental work, the experimental work can be better targeted and the accuracy and reliability of the process simulation can be increased.

With the combination of distillation and vapor permeation into hybrid separation processes, or when using multistage membrane separation, the process gets more complex with a large number of streams being heated and cooled. Energy saving measures for these processes are investigated. The Pinch Technology is considered as a good tool for studying heat integration options, which is based on plotting composed enthalpy-temperature diagrams of the streams to be heated and cooled. The optimum heat exchange network for the considered streams can be determined according to these diagrams and with the use of a systematic approach and process synthesis rules.

Following the above described work, the technical realization of the pervaporation and vapor permeation processes is investigated for refinements and for alternative technologies. As described in chapter 2, the condensation technology has yet proven to be the most convenient

method for vacuum production at the permeate side of the membrane. Although it is relatively expensive it is a simple and common technology with a wide range of standard units and long years of industrial experience. However, this technology has shown some limitations by its use in the combination with pervaporation and vapor permeation. One disadvantage is the exponentially increasing refrigeration cost with decreasing temperature below a certain temperature range. Another disadvantage is that the condensation temperature and thus the permeate pressure cannot be arbitrarily decreased. The freezing point of the permeate mixture sets the lowest temperature limit in the condenser to avoid solids accumulation on the heat transfer area. Alternative technologies for vacuum production are investigated for potential application within pervaporation and vapor permeation processes. The technical feasibility is discussed and economic studies are carried out.

In chapter 4 the modeling and simulation of pervaporation and vapor permeation processes are reviewed. Rigorous, semi-empirical and empirical models are presented and discussed. The computer program developed for the modeling and optimization of the membrane units with the software Aspen Plus is presented in chapter 5. Results for economic and energy optimization of a typical application of ethanol dehydration is illustrated at the end of this chapter.

In chapter 6 the use of steam jet ejectors as a process integration alternative for hybrid dehydration processes is introduced and investigated. In this novel configuration the resulting low pressure steam from the jet ejector is used as an energy source to run the distillation column. Process simulations and economic evaluations are carried out for this process. Favorable implementation regions are identified, and the advantages and limitations of this modification are discussed.

In chapter 7 another novel technique for vacuum generation is realized by the absorption of the permeate vapors. This technology is suitable for the dehydration of organics as it can assist to the commercial scale available absorption refrigerators or heat pumps. Technical and economic advantages over the conventional condensation technology can be achieved by integrating the membrane into such units. Vacuum pressures as low as 8 mbar can be obtained under room temperature without refrigeration. Low vacuum ranges that are not possible by condensation due to freezing limitations can be achieved. Process simulations and feasibility investigation for the suggested process are presented and discussed.

## 4 Mass transport mechanisms and models

The detailed modeling of the transport processes through pervaporation membranes requires the consideration of the partial processes shown in Figure 4-1. The main complexity in modeling the overall process lies in the steps concerning the active layer because the membrane material introduces additional coupling effects to the mixture to be separated. Unique swelling behavior of different polymeric membranes and the multi-feature diffusion mechanisms through microporous ceramic membranes prohibit the development of a universal transport model for the membrane process.

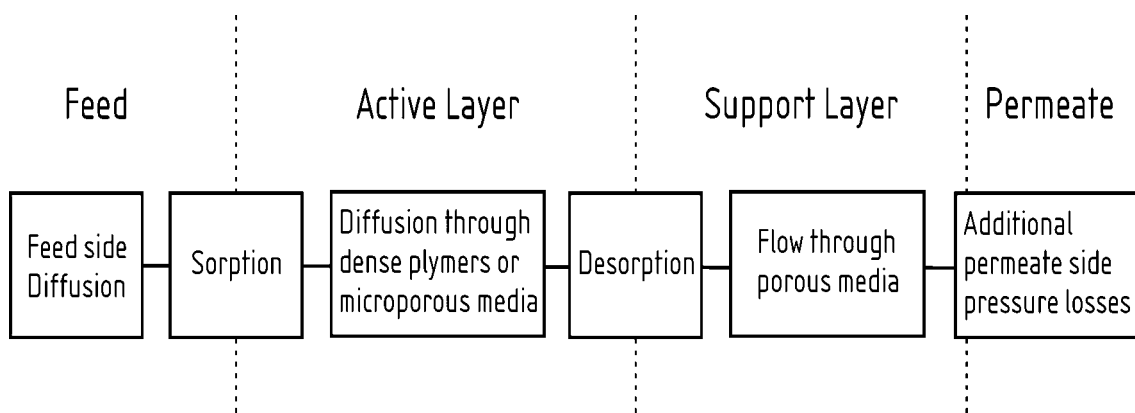


*Figure 4-1: Transport processes during pervaporation or vapor permeation separations*

Generally the slowest controlling step is either the sorption or the diffusion process, depending on the mixture to be separated and the used membrane material. However, in poor design or at improper operating conditions slow mass transfer at the feed side can limit the supply of the fast permeating component to the membrane surface. This limitation is known as feed side concentration polarization and it can be overcome or minimized by assuring high turbulence on the feed side of the membrane modules. Focusing on the support layer, the flow through the porous support and through the permeate side channels is more rapid than other transport steps. Yet, the permeate side pressure drop can have a great influence on the overall driving force for the permeation process. In the following sections the mass transport mechanisms within these steps are highlighted and different modeling techniques are introduced. Subsequently, the modeling of the membrane unit within the simulation software ‘Aspen Plus’ will be presented.

## 4.1 Feed-side mass transport

The feed-side mass transfer resistance resides in the ‘external’ diffusion process which may not be able to keep up with the possible rates of selective material transport through the membrane interface. This phenomenon, known as *concentration polarization*, is thus influenced by the intra-membrane flux as well as by the feed side hydrodynamics and concentrations. According to the film theory the resistance in the fluid phase can be expressed with molecular diffusion through a boundary layer with  $x_{bi}$  and  $x_{bi}^*$  the mole fractions of component ‘i’ in the bulk of the fluid and at the membrane interface respectively. Due to the selective material consumption at the membrane interface, unidirectional diffusion takes place, and a convective motion known as Stefan Flow compensates the consumption at the interface. Fick’s law for unidirectional diffusion for binary mixtures and low concentration of component  $i$  can be expressed as:

$$J_i = -D_{bi} \frac{c}{I-x_i} \frac{dx_i}{dz} \quad (4-1)$$

with  $z$  the path perpendicular to the membrane surface,  $c$  the total concentration and  $D_{bi}$  the diffusion coefficient of component ‘i’ in the fluid phase. Equation (4-1) can be integrated along the boundary layer thickness  $\delta_b$  to produce:

$$J_i = -c \frac{D_{bi}}{\delta_b} \ln \frac{1-x_{bi}^*}{1-x_{bi}} \quad (4-2)$$

and is expressed by the logarithmic averaged mole fraction  $\bar{x}_{bi}$  as:

$$J_i = -\frac{c}{I-\bar{x}_b} \frac{D_{bi}}{\delta_b} (x_{bi} - x_{bi}^*) \quad (4-3)$$

By the introduction of the mass transfer coefficient as

$$k_{bi} = \frac{D_{bi}}{\delta_b (I-\bar{x}_{bi})} \quad (4-4)$$

the expression for the flux will reduce to:

$$J_i = -k_{bi} c (x_{bi} - x_{bi}^*) \quad (4-5)$$

The mass transfer coefficient through the boundary layer  $k_{bi}$  is estimated as a function of feed hydrodynamics using the Sherwood correlation according to the flow regime shown exemplary as reviewed by Klatt [71] in table (4-1) for plate-and-frame membranes

*Table (4-1): Mass transport correlations for-plate-and-frame membranes*

Flow regime	Relation
Laminar, not fully developed	$Sh = 1.62 (Re Sc \frac{d}{L})^{1/3}$
Laminar, fully developed	$Sh = (3.66^3 + 1.62^3 Re Sc \frac{d}{L})^{1/3}$
Turbulent	$Sh = 0.026 Re^{0.8} Sc^{0.3}$

by using the dimensionless numbers Sherwood,  $Sh = k_{bi} d_h / D_{bi}$ , Reynolds,  $Re = \rho d_h v / \mu$  and Schmidt,  $Sc = v / D_{bi}$ . However, Sherwood number may be modified for unidirectional diffusion to be  $Sh = k_{bi} (1 - \bar{x}_{bi}) d_h / D_{bi}$  [72].

For plate and frame modules the hydrodynamic diameter is calculated by:

$$d_h = \frac{4 \times \text{volume between plates}}{\text{wetted surface between plates}} \quad (4-6)$$

A number of such transfer correlations for different geometries can be found in literature. Gekas and Hallstörm [73] reviewed different existing Sherwood correlations applicable to turbulent cross flow membrane operations.

In the case of nonideal multicomponent mixtures the Maxwell-Stefan approach is preferred as it considers the intermolecular interactions. This approach is illustrated in section 4.3.1.

## 4.2 Modeling the sorption process

The term ‘sorption’ is used to describe the initial penetration and dispersal of permeant molecules into the membrane surface. The term includes phenomena such as absorption, adsorption, incorporation into micro-voids and cluster formation. The permeant may undergo several modes of sorption simultaneously in the same material. In addition, the distribution of permeant between the different sorption modes may change with concentration, temperature, and swelling of the matrix and as well as with time.

#### 4.2.1 Sorption in organic membranes

The sorption of molecules from gases or liquids by polymers has been studied extensively, and several models have been proposed to describe the experimental sorption data as a function of sorbate concentration, partial pressure or activity.

**Henry's Law** is obeyed in the simplest ideal case at a low sorbate activity when the solubility coefficient is independent of sorbed concentration. The sorption isotherm is a linear relation of concentration versus activity in the fluid phase and can be expressed as:

$$\phi_i = S_i a_i \quad (4-7)$$

where  $\phi_i$  is the volume fraction of the sorbate in the polymer,  $a_i$  its activity in the fluid phase and  $S_i$  is the solubility coefficient. Due to its simplicity, Henry's law is often used as a first approximation, or for systems with little concentration change.

**Langmuir model** is derived by considering mono-layer sorption [75] into pre-existing voids which act in a manner equivalent to that of specific sites, and is given by:

$$\phi_i = \frac{\phi_i^H b_i a_i}{1 + b_i a_i} \quad (4-8)$$

where  $b_i$  is the hole affinity constant representing the ratio of rate constants of sorption and desorption of penetrant in the holes, and  $\phi_i^H$  is the hole saturation constant. This equation can simulate the isotherms only in a few cases for glassy polymers. However, it is a common way for expressing the adsorption isotherms for crystalline adsorbents like zeolites as shown in section 4.2.2.

**The dual sorption model** which was derived initially for glassy materials [76], is based on Henry's law and Langmuir equation. The population of molecules described by the Langmuir equation is assumed to be specifically adsorbed in the polymer matrix while those described by Henry's law are nonspecifically absorbed. In addition to providing a new description for sorption isotherms in complex media, the dual sorption theory allowed new interesting insights into the diffusion phenomena in polymeric materials. Related theories have recently somewhat overcome the difficulties encountered with polymers inducing high swelling ratio for which the initial dual sorption theory has been proved to be inaccurate.

A **mechanistic approach** was quite recently shown to be a very good alternative to the former models. This approach considers the sorption phenomenon as a competitive process of sorption on two different sites, i.e. a polymeric site or another previously sorbed molecule. This model (referrd to as the ENgaged Species Induced Clustering model, ENSIC) enabled the sorption modeling for a very broad range of systems [77].

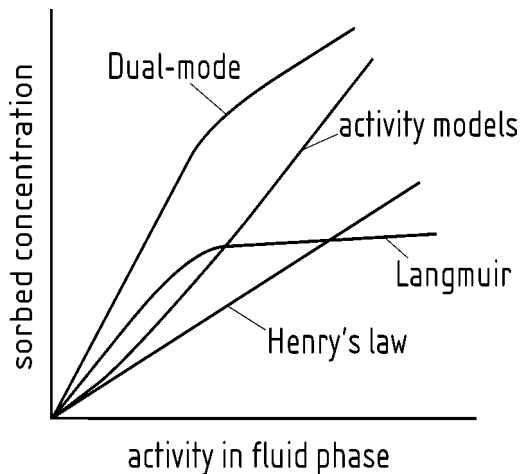


*Figure 4-2: Typical isotherm plots calculated from different models*

Other tools, similar to those used for modeling conventional phase equilibrium, are available for the treatment of polymer-solvent mixtures. Either ‘activity coefficient models’ (excess Gibbs free energy models ) or ‘equation of state models’ as shown in Table (4-2) can be used. A number of them are meanwhile available in commercial simulation software, and recent reviews [78,79] give guidelines for selecting the proper model for each specific system.

*Table (4-2): Representative thermodynamic property models*

Activity coefficient models	Equation-of-state models
Flory-Huggins	Sanchez-Lacombe
UNIQUAC	SAFT
UNIFAC	Polymer-SRK
Polymer-NRTL	

While the ‘equation of state models’ are preferred at high pressures and near the critical conditions, the ‘activity coefficient models’ are recommended for polar systems at low pressures. As the systems under investigation substantially contain polar components, two representative ‘activity coefficient models’ are introduced below in more detail.

**Flory-Huggins approach** due to Flory [80] and Huggins [81] is one of the most used approaches for modeling the sorption process in polymers. In the frame of this theory, which is based on a basic lattice concept, the modeling of the sorption process is given by:

$$\ln a_i = \ln \phi_i + \left(1 - \frac{\bar{V}_i}{\bar{V}_M}\right) \phi_M + \chi_{iM} \phi_M^2 \quad (4-9)$$

where  $\bar{V}_i$  and  $\bar{V}_M$  are the molar volumes of the sorbate and membrane polymer respectively, and  $\chi$  is Flory-Huggins interaction parameter. Despite its theoretical restriction to non-polar species this theory has been applied to a wide range of systems and the initial theory has been lately refined to account for sorption in systems of ever increasing complexity.

**The UNIQUAC approach**, originally proposed by Abrams and Prausnitz [82], accounts for the different sizes and shapes of the molecules as well as for the different intermolecular interactions between the mixture components including polymeric compounds. It requires binary interaction parameters for the description of multi-component mixtures, and can be expressed as:

$$\begin{aligned} \ln a_i = & \ln \phi_i + \frac{Z}{2} q_i \ln \frac{\theta_i}{\phi_i} + l_i - \sum_{j \neq M}^n \phi_j \frac{r_i}{r_j} l_j - r_i \phi_M \left( \frac{Z}{2} \left(1 - \frac{q_M}{r_M}\right) - 1 \right) + q_i^* \\ & - q_i^* \ln \sum_{j=1}^M \theta_j \tau_{ij} - q_i^* \sum_{j=1}^M \frac{\theta_j^* \tau_{ij}}{\sum_{k=1}^M \theta_k^* \tau_{kj}}, \\ \theta_i = & \frac{\phi_i (q_i / r_i)}{\sum_{j=1}^n \phi_j (q_j / r_j)}, \quad \theta_i^* = \frac{\phi_i (q_i^* / r_i)}{\sum_{j=1}^n \phi_j (q_j^* / r_j)}, \quad l_i = Z/2 \cdot (r_i - q_i) - (r_i - 1) \end{aligned} \quad (4-10)$$

where  $\theta_i$  and  $\theta_i^*$  are the surface fractions which can be calculated from  $r_i$ ,  $q_i$  and  $q_i^*$  which are dimensionless parameters for the relative molecular size and surface of component i related to the size and surface of a CH<sub>2</sub> segment in polyethylene respectively. The parameters  $\tau_{ij}$ ,  $\tau_{ji}$ ,  $\tau_{iM}$  and  $\tau_{Mi}$  represent the interactions of the sorbents with each other and with the membrane material.  $Z$  is the coordinate number and assumed to be equal to 10. Equation (4-10) is a modified version of the original UNIQUAC model extended by an additional term containing the parameter  $q_i^*$  (effective surface of the molecule) which is needed in the case of systems containing molecules which form hydrogen bonds [83]. This model has been applied successfully for modeling systems deviating strongly from ideality [84,85].

#### 4.2.2 Adsorption in inorganic membranes

The membranes made of inorganic materials have defined internal structures and no swelling takes place. However, the sorption process of gases and liquids by these materials is not less complex than by polymeric ones. The pore size and pore size distribution affects the adsorption and diffusion mechanisms as will be illustrated in detail in section 4.3.2. The interaction forces between the sorbates and the membrane surface and pore walls also affect the extent of the adsorption process. Like by organic materials the sorption may obey Henry's law at low sorbate concentration. At higher concentration the equilibrium relationship becomes curved. The commonly observed forms of isotherms were classified by Brunauer into five types illustrated in Figure 4-3 [86]. This classification has become a standard and the shapes of isotherms are often referred to in the literature by these five numbers.

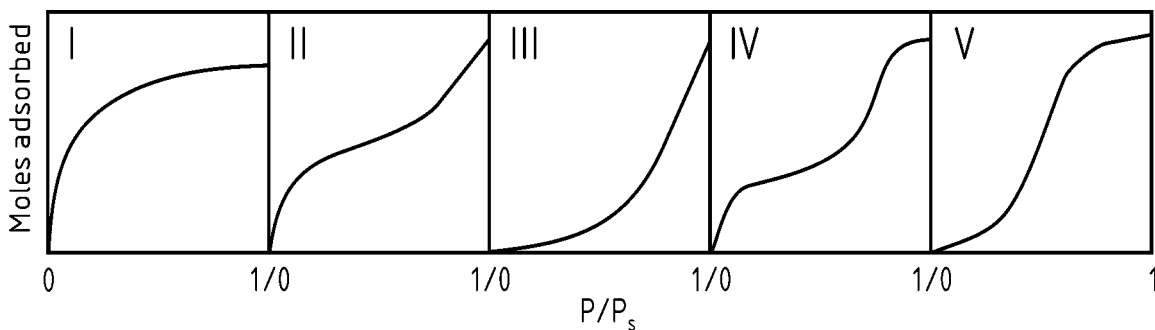


Figure 4-3: The Brunauer classification of isotherms

Reference to the isotherm for water vapor shows that  $\text{H}_2\text{O}-\text{NaA}$  is type I,  $\text{H}_2\text{O}$ -alumina is type II,  $\text{H}_2\text{O}$ -carbon is type III, while  $\text{H}_2\text{O}$ -Silica gel is type IV. Type I is characteristic of adsorption in microporous material where the saturation limit corresponds to complete filling of micropores. The increase in the amount adsorbed in the other isotherm types is explained by multilayer adsorption or capillary condensation which is dependent on the level of interaction energies between sorbate-solid and sorbate-sorbate. Type I can be well described by **Langmuir model** introduced in section 4.2.1. Other models with more parameters up to 4 or 5 can describe all types of isotherms. The **Brunauer, Emmett and Teller (BET) theory** is the basis of many of such models [87].

For multicomponent adsorption the **adsorbed solution theory** has been used as a basis of many modeling approaches [88]. This theory is based on the visualization of the adsorbed phase as an adsorbed solution. Equilibrium between the fluid phase and the adsorbed phase is then described analogously to vapor/liquid equilibria.

## 4.3 Modeling the diffusion process

The diffusion of the sorbed components through the active layer of the membrane is rather difficult to describe by a general fundamental model. Diffusion mechanisms depend primarily on the membrane material and sometimes different mechanisms take place simultaneously in the same membrane. In the next sections the diffusion processes in polymeric and ceramic pervaporation membranes are reviewed, and the modeling techniques are briefly addressed.

### 4.3.1 Diffusion in dense organic membranes

A variety of structural and morphological characteristics of the polymer affect solute diffusion through a membrane composed of a polymeric material. On the macro-scale, thickness, pore structure (including size, size distribution, and type), laminations, or asymmetry of the membrane are found to influence mass transfer rate and selectivity. Other features become important on the micro-scale: fixed charges, dipoles, crystallinity, degree of swelling, degree of cross-linking, and thermodynamic transitions related to macromolecular relaxation phenomena (glassy/rubbery transitions in the presence of a solute and a swelling agent).

**The glass transition temperature**, which corresponds to the transition from glassy to amorphous (rubbery) state, has a very marked influence on the diffusion mechanism. In the rubbery state, the polymer chains are movable and behave like a viscous fluid. The mobility of the polymer chains result in a continuous forming and closing of molecular-scale gaps between the chains. Thus, these gaps can serve as permeation paths for the molecules diffusing through amorphous polymers. In the glassy state, the mobility of the polymer chains is very constricted. However, unrelaxed molecular-scale gaps are frozen during quenching from the rubbery state or during casting from solution. As these gaps are of defined structure and location, the size and shape of the permeant are important parameters affecting the permeation through glassy polymers.

In conclusion, diffusion is controlled by the ease of forming enough free space in the membrane to enable the unit diffusion step to occur. In the **free volume theory** [89], this is discussed in terms of a probability of finding enough local free volume. The diffusion coefficient  $D$  may be related to this probability in the simplest case by

$$D = RTA_d \exp\left(-\frac{B_d}{V_f}\right) \quad (4-11)$$

where  $R$  is the universal gas constant,  $T$  is the absolute temperature,  $B_d$  is a parameter describing the amount of free volume needed and is proportional to  $\sigma$ , the Lennard-Jones size parameter and  $A_d$  is a parameter related to the size and shape of the permeant and can also be correlated to its molecular weight and to its  $\sigma$ .  $V_f$  is the fractional free volume, which is related to the volume of the polymer chains [90]. However, for glassy polymers  $V_f$  is always related to a hypothetical volume extrapolated from the rubbery state [91] as shown in Figure 4-4. The free volume model has been refined and modified in further studies to account for intermolecular interactions and for the swelling of the polymer matrix [92].

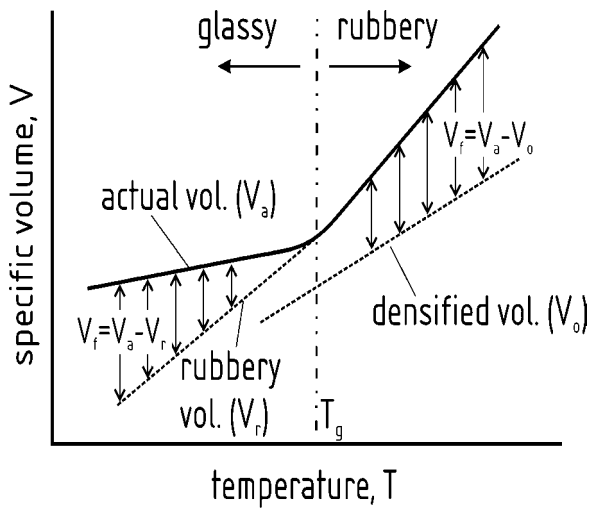


Figure 4-4: Different definitions of the free volume

From the activation energy viewpoint, the diffusion process is discussed in terms of the energy needed to create the free space. This is the basis of the Monte Carlo simulations and molecular modeling techniques [93,94]. For this way of modeling, as well as for the free volume theory, the flexibility of the polymer chains and the cohesive energy of the polymeric structure are important as they relate to chain mobility.

The modeling of the diffusion process may be carried out by Fick's law considering the concentration or activity difference as driving force. However, the Maxwell-Stefan equations are more suitable for calculating the diffusion fluxes in the case of nonideal systems [95]. Although they were originally developed for liquid systems, they are utilized by considering the membrane solid phase as a stationary liquid as proposed by Heinz and Stephan [96]. Based on the momentum balance, these equations relate the forces acting on the molecules of

each species (the gradient of chemical potential) to the friction between this species and any other species.

For binary diffusion, the flux  $J_i$  can be calculated as

$$J_i = -c_t D \Gamma \nabla x_i \quad (4-12)$$

where  $c_t$  is the total concentration,  $D$  is the Maxwell-Stefan diffusivity that has the physical significance of an inverse drag coefficient,  $\nabla x_i$  is the mole fraction gradient, and  $\Gamma$  is a thermodynamic factor portraying the nonideal behavior and can be calculated as

$$\Gamma = 1 + x_i \frac{\partial \ln \gamma_i}{\partial x_i} \quad (4-13)$$

where  $\gamma_i$  is the activity coefficient of component  $i$  in the binary mixture and can be calculated by a proper thermodynamic activity coefficient model.

For  $n$  components a  $(n-1)$ -dimensional matrix notation is used:

$$(J) = -c_t [B]^{-1} [\Gamma] (\nabla x) \quad (4-14)$$

where  $(J)$  and  $(\nabla x)$  represent column vectors of  $(n-1)$  components. The elements of the matrix  $[B]$  is derived in terms of the Maxwell-Stefan diffusivities  $D_{ij}$  as follows:

$$B_{ii} = \frac{x_i}{D_{in}} + \sum_{\substack{k=1 \\ k \neq i}}^n \frac{x_k}{D_{ik}}, \quad B_{ij} = -x_i \left( \frac{1}{D_{ij}} - \frac{1}{D_{in}} \right), \quad i, j = 1, 2, \dots, n-1 \quad (4-15)$$

while the elements of the matrix  $[\Gamma]$  that are derived from the chemical potential gradient can be written as:

$$\Gamma_{ij} = x_i \left( \frac{\partial \ln x_i}{\partial x_j} + \frac{\partial \ln \gamma_i}{\partial x_j} \right) \quad (4-16)$$

The main difficulty by using these equations is the proper determination of the interaction parameters especially between the diffusing components and the membrane material. Heinz and Stephan [96] and recently Bausa and Marquardt [97] have shown a good agreement of the Maxwell-Stefan modeling with the experimental data of different polymeric membranes.

### 4.3.2 Diffusion in microporous inorganic membranes

The diffusion in microporous inorganic membranes is at least as complex as the diffusion in dense organic membranes illustrated in the former section. Interaction forces and surface diffusion play an important role beside the molecular sieving effects of the membrane. The major transport mechanisms that can govern the permeation of gases or vapors in porous membranes are summarized in Figure 4-5.

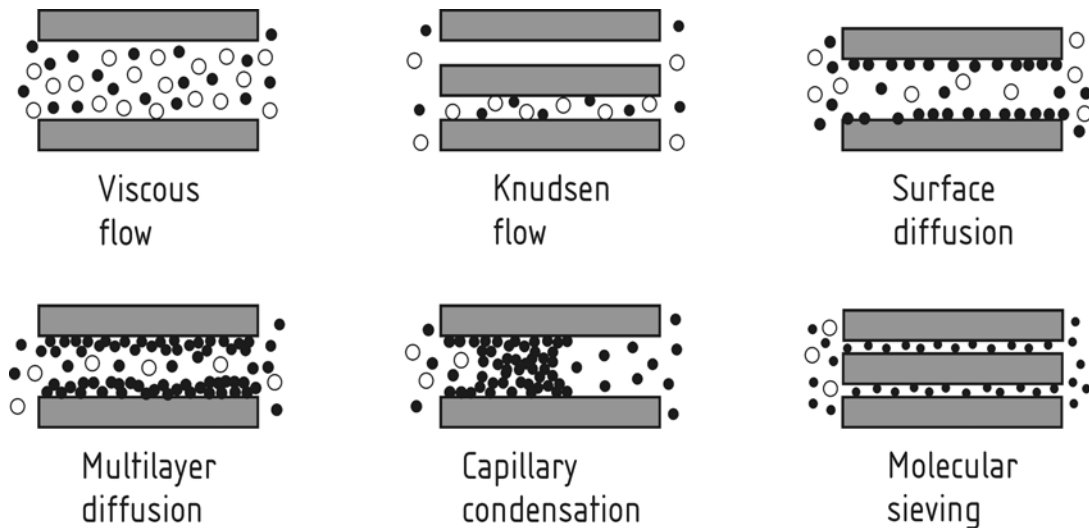


*Figure 4-5: Transport mechanisms through porous and microporous media*

**Viscous flow**, or Poiseuille flow, takes place when the mean pore diameter is larger than the mean free path of gas molecules (pore diameter higher than few microns). The gas acts as a continuum fluid driven by a pressure gradient and molecule-molecule collisions dominate over molecule-wall collisions. In such conditions, no separation can be attained [98].

**Knudsen flow** is achieved when the pore dimension decreases (down to fractions of a micron) or when the mean free path of molecules increases, which can be achieved by lowering the pressure or raising the temperature. The molecules collide more frequently with the pore walls of the membrane rather with one another. The fluxes are then proportional to the square root of the molecular weight of the different gaseous compounds [98].

**Surface diffusion** may also take place as a part of the diffusion process. It can contribute to the separation selectivity when one of the permeating adsorbed molecules can preferentially physisorb on the pore walls [99]. By higher interactions between the adsorbed molecules themselves multilayer adsorption and hence **multilayer diffusion** occurs. The multilayer

diffusional flux is generally much larger than the gas phase flux and can be considered as a two dimensional fluid ‘slipping’ over the surface [100].

**Capillary condensation** is enabled when a pore is blocked by condensate. The condensed components evaporates at the permeate side, where a low pressure is imposed. The meniscus formed at the feed side promotes further condensation due to the decrease in vapor pressure that can be described by Kelvin equation [100].

**Molecular sieving** is achieved when pore diameters are small enough to let only smaller molecules permeate while mechanically preventing the bigger ones from getting in. Provided the pores are monodispersed in dimension, selectivity may reach very high values.

The first two of the above mechanisms, the viscous and Knudsen flow are considered for modeling the support layers of pervaporation and vapor permeation membranes as will be described in section 4.4. The last four mechanisms take place in the active layer of these membranes. Modeling this complex process can be carried out using Fick’s law implementing concentration dependent diffusivities. The correlations for the diffusivity can determined experimentally and/or with the help of molecular modeling techniques [101,102]. The chemical potential gradient is usually used as a driving force by these techniques. The Maxwell-Stefan approach has been also successfully used for modeling the diffusion in the active layer of inorganic microporous membranes [103,104].

#### 4.4 Flow through the support layer

The vapor or gas mixture permeating through the active layer has to move through the support layer of the membrane, which is often a micro- or ultrafiltration membrane. The transport mechanism is a complex combination of viscous flow, Knudsen diffusion (see Figure 4-5), and continuum diffusion. The Knudsen and diffusive transport is controlled by concentration gradients, while the viscous non-separating flow is caused by total pressure gradients. In the transition region between the Knudsen and continuum regime, both molecule-molecule and molecule-wall interactions have to be considered. The result is slip flow with continuum transport in the bulk of the pore and “slip” near the pore surface caused by the molecule-wall interaction.

The combination of the above stated mechanisms for a porous medium may be described for the entire pressure range by the **dusty gas model** [98], which has been used to describe transport in porous membranes [105] and support structures [106] with estimated morphological parameters. The dusty gas model in its general form for component  $i$  in a mixture of  $n$  components is given by

$$\frac{RT}{D_{ik}} J_i + \sum_{j=1}^n \frac{RT}{D'_{ij}} (x_j J_i - x_i J_j) = -\nabla p_i - \frac{x_i}{D_{ik}} \frac{B_o p}{RT\eta} \nabla p \quad (4-17)$$

where  $J_i$  is the molar flux of component  $i$ ,  $x_i$  is its mole fraction,  $p$  and  $p_i$  are the total and partial pressure respectively and  $D_{ik}$  and  $D_{ij}$  are the Knudsen and continuum coefficients, respectively, given as

$$D_{ik} = \frac{4}{3} K_o v_{Mi}, \quad D'_{ij} = \frac{\epsilon}{\tau} D_{ij} \quad (4-18)$$

where  $v_{Mi}$  is the mean molecular speed of the gas molecules of component  $i$ ,  $D_{ij}$  is the intrinsic binary diffusion coefficient. The structure of the porous medium is described by three morphological parameters  $B_o$ ,  $K_o$  and  $\epsilon / \tau$ .  $B_o$  adjusts the term of viscous flow diffusion and is characteristic of the medium and independent of the gas used. For straight cylindrical capillaries,  $B_o$  is equal to  $d^2/32$  as in the Hagen-Poiseuille equation, where  $d$  is the diameter of the capillary.  $K_o$  is the parameter of the Knudsen and slip diffusion and depends primarily on the morphology of the medium, but also slightly on the absolute pressure and the gas. The effective porosity  $\epsilon / \tau$ , which is the ratio of porosity and tortusity, adjusts the continuum diffusion coefficient to the structure of the pore medium. These parameters are usually much easier to measure experimentally than to calculate it from the geometry, which in fact is seldom known with any precision.

Beuscher and Gooding [106] solved the general form of the dusty gas model for two components A and B, which may be useful in modeling many membrane processes, as follows:

$$J_A = \delta_A x_A J - \frac{D_A}{RT} \nabla p_A - (1 - \delta_A) x_A \frac{B_o p}{\eta RT} \nabla p, \quad (4-19)$$

$$D_A = \left( \frac{1}{D_{AB}} + \frac{1}{D_{AK}} \right)^{-1}, \quad \delta_A = \frac{D_A}{D_{AB}}$$

The total flux  $J$  in the above equation is calculated as follows:

$$\begin{aligned} J &= -\frac{K_{AB}}{RT} \nabla p - \frac{R_{AB}}{RT} \nabla p_A, \\ K_{AB} &= \frac{D_B}{1 - \delta_A x_A - \delta_B x_B} + \frac{B_o p}{\eta}, \quad R_{AB} = \frac{D_A - D_B}{1 - \delta_A x_A - \delta_B x_B} \end{aligned} \quad (4-20)$$

Generally the effect of the support layer on the whole membrane performance is small in the case of pervaporation or vapor permeation. However, its rigorous modeling may be complex as it requires a number of parameters that are specific for each membrane. The effect of the support layer has been sometimes neglected [63,107], calculated empirically [72] or approximated by a bundle of parallel cylindrical capillaries [96,97].

## 4.5 Empirical and semi-empirical modeling

In the former sections the detailed modeling of the transport processes considered in pervaporation and vapor permeation processes is presented. Yet, quite a large variance of models, especially for modeling the transport through the active layer, are in use. It is rather difficult to develop an universal model that can be applied for all types of membrane materials. This type of detailed modeling may give a good insight into the transport mechanisms in the membrane process, and a high accuracy simulation of specific separations with specific membranes. However, at an early design stage without availability of experimental data, or for the purpose of general process synthesis or process design, more simple empirical and semi-empirical models are often used. The solution diffusion model is the basis of most of these models. It accounts for the solution-diffusion-desorption steps with a general driving force term and a permeability term, which is derived by combining Henry's law of sorption and Fick's law of diffusion as follows:

$$J_{Pi} = \frac{S_i D_i}{\delta} \cdot (p_{iF} - p_{iP}) = L_i \cdot (p_{iF} - p_{iP}) \quad (4-21)$$

where  $L_i$  is the permeability coefficient which includes  $S_i$  and  $D_i$ , the sorption and diffusion coefficients and  $\delta$ , the thickness of the active layer of the membrane. The driving force is described by  $p_{iF}$  and  $p_{iP}$ , the partial pressure of component  $i$  in the feed and permeate side respectively. The above expression is generalized and is commonly used in different forms that are in general given by:

$$J_{P_i} = L_i \cdot (\text{driving force}) \quad (4-22)$$

The driving force can be considered, however, to be as fugacity, activity, or chemical potential difference. The permeability coefficient will have accordingly different units depending on the driving force expression used. The decision which term should be used is often taken after testing the different types on experimental data [19]. In semi-empirical approaches, the permeability coefficient is correlated to the process parameters by physical founded, and partly by empirical approaches. Rautenbach and Blumenroth [17] correlated permeability to temperature according to an Arrhenius-type relation and to the permeate pressure in an empirical way.

## 4.6 Simulation of the membrane process in Aspen Plus

As stated in chapter 3, the present work is concerned with the overall separation process rather than with a detailed investigation of a certain membrane. For that reason, a computer program is developed for the simulation of the membrane step according to the presented solution diffusion model introduced in section 4.5. Yet, it is extendable to make use of different rigorous thermodynamic and diffusion models described in sections 4.1 to 4.4 according to the membrane used. The advantage of the simplified modeling is the capability of varying the membrane transport properties, expressed by the permeability coefficients, during the simulations. Thus different membranes can be compared for a specific application and the membranes can be then tailored for different processes. The experimental work carried out in parallel to this study [108,109,110] gives guidelines and basis for the transport parameters assumed and optimized in the process simulation.

Within the present work, the modeling and simulation of the separation processes is implemented with the commercial flow-sheeting software ‘Aspen Plus’. This software offers models for various basic unit operations that can be connected in flow-sheets. Operations like membrane processes, which are not included in the standard model library, can be integrated into the process flow-sheet as a ‘user model’ that connects to a user-made ‘Fortran’ or ‘Excel’ subroutine describing the membrane. The software also enables different useful techniques for the analysis of the flow-sheets that includes sensitivity analysis, trial and error possibilities, and optimization routines.

In the following a general model for material balance and membrane area calculations is presented. It is valid for vapor permeation and pervaporation of binary mixtures. However, for pervaporation a modification is implemented to account for the temperature drop and to calculate the optimum number of stages required. The main assumptions in this model are:

1. Negligible pressure-drop along either side of the membrane surface.
2. Plug-flow along the feed side of the membrane.
3. Cross-flow along the permeate side, i.e. unhindered withdrawal of permeate.

The membrane module with the main design variables is shown schematically in Figure 4-6.  $J$  is the molar permeation flux,  $n$  and  $x$  are the molar flow rate and the mole fraction of the faster permeating component. The subscripts  $F$ ,  $P$  and  $R$  refer to the feed, permeate and retentate streams respectively. The superscripts refer to local streams flowing on both sides of a differential element of an area  $dA$ .

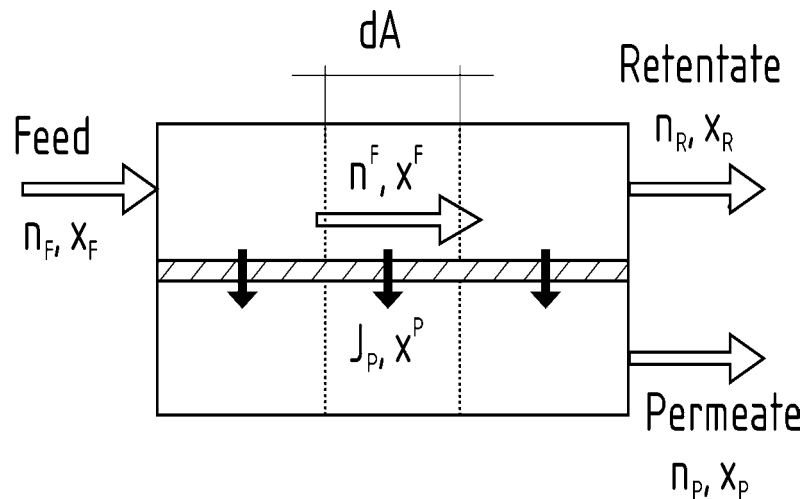


Figure 4-6: Material balance variables and flow assumptions for the membrane module

The overall and component material balance around the whole membrane module result in the following two equations:

$$n_F = n_P + n_R \quad (4-23)$$

and

$$x_F n_F = x_P n_P + x_R n_R \quad (4-24)$$

By considering the differential element shown in the above figure, the local molar flow on the permeate side equals the decrease in the molar flow on the feed side. Thus, the overall material balance around this element can be written as:

$$dn^P = -dn^F \quad (4-25)$$

A component material balance around a differential element of the membrane result in the following equation:

$$-x^P \cdot dn^P = d(x^F \cdot n^F) = x^F \cdot dn^F + n^F \cdot dx^F \quad (4-26)$$

After substituting for  $dn^P$  from equation 4-25 and variables separation, the above equation becomes to:

$$\frac{dn^F}{n^F} = \frac{dx^F}{x^P - x^F} \quad (4-27)$$

The integration of the above equation along the concentration interval from feed to retentate gives the ratio between permeate molar flow rate  $n_P$  and feed molar flow rate  $n_F$ .

$$\theta = \frac{n_P}{n_F} = 1 - \exp\left(\int_{x_F}^{x_R} \frac{dx^F}{x^P - x^F}\right) \quad (4-28)$$

The ratio  $\theta$  is called the module cut rate and introduces an additional mass balance information to the overall and component mass balance equations. Using this three equations the material balance can be solved for a given permeate or retentate specification.

The integral on the right side of equation 4-28 can be solved numerically, if experimental data about  $x^P$  versus  $x^F$  are available for the process conditions considered. The integral is the area under the curve of  $1/(x^P - x^F)$  versus  $x^F$ . However, it is planned in the present study to model the membrane process using general permeability coefficients derived from the solution diffusion model as illustrated in equation 4-21. Thus, the main obstacle will be that the permeate composition is unknown at the beginning and it has to be expressed as a function of the feed composition and the permeability coefficients. Considering cross flow conditions,  $x^P$  can be calculated as the ratio of the molar flux of the permeating component to the total flux as follows:

$$x_i^P = \frac{J_{Pi}}{J_P} \quad (4-29)$$

The flux is expressed as a product of a permeability term,  $L_i$ , and a driving force term (e.g. partial pressure difference) as follows:

$$J_{Pi} = L_i (x_i^F p_F - x_i^P p_P) \quad (4-30)$$

By considering a binary or a quasi-binary mixture with the faster permeating component  $i$  and the rest of the mixture  $j$ , the permeation of the slow component can be expressed by:

$$J_{Pj} = L_j [(1 - x_i^F) \cdot p_F - (1 - x_i^P) \cdot p_P] \quad (4-31)$$

By substituting for  $J_{Pi}$  and  $J_{Pj}$  in equation 4-29 and a quadratic equation of the variable  $x_i^P$  is obtained. After solving,  $x_i^P$  can be expressed as a function in  $x_i^F$  as follows:

$$\begin{aligned} x_i^P \Big|_{1,2} &= \frac{-K_b \pm \sqrt{(K_b)^2 - 4K_a K_c}}{2K_a}, \\ K_a &= p_P (L_j - L_i), \\ K_b &= L_i p_P + L_j (p_F - p_P) + x_i^F p_F (L_i - L_j), \\ K_c &= -L_i x_i^F p_F \end{aligned} \quad (4-32)$$

For given permeability coefficients of the components of the binary or quasi-binary mixtures,  $L_i$  and  $L_j$ , and for given feed and permeate pressures, the above expression can be substituted in equation 4-28 to calculate the module cut rate  $\theta$  in order to solve the material balance.

The starting point for calculating the membrane area required for a given separation is the definition of the total permeation flux,  $J_P$ . It can be expressed as the change in the local flow rate along the feed side with respect to the membrane area as follows:.

$$\frac{dn^F}{dA} = J_P \quad (4-33)$$

It should be noted here that  $J_P$  is the local flux at the differential element  $dA$ , which changes from location to location according to the local feed and permeate side compositions. By rearranging and integrating the above equation the membrane area  $A$  can be calculated as follows:

$$A = - \int_{n_F}^{n_R} \frac{dn^F}{J_P(n^F)} \quad (4-34)$$

The total permeation flux  $J_P$  has to be expressed as a function of the local molar flow at the feed side  $n^F$ . This integral as well as the integral in equation 4-28 can be solved numerically by discretizing the concentration interval in a certain number of elements and calculating for each element the local parameters on both sides of the membrane. The integral is in the case of the above equation the area under the curve of  $1/J_P$  versus  $n^F$ . This integral may be expressed in the terms of the cut rate  $\theta$  by considering its definition as:

$$n^F = (1 - \theta) n_F \quad (4-35)$$

thus:

$$dn^F = -n_F d\theta \quad (4-36)$$

by substituting for  $dn^F$  in equation 4-34 it becomes to:

$$A = n_F \int_o^\theta \frac{d\theta}{J_p(\theta)} \quad (4-37)$$

There are two common ways for expressing the selectivity of the membrane for binary separation. The first way is to express it by the selectivity coefficient which is the ratio of the component permeabilities as:

$$\alpha_L = \frac{L_A}{L_B} \quad (4-38)$$

where it is conventional to consider A as the faster permeating component. In a quasi-binary system like the separation of water from a mixture of solvents, the rest of the components are considered as B. It is assumed thereby that they have the same small permeability coefficient.

The second way for expressing the selectivity is similar to the common way in the thermal separations by the compositions of the separated products.

$$\alpha_x = \frac{x_P/(1-x_P)}{x_R/(1-x_R)} \quad (4-39)$$

where x refers to the mole fraction of the faster permeating component in both the permeate and retentate streams.

With the equations presented above, the modeling of pervaporation and vapor permeation processes can be carried out in a simple and straight forward way. They can rely on

experimental data of a certain membrane or make use of permeability coefficients, yet they can be extended for rigorous calculations. This way of modeling is very useful for the purpose of process design and process evaluation, especially when the membrane unit is a part of a complex plant or if it is combined to another thermal separation unit in a so called ‘hybrid’ separation process. For the evaluation of such processes such modeling techniques are preferred as they are less time consuming than the rigorous ways and more accurate than the short cut modeling techniques.

However, at the early design stage the necessary information (experimental data) may not be available for the permeability coefficients to be determined with a significant accuracy. Petersen and Lien have presented a simple algebraic model [63], with which the material balance around the membrane can be solved and the required surface area for a certain separation can be calculated. For this model only an averaged separation factor and an averaged flux of the membrane for the investigated concentration interval are required. This model was first published in the work of Naylor and Backer [111], who derived a calculating approach for the gaseous-diffusion-stage like that of McCabe and Thiele for distillation. The calculation procedure can be summarized in the following algebraic equations:

$$\theta = \frac{n_p}{n_f} = 1 - \exp \left[ \frac{I}{\bar{\alpha}_x - I} \cdot \left( \ln \left( \frac{x_R}{x_F} \right) - \bar{\alpha}_x \cdot \ln \left( \frac{I - x_R}{I - x_F} \right) \right) \right] \quad (4-40)$$

and

$$A = \frac{n_f \theta}{\bar{J}_p} \quad (4-41)$$

where  $\bar{J}_p$  and  $\bar{\alpha}_x$  are the logarithmic mean values of the total flux and the separation factor of the membrane at the feed and retentate compositions.

In addition to the earlier stated general assumptions this model is based on the assumption that a linear relation exists between  $J_p$  and  $x^F$  and between  $\ln \alpha_x$  and  $x^F$ . This assumption is valid only if the fugacity or the partial pressure of the permeate side is of a negligible value when compared to that of the feed. The flux can then be considered to be proportional to the concentration or partial pressure of the faster permeating component in the feed side. This is a reasonable assumption for the dehydration examples if the required purity of the retentate is not very high, so that there is still a considerable amount of water at the feed side, which

keeps the driving force high, i.e still  $p_{iF} > p_{iP}$ . This is realized for example by the azeotrope separation of aqueous isopropanol, where the required separation is concentrating isopropanol from about 85% to 89%. An example of requiring a high product purity is the dehydration of ethanol, where it is required to concentrate the sub-azeotropic ethanol from <95.5% up to 99.5% or higher. For this type and for similar dehydration problems the local flux is not a linear function of the local feed side composition. When these nonlinearities appear, the above algebraic model will not provide sufficient accuracy, and the design calculations has to be better done by the differential model presented before.

## 4.7 Calculation of pervaporation stages

In pervaporation processes the permeate evaporates out from the liquid feed stream. The only source for the latent heat of vaporization is the sensible heat of the liquid. This heat is usually supplied to the feed stream by intermediate heat exchangers as shown in Figure 2-2(a). In the simulation of pervaporation processes, the material balance equations presented in section 4.6 for a membrane differential element are extended by the energy balance equation:

$$n^F h^F = n^R h^R + n^P h^P \quad (4-42)$$

where  $h$  is the average molar enthalpy of the stream at the considered differential element, and the superscripts  $F$ ,  $R$  and  $P$  refer to the local feed, retentate and permeate respectively. Thus the temperature drop can be calculated for each element from the enthalpy of its retentate. The calculation of the pervaporation stages is realized in Aspen Plus by a looping procedure. The loop contains a membrane module and a heater. The material and energy balance calculations take place in the membrane ‘user model’. In the heater, the temperature of the retentate is raised to a defined feed temperature and it is recycled to the same membrane module. The retentate composition of each run is determined either by a predefined constant temperature drop for each stage or by a predefined constant stage area. Both options have been practiced commercially [44]. An additional subroutine is responsible for saving the intermediate results of the stages and for ending the calculations when the required retentate purity has been reached. The number of runs corresponds to the number of pervaporation stages.

The total number of stages and size of each of the stages, and tolerated temperature drop per stage are matters of optimization for the respective application and plant. Increasing the

number of stages would result in savings in the membrane area as the temperature drop per stage is smaller and the operation takes place at a higher averaged temperature. On the other hand, too many stages and heat exchangers would be also expensive and cause hydraulic pressure losses.

## 5 Optimizing membrane dehydration processes

The state of the art of solvent dehydration processes is introduced in section 2.5. In many cases the membrane unit is coupled to a distillation column as shown in section 2.5.3. The permeate stream which supposed to have a certain organics content is usually recycled to the distillation column in order to decrease the losses. Another feature of the solvent dehydration processes is that the required product purity is usually very high, i.e. a nearly complete dehydration is required in most applications. This feature is always combined with difficulty, as the driving force for the permeation of water vanishes near the required water-free composition. This is always indicated by an exponential increase of the required membrane area above a certain purity. Increasing the driving force by varying the process conditions is expensive as it means a lower condensation temperature that can produce a lower vacuum at the permeate side (details of the technical configuration of pervaporation and vapor permeation units are shown in section 2.2).

In the following sections the pervaporation and vapor permeation processes are optimized by considering the above special features of solvent dehydration. The process parameters like temperatures and pressures as well as membrane separation properties like permeability and selectivity are considered during this optimization. The results of these theoretical studies could help in pre-tailoring the membrane structure and hence its separation properties for each specific process.

### 5.1 Effect of the membrane selectivity

In recent years the membrane-making research is concerned with improving the membrane materials to achieve higher fluxes, proper selectivities and stable structures. The main challenge in the field of gas separation is to increase the membrane selectivities, especially for air fractionation or for conditioning of natural gases. In contrast, pervaporation membranes especially those for dehydration have shown much higher selectivities up to several thousands for both organic and zeolitic membranes. In this section the concept of ‘optimum selectivity’

and the advantages of low-selectivity membranes for the high purity separation are highlighted and analyzed.

### Illustrative application

Most of the dehydration tasks of organics are high purity separations, i.e. a nearly complete removal of water is always required. The feed conditions may vary from case to case according to application. The ethanol dehydration has become a classical application for testing and evaluating the membrane dehydration performance, because it is until today the largest customer for dehydration membranes. An azeotrope exists in the ethanol water system at nearly 95.6 mass% ethanol, thus a typical feed to the membrane originates from a prior distillation step and can be received in the vapor phase as a feed to the membrane step. The selected separation presented in Figure 5-1 is a typical dehydration task, in which 1000 kg/h of an aqueous solution of 93% by wt. ethanol should be concentrated up to 99.9%.

For the first calculations a poly-vinylalcohol (PVA) membrane is selected. Its water permeability is comparable to that of a Sulzer ChemTech (formerly GFT) standard dehydration membrane [15,72], or to the modified PVA membrane of GKSS [108,109,110]. Constant permeation coefficients for water and ethanol are assumed along the investigated concentration interval. This could be accepted for narrow concentration intervals, especially in this early design phase, where no extensive experimental data are available for the membranes. More exact assumptions could be considered in a later phase of design and optimization as a second iteration after the suggested membranes have been developed and tested. First, a selectivity of 2000 is considered. The feed pressure is 1 bar and the permeate pressure is 20 mbar.

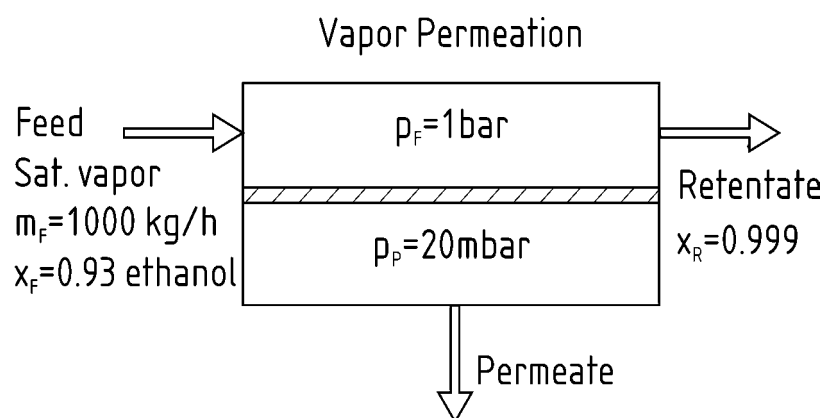


Figure 5-1: A typical dehydration task which is studied in the following sections

The driving force for water transport represented as partial pressure difference between feed and permeate is illustrated in Figure 5-2 as function in the retentate composition. As expected, above a certain ethanol purity, here 99 wt%, the driving force vanishes as the water concentration on the feed side becomes very low. As a result, the required membrane area increases exponentially in this region as shown in the same figure. This area is calculated using the differential model presented in section 4.6.

To increase the driving force for fixed feed conditions, either the permeate pressure or the water concentration in the permeate should be lowered. Decreasing the permeate pressure is accompanied by cost increase, as it would be required to lower the condensation temperature to unfeasible levels. In addition, too low condensation temperatures could result in ice formation on the cooling surfaces of the condenser when the freezing point of the permeate mixture is reached.

The decrease of the water concentration in the permeate stream could be realized by two ways. The permeate can be diluted either by an inert (sweeping) gas or vapor or by lowering the permeate selectivity to allow for an increased permeation of ethanol. The last way may be more useful than using sweeping gases, as the reduced selectivity is, as a general rule, accompanied by an increased permeability. This plays an additional role in reducing the required membrane area.

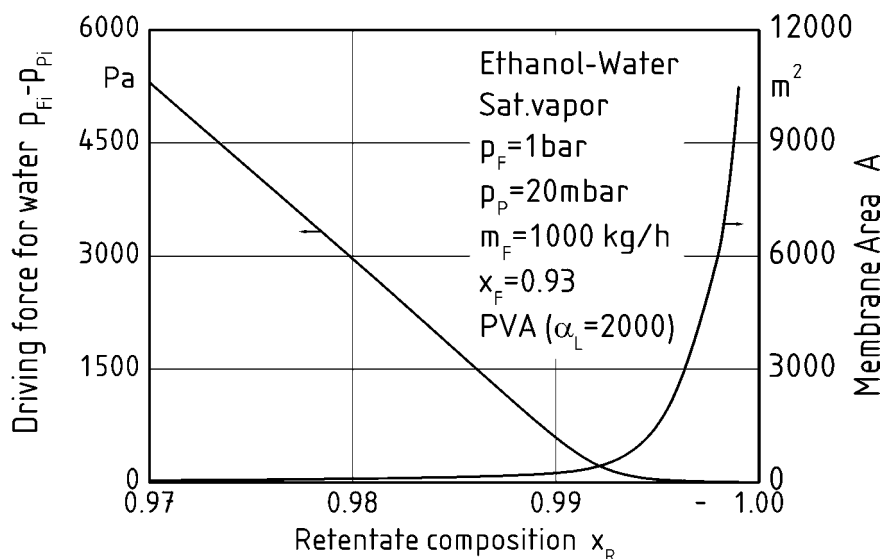
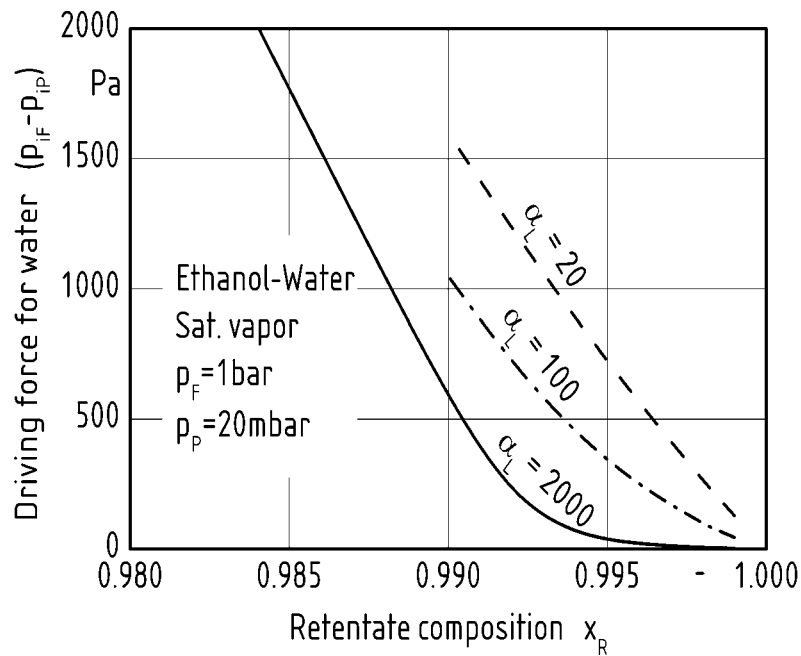


Figure 5-2: Driving force and membrane area as functions in retentate composition

However, it is interesting at this stage to analyze the effect of reducing the membrane selectivity without considering the expected associated increase in permeability. To realize this during the simulation, the permeation coefficient for water is kept constant while reducing the selectivity by increasing the permeation coefficient for ethanol. The pressure on the permeate side is also held constant to limit the investigation to the effect of the selectivity. The increase in the driving force by reducing the selectivity to 100 or to 20 by the above described manner is shown in Figure 5-3 for the region above 99 wt% ethanol.



*Figure 5-3: Partial pressure difference as a function of the retentate composition for different selectivities*

As a result, the membrane area required for separation is strongly reduced as shown in Figure 5-4. Thus an enormous decrease in the capital cost of the membrane unit is expected. However, the ethanol concentration in the permeate stream will be higher than that in the case of high selectivity as shown in Figure 5-5. If the permeate stream is recycled to a distillation column in a hybrid process configuration, no ethanol will be lost. The only attention that should be taken is that it should be recycled to the right position in the column that is equivalent to its composition.

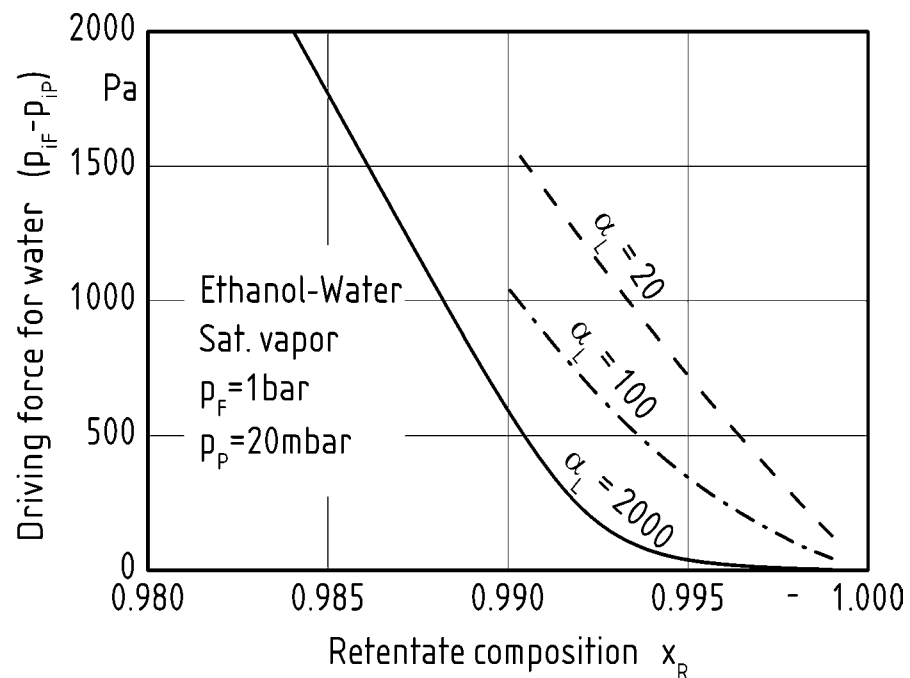


Figure 5-4: Membrane area as function of the retentate composition for different selectivities

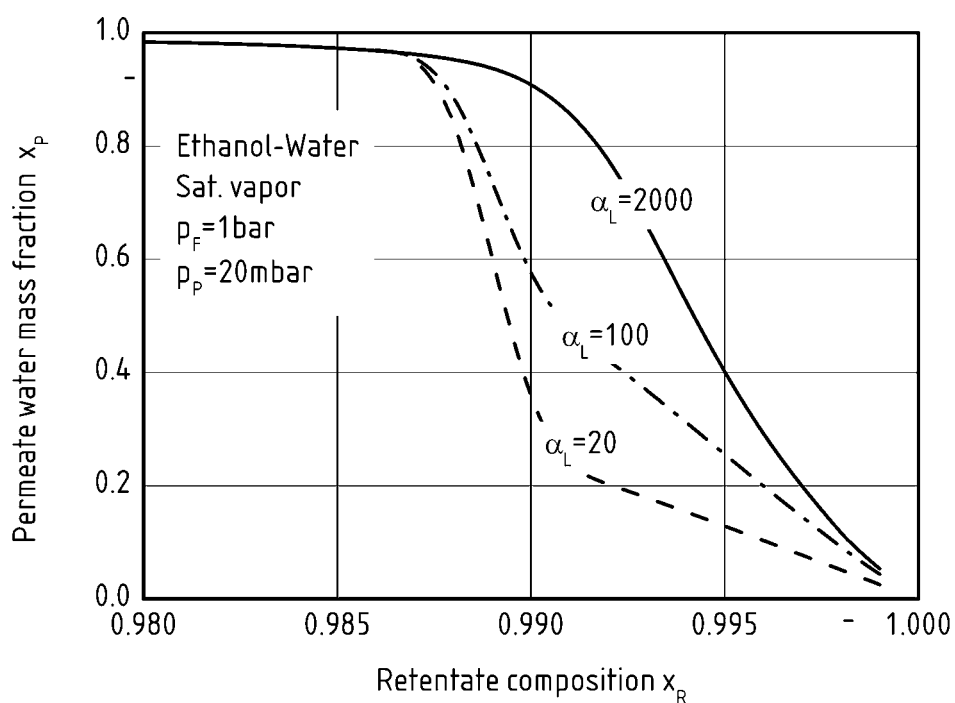


Figure 5-5: Local permeate composition as function of the retentate composition for different selectivities

The results of material balance calculations for the hybrid process are shown in Figure 5-6. The calculations are based on a column feed of 7 wt% ethanol, which is a typical composition of the product beer of a fermentation unit [112]. These results show that the mass flow of the recycled permeate stream is always lower than 1% of the column feed, so its recycle will not result in hydrodynamic drawbacks to the column.

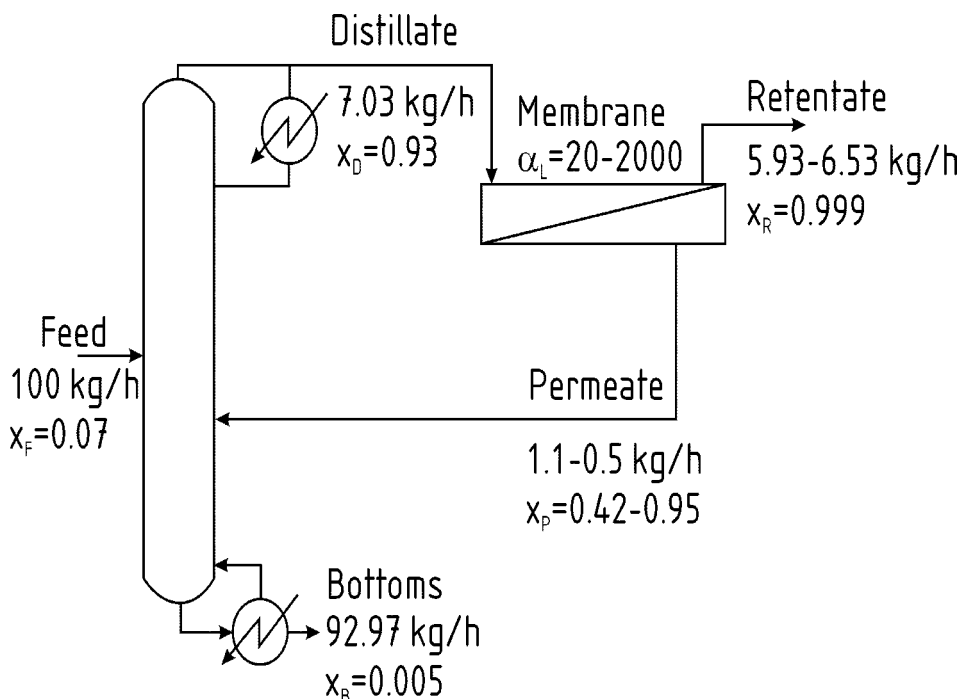


Figure 5-6: Mass balance for a hybrid process for ethanol dehydration

The increased permeability for ethanol will certainly result in an increase of the mass flow of the permeate stream as shown in Figure 5-7. This increase in flow rate will elevate the cost of the condensation and vacuum system that is used for the removal of the permeate. Thus, lowering the membrane selectivity has two contradicting effects on the total cost of the unit. Nevertheless, one can expect cost savings in the case of using low-selectivity membranes rather than by using high-selectivity ones for this high purity application. For the presented case study, the enormous savings in the membrane area would not be abrogated by the costs resulting from the increase in permeate flow. However, at this point it becomes clear that a certain optimum membrane selectivity exists for each specific application as shown in Figure 5-8. To calculate this selectivity, the whole membrane process including all the periphery equipment for condensation and vacuum production has to be simulated, and the annual total cost should be estimated as shown in the following section.

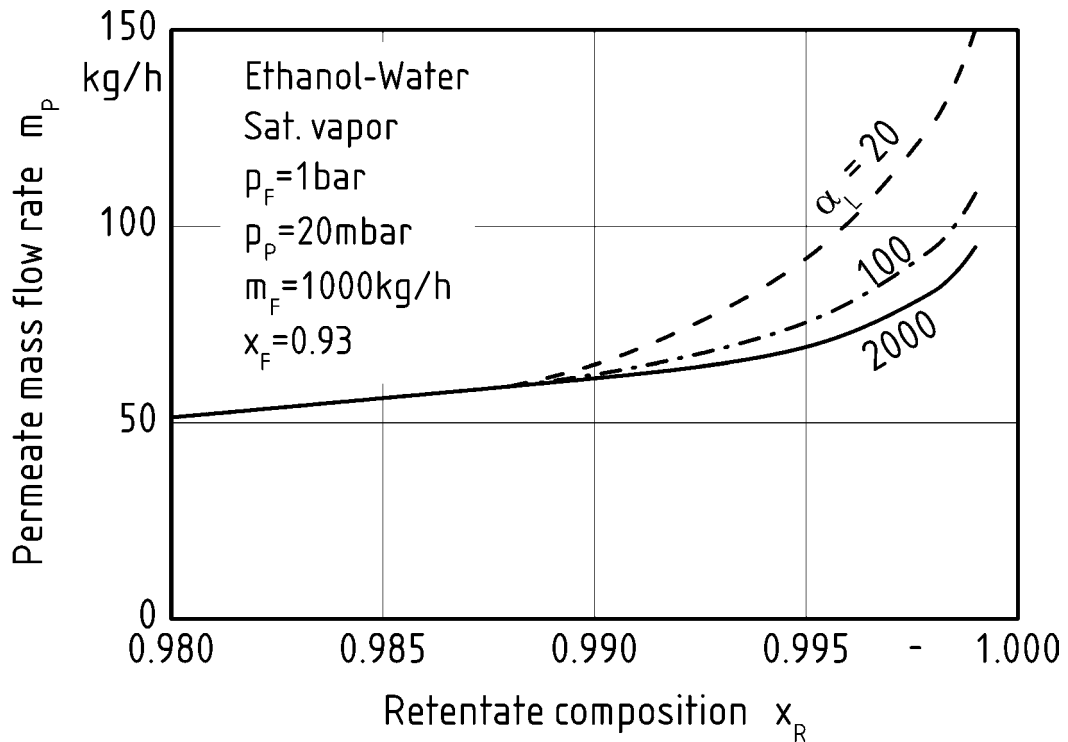


Figure 5-7: Permeate mass flow as a function of retentate composition for different selectivities

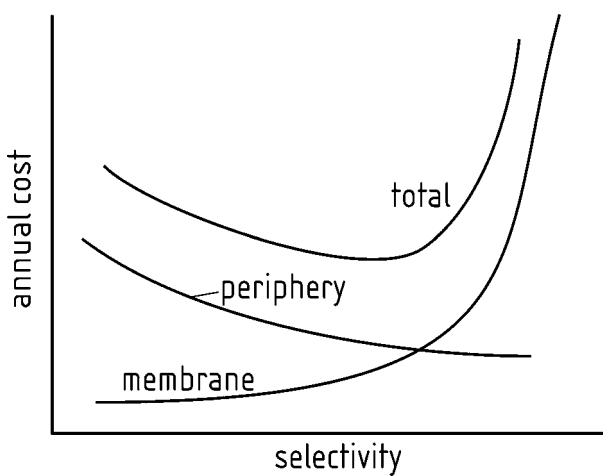


Figure 5-8: Effect of selectivity on annual cost in high purity applications

## 5.2 Optimization calculations

In this section, a methodology for the optimization of pervaporation and vapor permeation processes is introduced. Different process parameters as well as the membrane selectivity can be optimized for different separation processes. The optimization method is implemented exemplary on the application introduced in section 5.1.

For carrying out a detailed optimization the whole membrane system has to be pre-designed, the major equipment have to be sized, and the annual cost should be minimized. For this purpose a simulation program is developed with the process simulation software “ASPEN Plus” (Aspen Technology Inc., Ten Canal Park, Cambridge, MA 02141-2201 USA). The main flow-sheet and the main calculation loops are shown in Figure 5-9. The differential model presented in section 4.6 is implemented in a FORTRAN subroutine that is coupled to the main program as a ‘user model’. After material balance, energy balance and area calculations, the membrane and module costs are estimated.

A leakage air stream is inevitable in any vacuum system; however, the amount of leakage is important for subsequent calculations of the condenser and the vacuum pump. An air stream of assumed volumetric flowrate is mixed with the permeate stream and sent to the condenser. To decrease the load to the vacuum pump, the permeate mixture is condensed and subcooled. Only a very little equilibrium amount will remain with the leakage air in the gaseous phase. The condensation temperature is varied within an iteration loop. The results of creating this simulation loop are the determination of heat transfer area and condenser volume, the design specifications of the refrigeration unit and the vacuum pump, and the total annual cost of this condensation and vacuum system. The result using the inner loop is the determination of optimum subcooling temperature, which gives the minimum total cost of this part of the system. The effect of the condensation temperature on the cost of the condensation and vacuum system is shown schematically in Figure 5-10. While the vacuum costs decrease nearly linearly with decreasing temperature due to decreased amount of equilibrium vapor, the refrigeration costs increase exponentially under a certain temperature range. To find the optimum condensation temperature, it is raised gradually starting from a value far below the dew point of the permeate mixture and the optimum is reached when the slope of the curve of the total cost changes from negative to positive.

From the calculated condenser volume, the flow rate of the leakage air stream is corrected and the outer loop of the leakage air is run till it converges to a constant air stream. The global variables that could be manipulated through the whole program are the membrane selectivity (i.e. the ethanol permeation coefficient) and the permeate pressure. The water permeation coefficient is held equal to that of the most selective membrane.

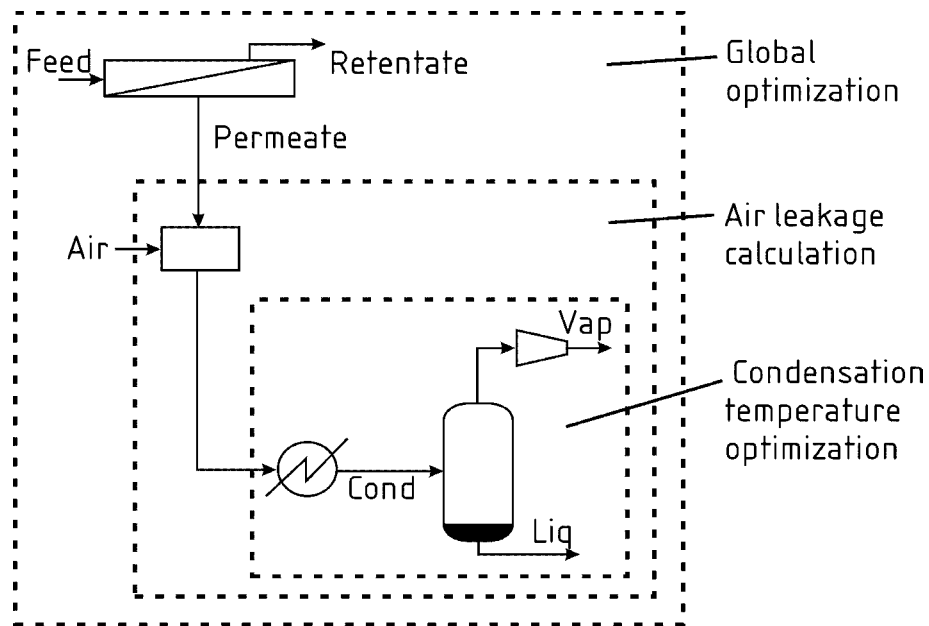


Figure 5-9: Main loops of the optimization program

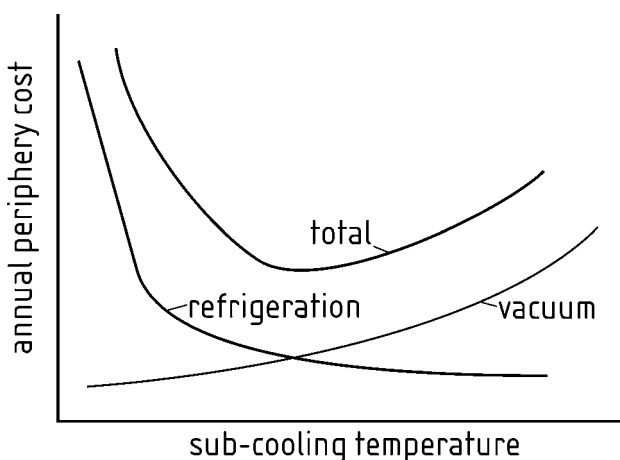
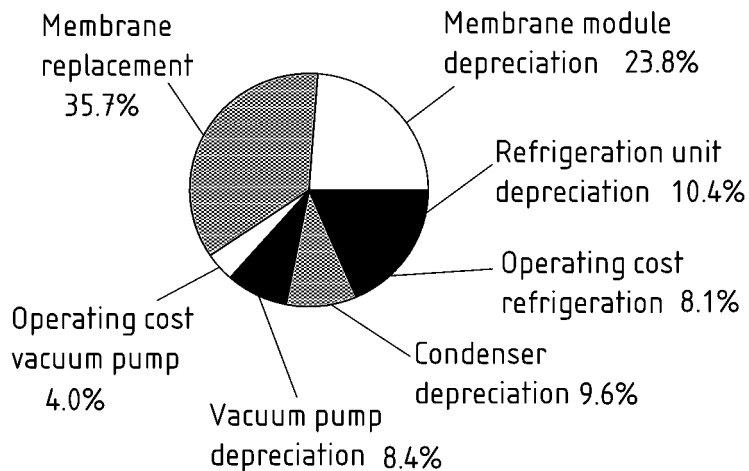


Figure 5-10: Optimum condensation temperature

A typical structure of the total annual cost is presented in Figure 5-11. The membrane replacement costs held the highest share of the total annual cost because of the increased specific area of the membrane as the required purity is exceedingly high. Throughout these cost calculations the membrane material is depreciated along three years, the membrane modules along 6 years and all other parts of the system along ten years. The main operating costs of the refrigeration system and of the vacuum pump are electric power costs. The functions for the fixed and operating costs are developed on the basis of offers from different manufacturers and from data from large scale chemical companies. These functions can be found in detail in Appendix A at the end of the thesis.



*Figure 5-11: Typical cost structure of the membrane unit*

$$m_F = 1000 \text{ kg/h}, x_F = 0.93, x_R = 0.999, p_F = 1 \text{ bar}, p_P = 8 \text{ mbar}, \alpha_L = 40$$

The total cost as the sum of mentioned costs in Figure 5-11 is illustrated in Figure 5-12 as function of the manipulated variables, the selectivity and permeate pressure. Some of the curves are broken, otherwise the temperature of the heat transfer surface in the condenser would be lower than the freezing point of the permeate mixture. This could result in the formation of ice crystals on the heat transfer surface, which could block the operation. The curves show optimum selectivities between 20 and 40 and optimum operating pressures between 4 and 6 mbar. These low selectivities may be a surprising result, however this result is specific for this separation problem where a very high purity is required.

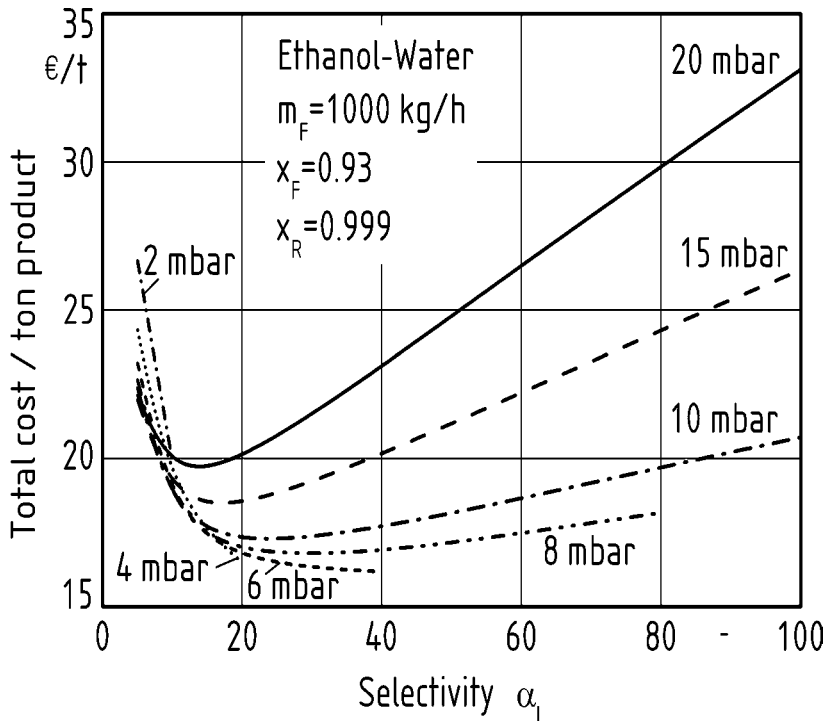


Figure 5-12: Total cost as function of membrane selectivity and permeate pressure

The same methodology was used to compare three different process schemes, which are shown in Table (5-1). The first is a conventional scheme with the membrane modules fitted with one type of membrane and equipped with a condensation and vacuum system. The second utilizes two different types of membranes in series integrated in the same system. Thus the membrane separation properties can be optimized for two concentration regions. In the third scheme the two membranes have different condensation and vacuum systems. The three schemes are studied for two different separation tasks, one is the dehydration from 93% to 99.9%, and the other is from 83% to 99.9%. The composition between the two membranes is assumed to be 99% for the last two cases. The results are shown in Table (5-1). A heuristic rule can be derived, that a higher selective membrane is needed at high concentrations of the faster permeating component, and a lower selectivity is favored for the regions of lower concentration. Based on the earlier stated assumption of constant water permeability, the use of two different membranes in series will bring savings up to 6% of the total annual cost for the first separation problem, for the second up to 14% where the concentration interval is larger.

Table (5-1): Three process schemes compared for two dehydration tasks

		1 <sup>st</sup> mem.	2 <sup>nd</sup> mem.	1 <sup>st</sup> mem.	2 <sup>nd</sup> mem.
93%-99.9%	P <sub>p</sub>	6 mbar	6 mbar	10 mbar	4 mbar
	α <sub>L</sub>	30	100	20	40
	rel. cost.	100	94.3		96.2
83%-99.9%	P <sub>p</sub>	8 mbar	8 mbar	10 mbar	4 mbar
	α <sub>L</sub>	40	200	20	1000
	rel. cost.	100	89.7		85.9

The general assumptions of negligible pressure drop, constant temperature, plug flow along the feed side, and cross flow along the permeate side are discussed in detail in the paper of Pettersen and Lien [63] and of Naylor and Backer [111]. The assumption that the less selective membranes have the same water permeation coefficient as the most selective membrane is a very conservative assumption concerning the calculation of the membrane area and the membrane cost. Usually the less selective membranes allow higher fluxes [72]. Therefore the cost savings of the less selective membranes demonstrated in the previous separation example can be considered to be calculated on the very safe side. Much more cost savings are expected when considering the increase of the water flux as a result of a decreased selectivity.

For separations, where the water concentration in the retentate is relatively high, as by breaking the azeotrope of the iso-propanol water system, the low selectivity membranes would not give any cost savings if the calculations are carried out on the basis of the previously mentioned assumption of constant flux. However, if the flux increase by lowering the selectivity would be considered, the low selectivity would then offer cost savings.

The solid curve of Figure 5-13 may present schematically the real behavior of the flux against selectivity by considering different membranes with different selectivity for the same separation application. During the previous analysis the horizontal dotted line was assumed as the flux was held constant by lowering the selectivity. As a first approximation one could assume an inverse proportionality between flux and selectivity as shown by the straight dashed line of the same figure. That means that the optimization calculations could be carried out for membranes of the same separation index defined by

$$SI = J \cdot \alpha \quad (5-43)$$

This is analogous to the concept of the pervaporation separation index (PSI) introduced by Huang [113]. (Another common separation index is the Rony's extent of separation [114] which was refined by Sirkar [115] for single entry barrier separation processes. This index has been largely used for the characterization of gas separation stages [116, 117] and pervaporation [118]).

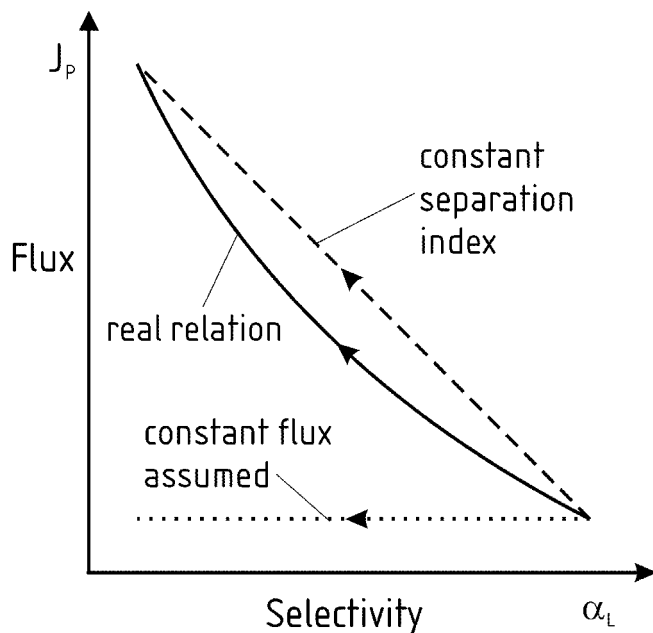


*Figure 5-13: Transport properties shown schematically for one membrane type*

The most exact relation between the flux and the selectivity of the considered membranes should be derived experimentally. Therefore, a number of different membranes with different separation properties must be developed for the same application. These membranes must be tested experimentally for one to get an idea about flux variation with respect to selectivity for this kind of membranes. Moreover, relationships between the permeation coefficient and the

process parameters should be determined for each membrane. This determination requires that a targeted set of experiments be completed to increase the accuracy of the optimization procedure.

Nevertheless, though the optimization method presented in the present study may not give the most accurate quantitative result, it gives a qualitative conclusion about using membranes of low selectivity in separations that require high retentate purity. However, increased reliability of rigorous or molecular modeling would save a great deal of experimental work that must be done when optimizing on the empirical basis.

Although the use of low-selectivity membranes may offer cost savings, the presented calculations were completed based on the assumption that the presence of the membrane step was within a hybrid process. That is, that the purity of the permeate stream was not assumed to be a constraint throughout the calculations. Permeate streams containing considerable amounts of the slow permeating component would be recycled to a distillation step without disturbing the distillation operation due its relatively small quantities. Increased amounts of the organic components in the permeate stream would decrease the mass flow of the product retentate. However, the cost calculations are based on a unit weight of the retentate.

For stand-alone membrane processes (i.e., those not coupled to a distillation column), a two-stage membrane process is suggested for membrane area savings. A scheme of such a process is demonstrated in Figure 5-14 for ethanol dehydration. However, it is applicable for any dehydration of organic solvents. The first stage is the dehydration stage with a low selectivity membrane. Its permeate stream of increased organics content is concentrated by a small membrane unit up to the concentration of the first feed. The second unit has a high selectivity membrane to produce high purity waste water as permeate. This unit is relatively small because its retentate purity is lower than that of the first one so that the water content of the retentate side is sufficient to create a reasonable driving force at the end of the separation. Moreover, its feed stream is much smaller than the main feed. Simulation and optimization of this two stage process result in an optimum selectivity for the first membrane between 40 and 50 with an optimum permeate pressure of 8 mbar, and a selectivity of 1000 for the second permeate purification membrane with an optimum permeate pressure of 110 mbar. The cost of the second stage comprises 10.5% of the total cost of the process. One should remark here that the membrane of the second stage should be a water stable membrane as its feed contains from 40 up to 60 wt% water.

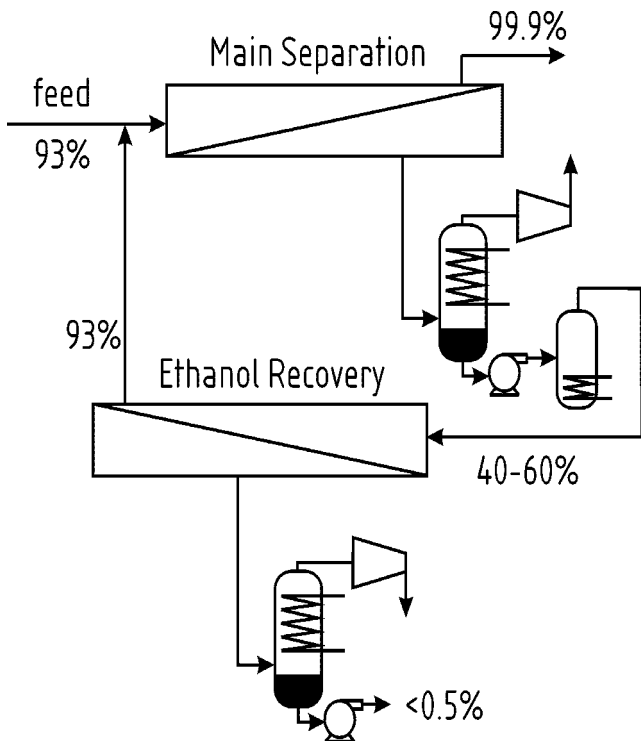


Figure 5-14: Two stage process for high product purity

A distillation unit could also be used for the solvent recovery as shown in Figure 5-15. For large scale processes the distillation will be the convenient one supposed that there will be no azeotropes or closely boiling regions in the concentration interval to be dealt with.

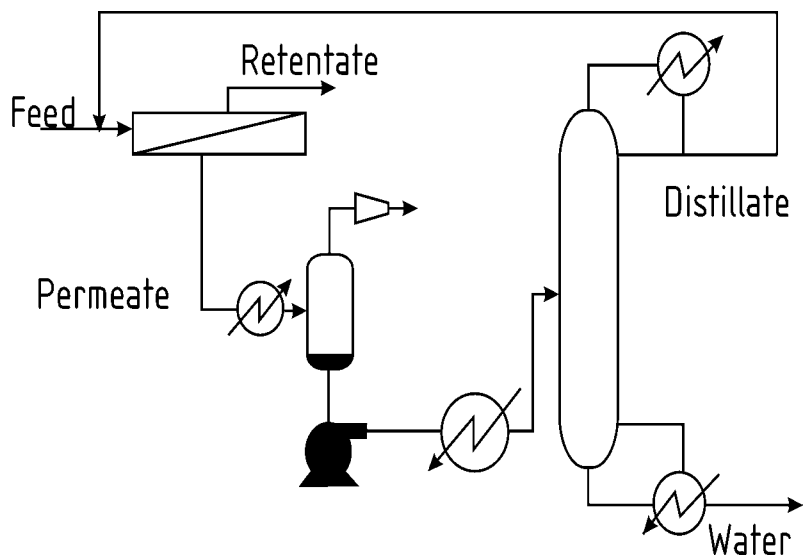


Figure 5-15: Two stage vapor permeation-distillation

### 5.3 Heat integration in multistage-separations

In the two stage separation processes presented in the previous section, several streams have either to be cooled or heated. This has been presented as to be carried out by external heating or cooling sources. Thus, a refrigeration unit is needed for condensing the permeate and steam or another heating source is necessary for reheating the condensed permeate and for supplying the heat necessary for the reboiler of the distillation column. However, a great deal of energy could be saved through proper heat exchange between the cold and hot streams.

The pinch technology is used to investigate the options for proper heat exchange within this process. It is based on drawing combined enthalpy-temperature curves of the process streams to be cooled and heated. According to these plots, the feasible heat exchanger networks can be determined. With the help of rules of thumb for heat integration [119] the proper scheme can be chosen and additional process modifications could be suggested. Applying this method on the process presented in Figure 5-15 it is found that operating both separation stages under different pressures would be a good option for heat integration. Thereby, the first stage should be the high pressure and the second should be the low pressure (atmospheric) separation stage. This would allow the hot retentate stream of the first stage to be used as a heating medium for the second stage operating under a lower temperature and pressure.

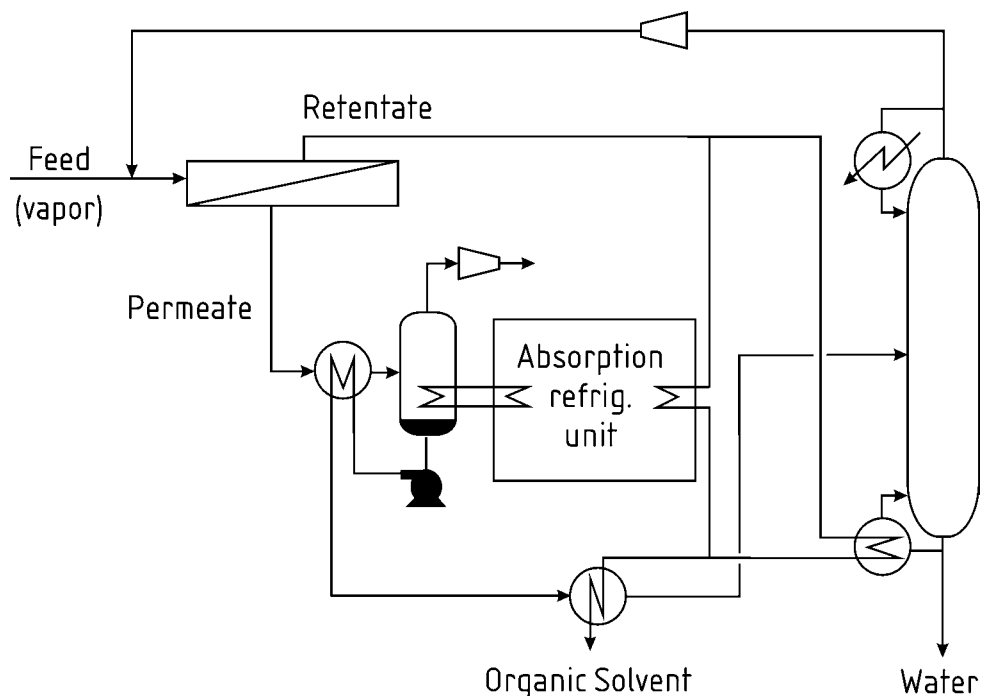


Figure 5-16: Options for heat integration for a two stage vapor permeation-distillation

The results of the heat integration for a vapor permeation unit are presented in Figure 5-16. Based on the application presented in sections 5.1 and 5.2, around 50% of the excess enthalpy of the vaporous retentate stream is used for running an ammonia absorption refrigeration unit that supplies the required refrigeration for cooling and condensing the permeate stream. Another 25% of the heat content is used for running the reboiler of the distillation column and the rest can be used elsewhere for heating purposes. A mass and energy balance diagram made for this study is presented in Appendix B

If the vaporous feed to the membrane originates from an atmospheric distillation column, it is not recommended to compress it to higher pressures due to the high cost. For stand-alone membrane units, however, the pressure of the feed can be raised to the maximum allowable value that the membrane can withstand. For polymeric membranes this value is today up to 5 bar [108]. Moreover, operating the two stage process by two different pressures is also in favor of the separation efficiency, as the high pressure at the membrane step will reduce the required membrane area, and distillation under atmospheric pressure has also many technical and economic advantages.

The heat integration calculations suggest the heat exchange between the condensed permeate stream and the vaporous permeate feed to the condenser. However, it would not be a real advantage due to pressure losses in this exchanger that would affect the vacuum level on the permeate side of the membrane. Moreover, the amount of heat exchanged in this exchanger is too small compared to the large amount of latent heat that has to be removed in the condenser itself.

## 6 Steam jet ejectors within hybrid processes

Hybrid processes of distillation and membrane separation are presented and discussed in section 2.5.3. They are considered as promising alternatives to azeotropic and extractive distillation. The driving force for the mass transfer across the membrane is realized generally by lowering the partial pressure of the permeating components on the permeate side. The most common technique is condensing the permeate stream prior a vacuum pump. The vacuum pump removes the non-condensed compounds and the leakage air. In most cases the condensed permeate stream has to be recycled to the distillation column so it has to be reheated as shown in Figure 6-1.

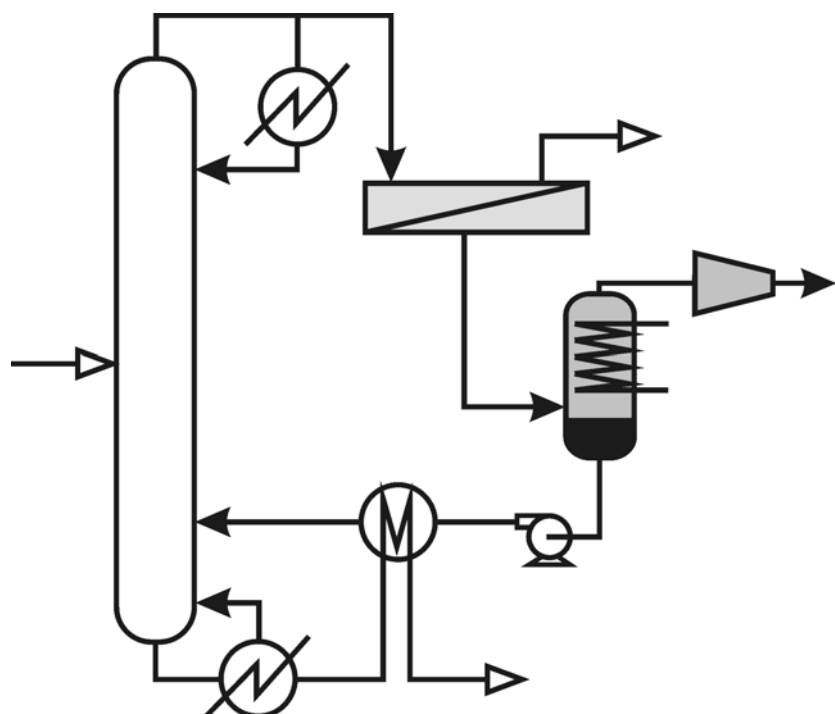


*Figure 6-1: Condensation-vacuum technology for the hybrid process*

As discussed in chapter 5, the condensation and refrigeration are characterized with high costs, and with some technical limitations. Within the hybrid process, the reheating after condensation highlights the high level of energy consumption combined within this technique and motivates the search for other process alternatives that can keep the permeate stream in its vaporous phase at this stage.

In this section the use of steam jet ejectors as a process integration alternative for hybrid dehydration processes is introduced and investigated. In this novel configuration the resulting low pressure steam from the jet ejector is used as an energy source to run the distillation column. Process simulations and economic evaluations are carried out for this process. Favorable implementation regions are defined, and the advantages and limitations of this modification are discussed.

## 6.1 Suggested process scheme

The suggested flow diagram is exemplary illustrated for the dehydration of isopropanol. A steam jet ejector is used to produce the vacuum pressure on the permeate side of the membrane, as shown in Figure 6-2. The vacuum is developed by accelerating a high pressure (motive) steam inside a converging diverging nozzle. As a result, the permeate vapors are drawn from the membrane module and mixed with the motive stream inside the ejector. The discharge vapor stream from the ejector can be used then for direct heating in the distillation column. The selectivity of the membrane is sufficient to produce a permeate stream of a composition greater than 98% water [120]. Such high selectivities are not uncommon by dehydrating organic solutions, especially when the water content in the retentate is not very low. The permeate stream is further diluted with the high pressure steam. The final composition of the produced stream will depend on the amount of the used high pressure steam. The permeate stream stays thereby in the vapor phase and its enthalpy potential is maintained. The produced low pressure steam can be also used for other heating tasks in the chemical plant.

The process looks simple when compared to the conventional condensation technique. The condenser, the reheat and the vacuum pump are all replaced by a single piece of equipment of low capital cost. The refrigeration and cooling are replaced by the use of steam. However, attention should be taken to the level of steam requirements for the ejector, as the mixing processes are generally characterized by low thermal efficiency. The steam consumption has to be carefully calculated for different practical examples in order to achieve a fair evaluation. The additional cost of biological treatment of the excess waste water has also to be considered.

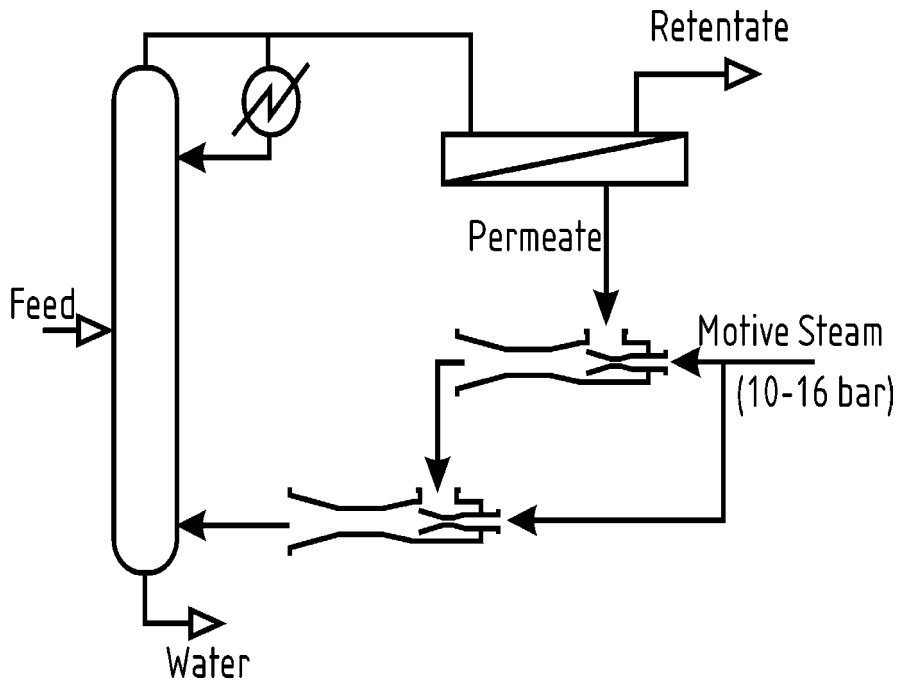


*Figure 6-2: Using steam jet ejectors within the hybrid process*

## 6.2 Operating principle of jet ejectors

Ejectors are momentum-exchange pumps. High pressure motive steam expands across a converging diverging nozzle and is thus accelerated to a supersonic velocity. The high velocity motive steam entrains the process gas or vapor aspirated through the suction port, and compression of the mixture is accomplished across a diffuser by conversion of velocity head to pressure head. The mixture entering the diffuser is still supersonic if the stage is designed for a compression ratio (discharge/suction pressure) greater than 2:1. Within the diffuser the mixture experiences a normal compression shock, after which its velocity is lower than the sonic velocity. At the diffuser exit section, most of the remaining velocity energy is converted into an additional pressure rise. At the discharge the vapor mixture is generally slightly superheated. Typical pressure and velocity profiles inside the jet ejector are shown in Figure 6-3.

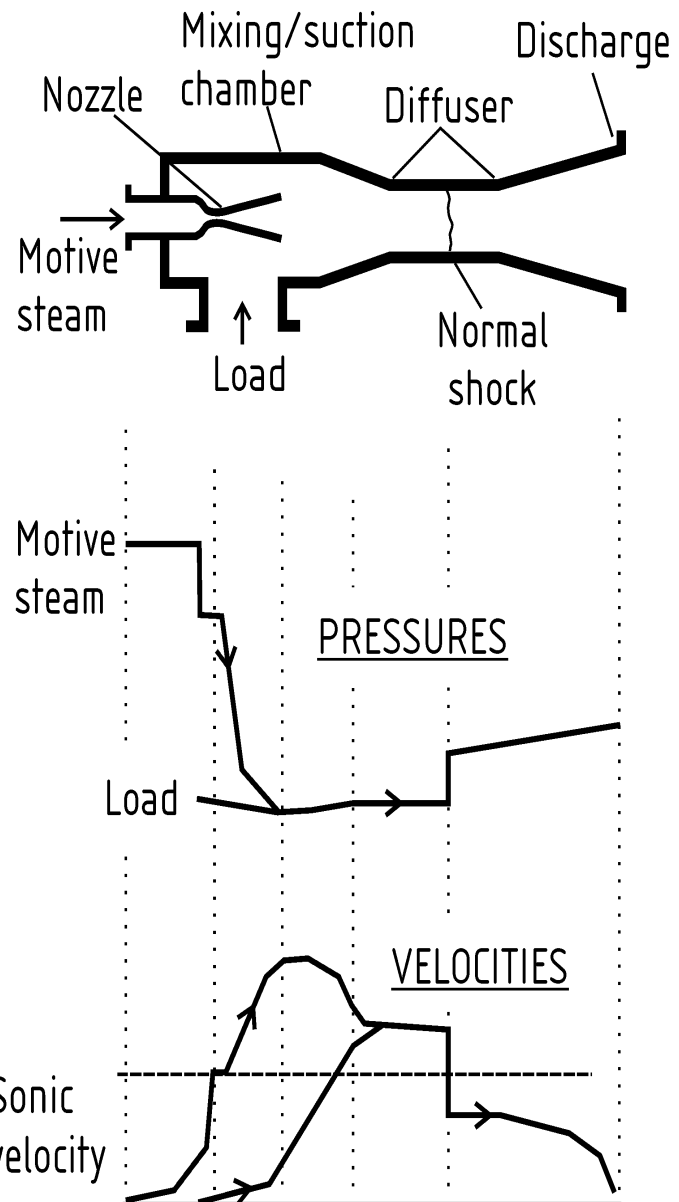


*Figure 6-3: Operating principle of the steam jet ejector*

### 6.3 Motive steam requirements

The motive steam requirements for an ejector stage can be calculated directly by application of the basic laws of thermodynamics and fluid mechanics. Ejector operation approaches an isentropic process. Overall ejector efficiency can be expressed as a function of the entrainment or mixing efficiency and the ratio of energy output and energy input. Fairly

sophisticated models [121,122] have been developed by using an integral-equation approach to describe ejector mass and momentum transfer. However, the most recommended calculation procedure [123] is based on the basic empirical procedure of the HEI [124]. In this procedure the dry air equivalent of the vapors entering the suction of an ejector stage is calculated. It depends on the composition of the load vapor stream and the molecular weights of its components. The next step is estimating the motive steam required to compress that air load from suction pressure to the discharge pressure. Motive steam is estimated by determining how much a 10 bar steam would be required. The amount of steam is empirically corrected for the actual motive steam pressure. Other corrections consider the temperature of the load stream and the stability at no load.

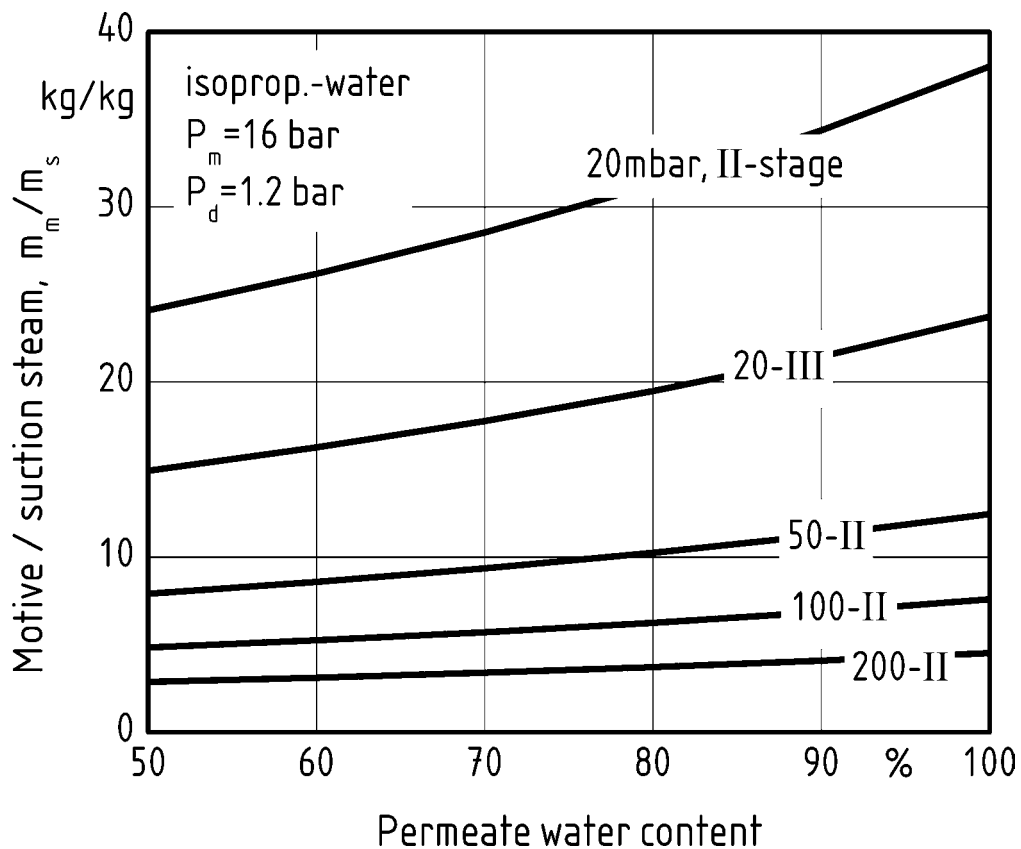


Figure 6-4: Motive steam requirements for different permeate mixtures

The above mentioned procedure is used to calculate the motive steam requirements for the suction of the permeate stream. The results for different isopropanol-water mixtures are presented in Figure 6-4. An exponential increase in the steam requirements below a certain vacuum pressure can be observed. Hence the use of ejectors at very low suction pressures is not expected to be feasible. However, in many dehydration tasks, permeate pressures are not

necessarily very low, especially when the water content specified in the product retentate is not extremely low. For these cases the use of the ejector could bring savings to the hybrid process. Economical and technical aspects have to be investigated to determine the proper regions, where the use of this alternative could be beneficial to the whole separation process.

## 6.4 Process control

Different methods can be used to control steam jet ejectors. The most common ways are throttling pressure drop in the line to the ejector or bleeding gas or vapor to the ejector suction line [125]. Condensable bleeds or recirculated vapor are normally used to control multistage ejectors. The required devices are a pressure controller and a control valve. In the conventional condensation additional control components are used such as level control for the condenser and temperature control for the reheat. Details of the control system for the conventional system can be found in [120] with comprehensive cost information. The saving of these components will be considered when comparing the economics of both alternatives. On the other hand, the ejector is designed for the maximum load of the specified process and the control lowers its efficiency to make it stable at lower loads. That will prevent the back streaming of the motive steam to the process. Increased flexibility of an ejector can be achieved by changing the nozzle according to the new design parameters.

## 6.5 Economic evaluation

The economics of the jet ejector alternative will be evaluated relative to the conventional condensation technique. The cost reductions can be divided into fixed and variable parts. The fixed part is saving the following equipment: the condenser operating under vacuum, the vacuum pump, the liquid pump and the reheat of the permeate. The variable part is saving the cooling water or the refrigeration costs. The added costs are the fixed cost of the ejector, the price difference between high pressure and low pressure steam, and the costs of the additional waste water treatment. The cost comparison is made on an annual cost basis. The equipment costs are depreciated on a period of eight years. It should be noted again that the

presented annual cost is not the total annual cost of the process, but it is only of the vacuum system behind the membrane module.

Functions for the fixed and variable costs were developed on the basis of offers from different manufacturers and data from large scale chemical companies. All the cost functions used for this economic evaluation can be found in Appendix A at the end of the thesis.

It should be noticed here that the losses by the pressure decrease of the steam before and after the ejector are relatively low, as the price of the 1.2 bar steam is about 75 % of that of the 16 bar steam as shown in Appendix A. Moreover, the added value of the permeate (suction) steam has to be considered. That lowers the effective price of the high pressure steam from the original price by the ratio  $A/A+1$ . The factor 'A' is the steam requirements ratio (motive/suction steam in kg/kg). This cost reduction will be noticeable by low values of 'A', i.e. by moderate vacuum pressures.

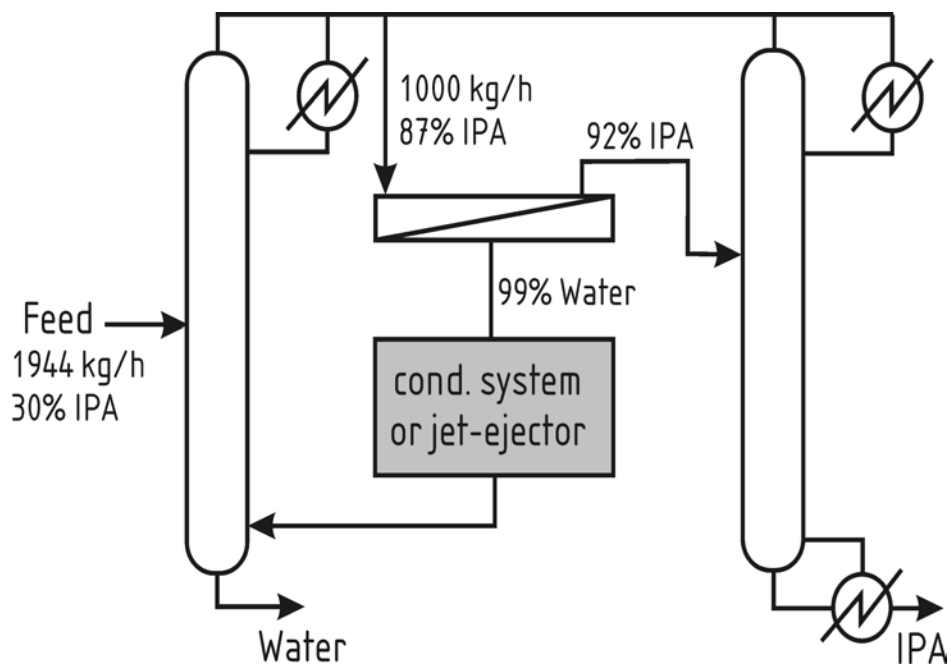


*Figure 6-5: Case studied for the dehydration of isopropanol*

A case study is carried out for the dehydration of iso-propanol. The process is shown in Figure 6-5. The feed to the first distillation column contains 30 mass% isopropanol. The membrane feed is 1000 kg/h with 87 mass% isopropanol, and has to be concentrated up to 92%. The permeate stream has a water content of 99%. A detailed cost analysis is made for

running the membrane separation under different vacuum pressures and for the same feed pressure of 1.2 bar. All the variable and fixed costs are calculated on an annual basis.

In Figure 6-6 the saved and added costs by implementing steam jet ejectors in comparison to the condensation are plotted against the permeate pressure to obtain a break-even diagram. These added and saved costs are described at the top of this section. The cases studied are connected with simple lines for the visual purpose. As a result of this study, the use of the steam-jet ejector option seems to be more favorable at relatively high permeate pressures where the steam requirements are relatively low.

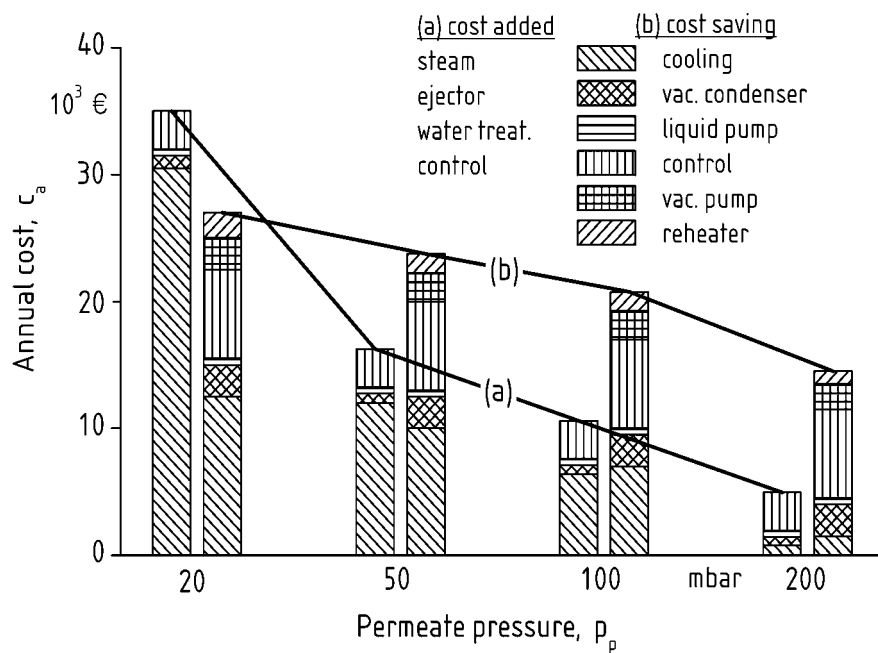


Figure 6-6: Annual total cost added (a) and saved (b) by the application of jet ejectors

Although the condensation cost increases with lower pressures, the exponential increase in the steam requirements with lower vacuum pressures makes the ejector alternative in that part less attractive. However, the use of very low vacuum pressures is limited to the applications, in which a very high retentate purity (absolute dehydration) is required. In several dehydration applications, in which the retentate purity is not extremely high, medium level vacuum pressures are used. Examples to that are overcoming middle range azeotropes as in the dehydration of isopropanol, or in hybrid combination to continuous reactors.

The cost advantages on an annual basis may appear quantitatively low when calculating the total annual cost of the whole process. On the other hand the fixed purchased cost of the

membrane unit is thereby dramatically reduced. For the above presented application we have estimated fixed cost savings in the whole membrane unit up to 30 per cent. That could assist in increasing the number of membrane applications in the chemical industry, as in many cases the relatively high capital cost delays and maybe discourages the decision of applying membrane technology.

Another reason that makes the ejector alternative inadvisable by permeate pressures lower than 50 mbar is the large amounts of steam discharged from the ejector. These large amounts would be redundant for the use as heating medium in the first column.

## 6.6 Other potential applications for steam jet ejectors

As illustrated in the previous sections, the low pressure steam produced from jet ejectors used in combination to dehydration membranes can be used as a heat source in the same plant. It will be more interesting if the heating task can be found in the immediate vicinity to- or in the same unit implementing the membrane separation. Hybrid combinations to distillation and to reactors may provide an attractive area for this application.

An interesting potential application is the three component separation methanol-isopropanol-water. The conventional separation of these components is done with at least three distillation columns and by using an entrainer like toluene to overcome the azeotrope between water and isopropanol. In an alternative hybrid process [67] using one distillation column and a pervaporation unit a side stream from the column is fed to the membrane where water is separated as a permeate. The retentate is recycled to one stage below the membrane feed for an undisturbed distillation process. Methanol is separated as a top product and isopropanol as a bottom product. As water builds a minimum azeotrope with isopropanol, it is possible to separate the water at the middle of the column via the dehydration membrane. To reduce the required membrane area the side stream is drawn from the point of maximum water concentration in the column. The integration of a steam jet ejector within this hybrid process is shown in Figure 6-7. As the temperature of the bottoms of the column is around the 82 °C (atmospheric boiling point of isopropanol), it is possible to heat the reboiler with the low pressure steam arising from the jet ejector due to the available temperature difference.

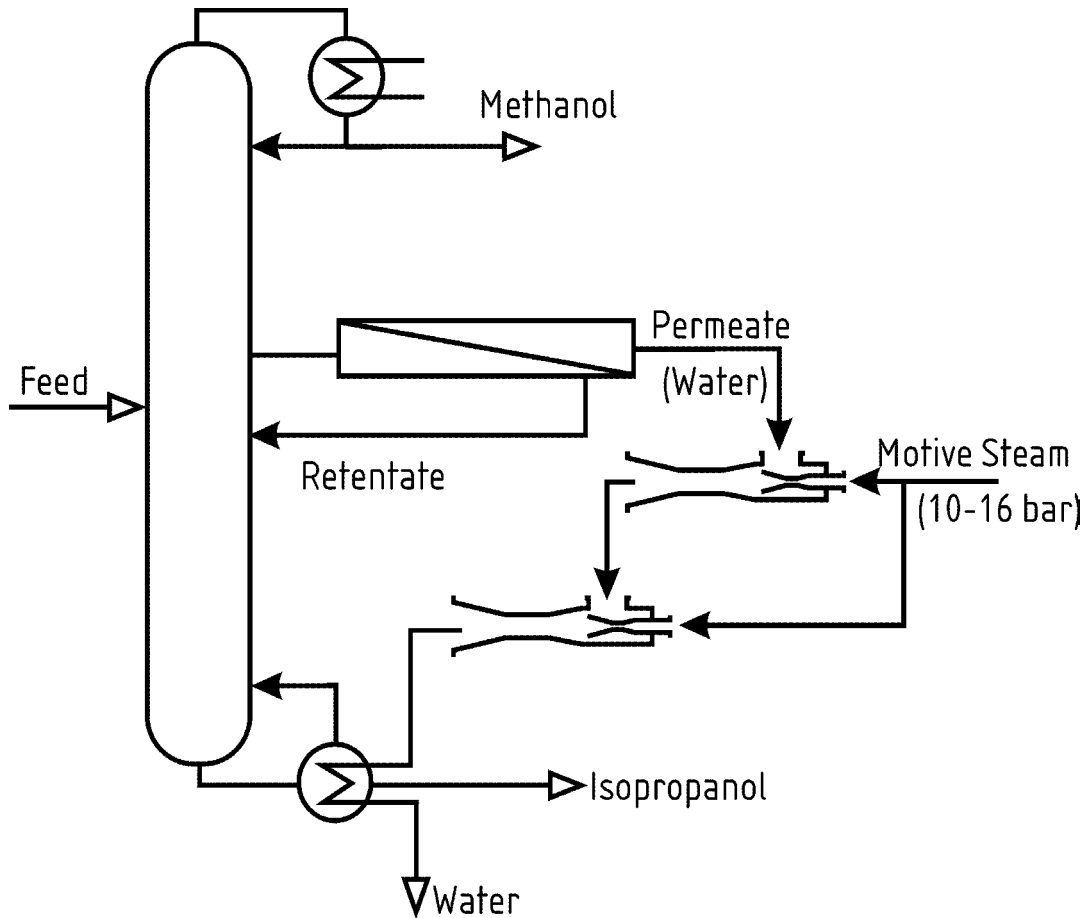
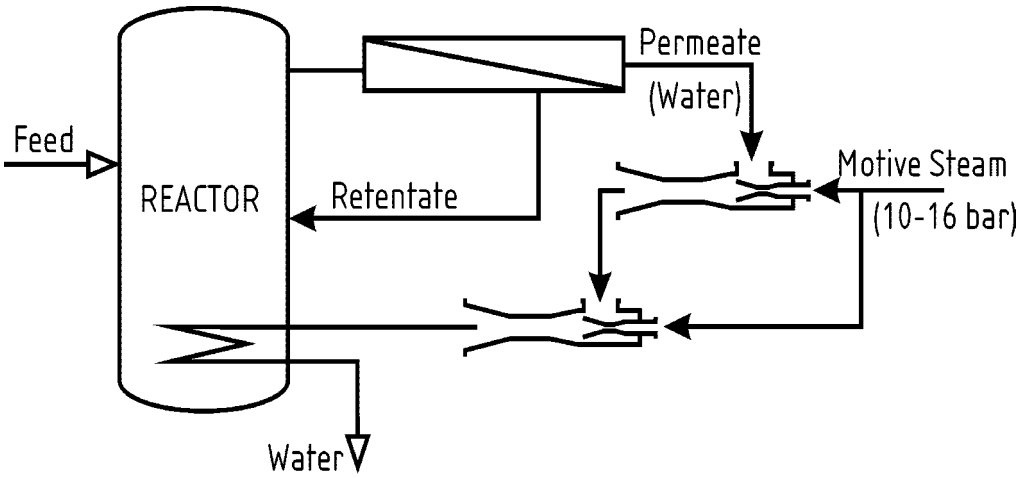


Figure 6-7: Use of steam jet ejectors within three component hybrid separation

The economics using jet ejectors in the application presented above will not differ very much from the case discussed before in section 6.5 as the produced low pressure steam is used for heating tasks inside the process.

Another possible application for the jet ejectors is its integration in the pervaporation or vapor permeation assisted chemical reactions as shown in Figure 6-8. The membranes are used for the dehydration of the produced water from different condensation reactions to shift the equilibrium towards the product side. The produced low pressure steam from the ejector can then be used for heating or evaporation tasks in the reaction medium. As a result, the same effect as in the presented isopropanol process can be achieved. The produced energy will stay inside the system, and the fixed cost and the total annual cost of the process can be reduced.



*Figure 6-8: Integrating steam jet ejectors into membrane reactors*

**Concluding this illustration:** The use of the suggested process combination seems to be useful in many cases. Its use will be especially attractive when excess high pressure steam is available, or when the produced low pressure steam can be directly used elsewhere in the process. Cost calculations show the feasibility of its use for moderate permeate pressure. However, a careful economic analysis has to be done each time for the case studied, as heating and cooling costs are unique for each industry and in each plant. Indeed, the suggested process could be considered as an additional option for the process integration and optimization of chemical plants containing, or are planning to use, membrane dehydration units.

## 7 Absorption assisted pervaporation

As discussed in chapter 1, the share of the membrane in the total cost of the unit is decreasing with increasing membrane fluxes and decreasing membrane prices. Thus efforts to optimize, modify and improve the periphery equipment would be worth while. The condensation technology that is yet the most convenient way for vacuum production in the pervaporation processes is therefore revised for energy and cost saving alternatives. In the previous section the use of steam jet ejectors within the dehydration of organics with hybrid processes is introduced and investigated. In this section a novel method for vacuum production by the absorption of the permeate vapors is introduced. This technology is suitable for the dehydration of organics as it can assist to the commercial scale available absorption refrigerators or heat pumps. Technical and economic advantages over the conventional condensation technology can be achieved by integrating the membrane into such units. Vacuum pressures as low as 8 mbar can be obtained at ambient temperatures without refrigeration. Low vacuum ranges that are not possible by condensation due to freezing limitations can be achieved. Process simulations and feasibility investigation for the suggested process are presented and discussed.

### 7.1 Limitations of the condensation technology

The different methods used for realizing the driving force necessary for permeation by pervaporation and vapor permeation are introduced and discussed in section 2.2. The steam jet ejection introduced in section 6.1 can be considered as an additional option within hybrid processes. However, the condensation technology has proven to be the most convenient method for vacuum production. Although it is relatively expensive it is a simple and common technology with a wide range of standard units and long years of industrial experience. However, this technology has shown some limitations by its use in the combination with pervaporation and vapor permeation. One disadvantage is the exponentially increasing refrigeration cost with decreasing temperature below a certain temperature range. Another disadvantage is that the condensation temperature and thus the permeate pressure cannot be

arbitrarily decreased. The freezing point of the permeate mixture sets the lowest temperature limit in the condenser to avoid solids accumulation on the heat transfer area. This freezing limitation is shown in Figure 7-1 for water-ethanol mixtures. In consequence of this limitation, the permeate pressure cannot be arbitrary lowered and thus the savings in the required membrane area are also limited. This limitation is known within the attempts to achieve a very high retentate purity, where the driving force for permeation diminishes. Exponential increase in the required membrane area is expected at this concentration range. One solution, which has its cost and feasibility limitations as discussed above is lowering the permeate pressure towards the absolute zero. Another feasible and realistic way is to use low selectivity membranes at this concentration region as illustrated in section 6.1. An intermittent operation of the condenser with heating and melting the formed ice has also been practiced [126]

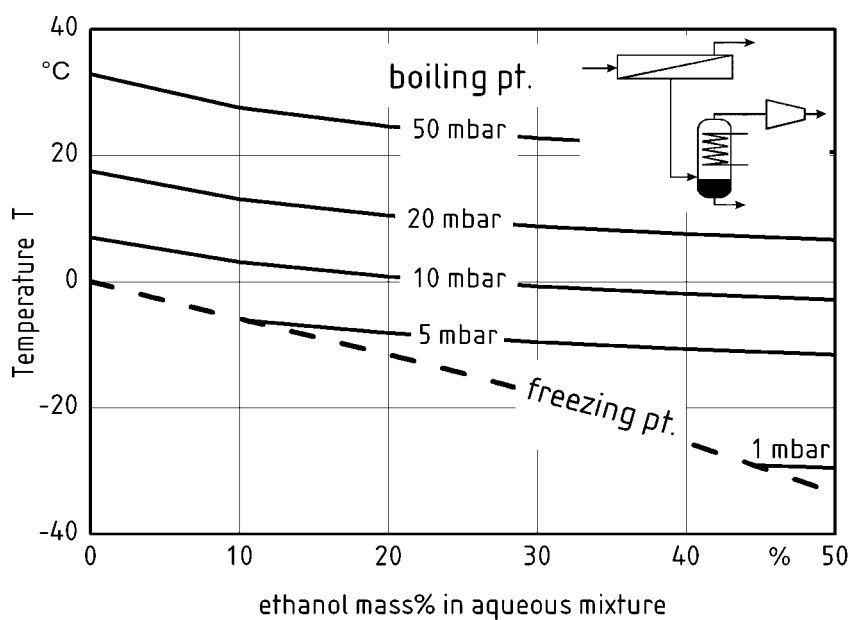


*Figure 7-1: Boiling and freezing points for different water ethanol mixtures*

In the following sections an alternative absorption technique for carrying out the PV and VP is introduced. This process modification is evaluated and compared to the conventional condensation technique. Within case studies for the dehydration of organic compounds the advantages and limitations of this novel technology are illustrated and discussed.

## 7.2 Suggested absorption technology

The absorption of the permeate stream is used for vacuum generation on the permeate side. An absorbent with a high affinity to the permeate mixture is contacted with the permeate vapor. The lean (dilute) absorption solution after absorbing the permeate should have a lower vapor pressure than the condensed permeate mixture at the same temperature. Thus compared to condensation, a lower vacuum pressure can be attained by equal temperature, or the same vacuum pressure can be attained by a higher temperature. Consequently the fixed and operating cost for the refrigeration process could be reduced and it could be even redundant if the absorption process runs at room temperature and cooled with normal cooling water.

The lean absorption solution is sent to a desorber where the absorbed permeate is stripped out of the solution. The required stripping energy could be attained from a low quality energy source in the chemical plant or it can be won out of the vaporous retentate stream in the case of vapor permeation. A flow sheet of that process is shown in Figure 7-2. The vapor stripped out of the desorber is condensed at a higher pressure compared to the permeate. Therefore in all cases normal cooling water can be used for it. The rich solution from the desorber is recycled back to the absorber. Heat is exchanged between the lean and rich solutions to lower the energy consumption of the process.

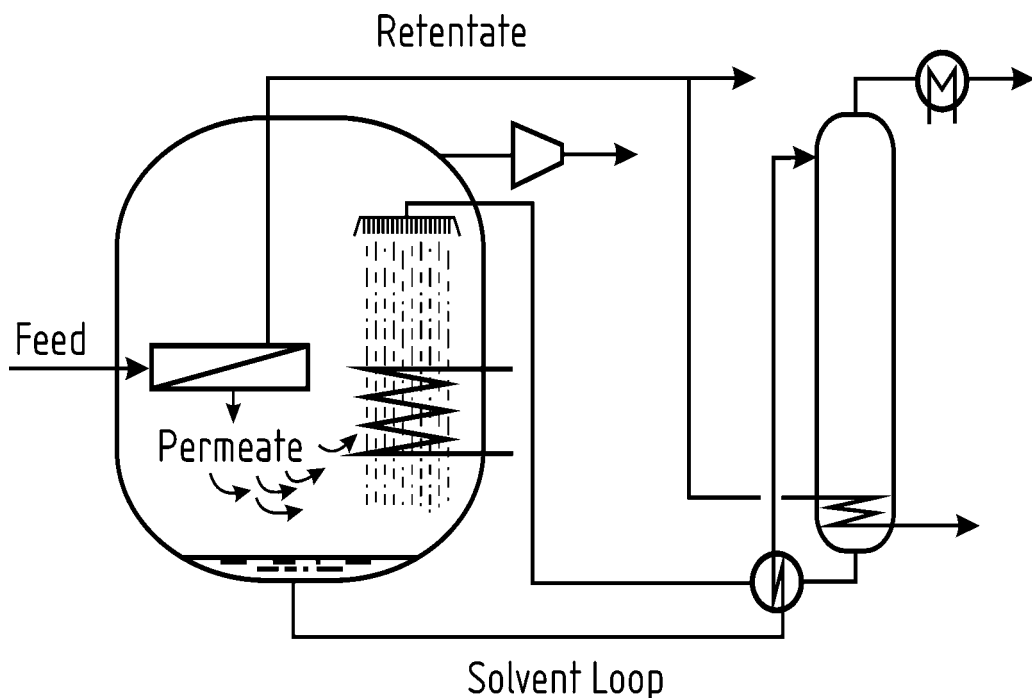


*Figure 7-2: Absorption technology for dehydration by vapor permeation*

The required area for heat transfer is realized by horizontal cooling pipes. The heat evolved by the absorption process is removed by a cooling medium, normally cooling water, flowing inside the pipes. The exiting cooling medium can then be used for another cooling step in the condenser of the stripped vapor.

### 7.3 Application to dehydration processes

An interesting application of the absorption technology is the dehydration of organic solvents. A number of hygroscopic solutions were developed and optimized for the absorption of water for other applications. These include a many well established drying processes implemented in different fields and absorption refrigeration processes with water as a cooling medium.

So applying the above introduced absorption technology on the dehydration of organics with PV or VP, a hygroscopic liquid is utilized for the absorption of the permeate. The lithium bromide (LiBr) solution is one of the most hygroscopic liquids found. The vapor pressure of water above LiBr solution as shown in Figure 7-3 is much lower than that of water at the same temperature. Some additives like ethandiol or propandiol slightly increase the vapor pressure above the solution, but they lower the crystallization temperature of LiBr [127,128].

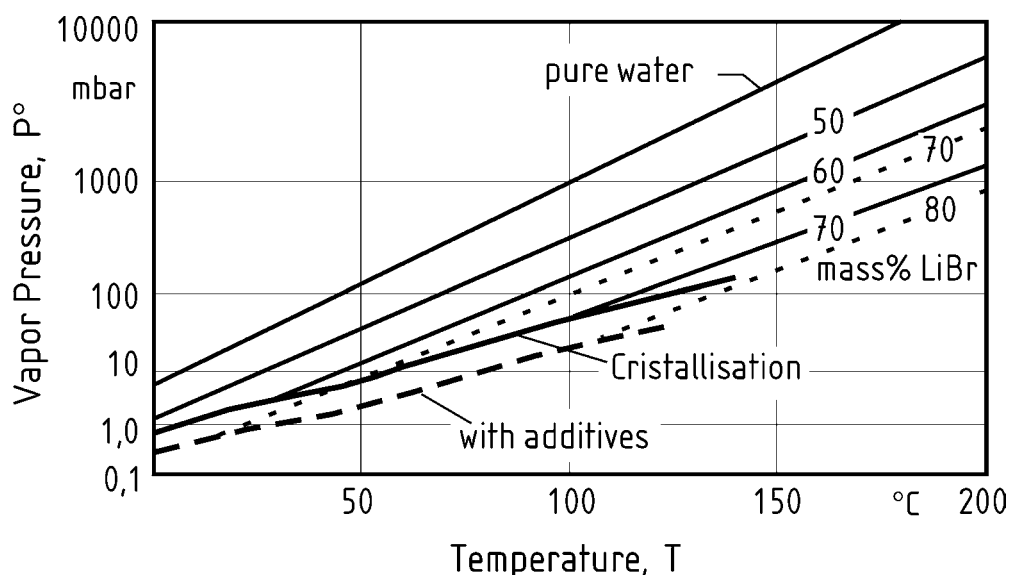


Figure 7-3: Vapor pressure over LiBr solutions [126,127]

A vapor pressure of 8 mbar can be achieved above a 60 mass% LiBr Solution at room temperature. A refrigeration to  $-10$  or  $-15$  °C is necessary to achieve such pressure by condensing the permeate mixture.

In addition to the above stated cooling temperature advantage, lower vacuum pressures could be achieved that were not possible by condensation due to the limitation of the freezing point at low pressures. Overcoming this limitation could result in the possibility of increasing the driving force, especially in the region of very low water content in the retentate, which would result in considerable reduction of the required membrane area.

### **7.3.1 Integration into absorption refrigeration cycles**

The above described absorption process may look more complex than conventional condensation. The absorbed solution has to be reconcentrated in the stripper. Simultaneous heat and mass transfer processes take place and the process has to be controlled. However, a similar process is found in absorption refrigeration units and absorption heat pumps. Generally a LiBr solution is the absorbing fluid and water is the refrigerant. There is a satisfactory amount of know how and experience on using these refrigeration cycles. The equipment and processes are standardized and the whole cycle is available as a finished product in the market.

A typical cycle is shown in Figure 7-4a. The cooling load is drawn out of the evaporator, where water evaporates under a very low pressure. Water vapor is then absorbed by a concentrated LiBr solution at the same pressure. The level of the vacuum depends on and is realized by the absorbing solution. A small vacuum pump is also necessary for drawing the leakage and the non-condensable components out of the process. The lean solution is pumped to the desorber, where the water vapor is stripped out of the solution. The solution is recycled to the absorber and the water vapor is condensed and drawn back to the evaporator by the pressure difference. The aim of the whole cycle is to convert heat supply to the desorber into refrigeration cooling at the evaporator. The refrigeration temperatures are not very low (4 to 6 °C) as they are limited by the freezing point of the refrigerant (water). Typical pressure levels are 8 mbar for absorption and evaporation and 100 mbar for the desorption process[127]. Our suggestion is to integrate the membrane modules into such processes with little modification. The membrane is considered to be the source for water vapor. It can replace the evaporator as

shown in Figure 7-4b. The cycle will be converted to an open system. The permeate stream is drawn out of the process as condensate.

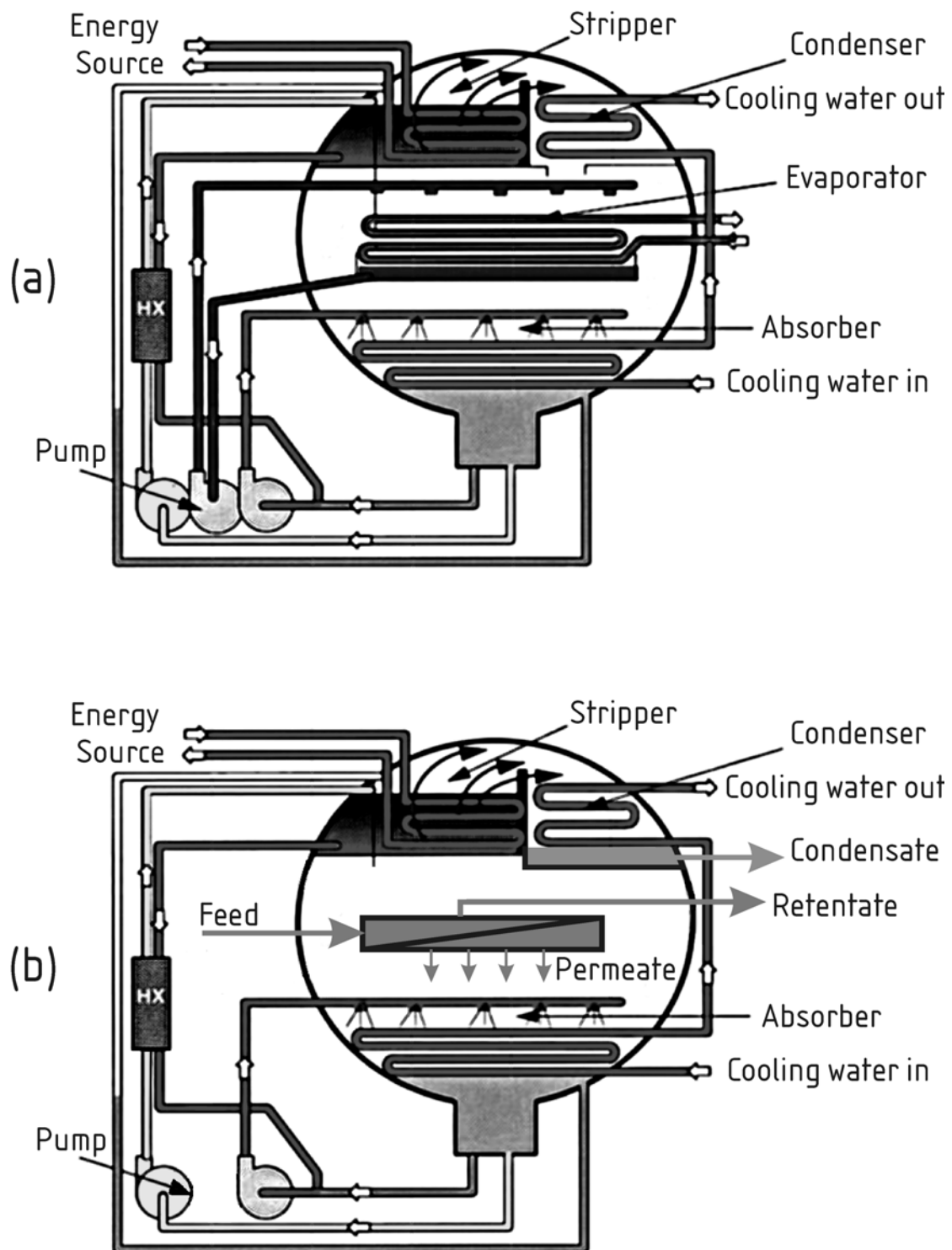


Figure 7-4: Integrating the membrane modules into the refrigeration cycle

Generally the absorption is carried out with the highest possible solution concentration. The only limitation thereby is the crystallization limit of the salt solution. With some additives, as discussed above, it is possible to lower the crystallization temperature of LiBr. This will bring an advantage of working with highly concentrated solutions and under low temperatures.

Aqueous LiBr has been known to be aggressive to many metals including carbon steel and copper. However, if the system is well sealed, little oxygen is present and corrosion rates are much slower. The manufacturers of absorption refrigerators have overcome the corrosion problems and such cycles have been used successfully in the last decades and are a well established market technology . LiNO<sub>3</sub> and Li<sub>2</sub>MoO<sub>4</sub> are common corrosion inhibitors for such systems.

A little amount of octyl alcohol is added to the LiBr solution to enhance the mass transfer. Convective motions are thereby generated on the gas-liquid interface due to different surface tensions (Marangoni-effect). On the interface the liquid molecules move from low to high surface tension regions generating high convection rates that increase the mass transfer coefficient.

### **7.3.2 Effect of lower membrane selectivity**

The membrane selectivity for the dehydration of organics is generally very high. Ceramic membranes offer even a further increased separation selectivity. Nevertheless, a small fraction of the organic solvent will always permeate with the water to the permeate side, especially if a very pure retentate is required. However, their effect will be negligible as they are diluted further with the absorbing solution as shown in section 7.3.3 by a factor 10:1. Nevertheless, for a thorough study two parameters should be investigated: the solubility of the organic part of the permeate into the absorbing solution, and the change in the vapor pressure above the solution.

It was found that LiBr and similar hygroscopic salts are soluble in most organic solvents. Many studies were carried out on the effect of different salts on overcoming the azeotropes in the water-organic distillation [129,130]. However, a slight decrease in the solubility of the salt in the water-alcohols solutions than in pure water is observed [131,132]. A slight increase in the vapor pressure due to the existence of ethanol is expected but cannot be quantified at the moment. However, experimental studies on organic additives to the LiBr-water system show that the crystallization point of the solution is further decreased, which would allow to

implement higher salt concentration [127]. As a result the presence of small amounts organic material in the salt solution has negative and positive effects with respect to our suggested application. Thus at this stage of basic process design we will assume that the positive effects would adjust the negative ones, and that the permeate can be considered as pure water. At further design stages thermodynamic data for the investigated system can be experimentally determined.

### 7.3.3 Process simulation and economic evaluation

The process simulation program introduced in chapter 5 is used for the simulation of the membrane unit with all its periphery equipment. The optimum condensation temperature and vacuum pressure of the permeate can be determined on an economic basis. The economic evaluation of the absorption alternative is made in comparison to the condensation technology. In the case study considered, the separation task is dehydrating 1000 kg/h from 95 to 99,9 mass% ethanol. The permeability of water considered in the simulations is based on a modified PVA membrane of GKSS [108]. Different membrane selectivities from 20 to 2000 are considered. The permeate pressure is 8 mbar for both alternative processes. An additional case of 2 mbar is also considered for the absorption alternative as it is not possible by condensation due to ice formation in the condenser.

Functions for the fixed and variable costs were developed on the basis of offers from different manufacturers and data from large scale chemical companies. The cost functions considered in this section are listed in Appendix A at the end of the thesis. The process alternatives are compared on the basis of the annual total cost. The membrane material is depreciated over 3 years, the membrane modules over 6 years and the rest of the peripheral and utility equipment over 10 years. The above mentioned computer program is extended to calculate the cost items of the absorption cycle.

The results are shown in Figure 7-5. The absorption alternative has shown cost advantage over the condensation at 8 mbar. Working under 2 mbar is more expensive as refrigeration will be required to lower the temperature of the absorption solution to achieve a vapor pressure of 2 mbar. It would be necessary if a further purification of the retentate is required. From the same figure one can derive that a certain mid-range membrane selectivity seems to be optimal for the studied separation case. A very high selectivity maybe not be favorable for this separation task with a high retentate purity as discussed before in section 5.1.

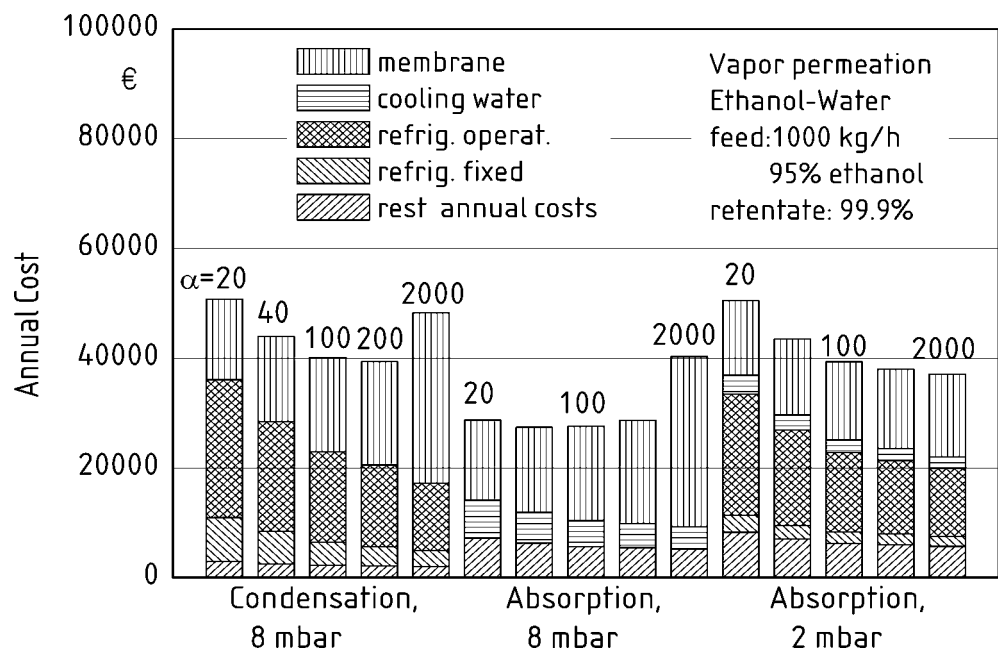


Figure 7-5: Comparing process alternatives for a typical dehydration task

At a permeate pressure of 8 mbar the permeate contains 1.1 and 9.8 mass % ethanol when using a membrane selectivity of 2000 and 200 respectively. This amount is then diluted in the absorbing solution to be 0.1 and 0.89 % in the effluent solution. As discussed in section 4.2 the effect of the presence of ethanol is neglected. Hence, the simulation of the absorption cycle is based on an ethanol free permeate at this basic design phase. In fact, the absorption cycle that could be used in this suggested process is one compact unit that can be bought as an one unit. The water (refrigerant) flow rate that corresponds to the permeate and the temperature and pressure levels should be enough for specifying such machine. However, for more understanding such a cycle has been simulated in more detail. The software ‘Aspen Plus’ does not provide thermodynamic data about the LiBr-water system. Therefore, the complete simulation of the absorption cycle is carried out using the software ‘ABSIM’ (Oak Ridge National Laboratory, Oak Ridge, TN 37831 6070 USA), which is a special software developed for the simulation of absorption refrigeration cycles. Results for mass and energy balance calculations for the absorption cycle used for the above case study are illustrated in Figure 7-6. The presented results are based on a membrane feed of 1000 kg/h and a membrane selectivity of 200.

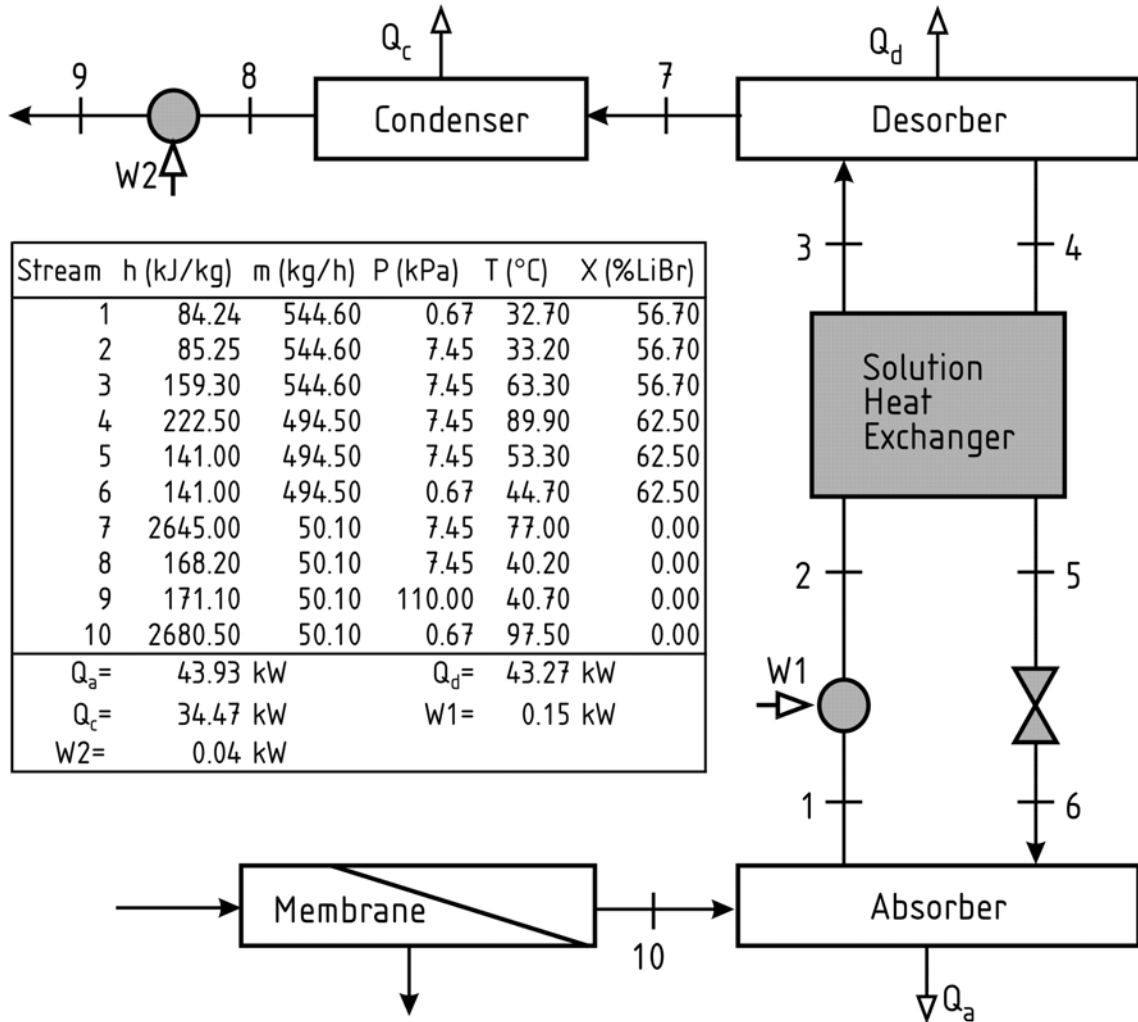


Figure 7-6: Mass and energy balance for the absorption desorption cycle

In another case study, it is required to dehydrate the 99,9 ethanol further to 99,95. This is an extremely difficult task, since the driving force for water permeation nearly vanishes in addition to other factors like feed concentration polarization which will not be discussed here. An extremely low permeate pressure is required to increase the driving force. However, it is not possible to produce a permeate pressure below 8 mbar by condensing the permeate due to freezing limitation. For an increased driving force a low selectivity membrane is needed as shown in Figure 7-7 . Another stage is necessary to purify the permeate as illustrated in chapter 5. Yet, with the presented absorption technology it is possible to reach a permeate pressure of 2 mbar with little refrigeration. From the results presented in Figure 7-7, the use of a high selectivity membrane in a single stage operation would be the most economic solution for such a high pure separation.

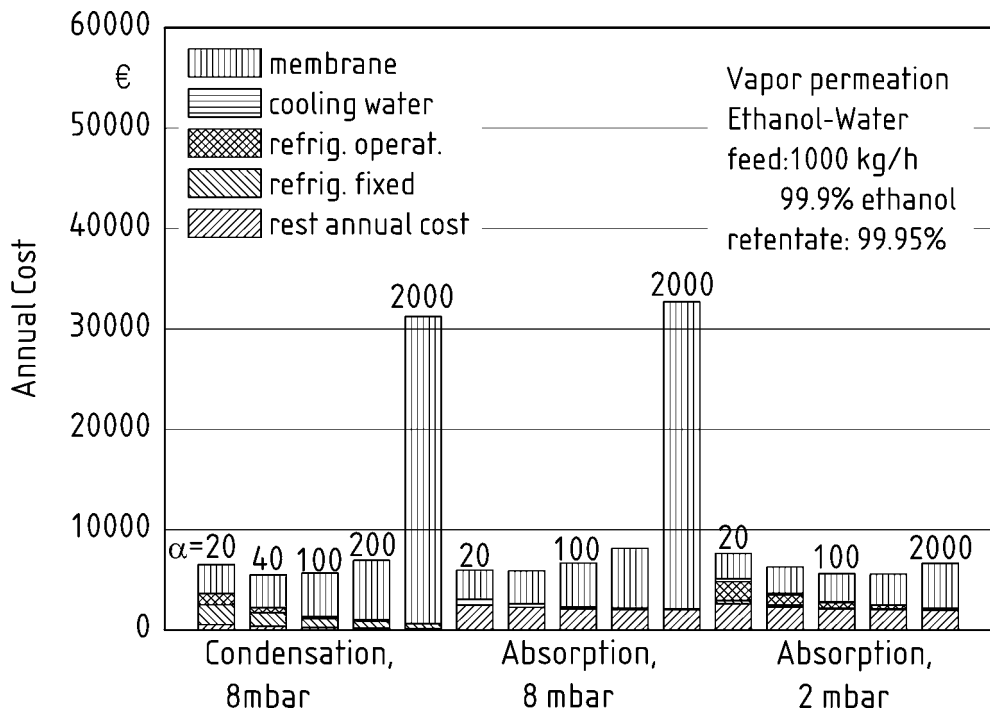


Figure 7-7: Comparing process alternatives for an ultra-pure separation

## 7.4 Technical evaluation

The presented process for carrying out pervaporation and vapor permeation processes combine both the selectivity of the membrane and the high affinity of the permeate towards the absorbing solution. It should be distinguished from other membrane absorption processes where a porous membrane is utilized as a contacting medium between the feed and the absorbing solution. In the presented configuration the membrane is not a contacting medium, but it is a selective barrier between the feed side mixture and the absorbing solution. The absorption process takes place outside the membrane module.

As illustrated above, the suggested process configuration could bring cost savings in the case of the dehydration of organic solvents. This should not rule out its feasibility in other membrane separation applications. The presupposition is the availability of a low vapor pressure solvent with a strong affinity towards the permeate mixture.

The presented modification in the LiBr absorption cycles turns it from a closed cycle to an open one. The use of the LiBr absorption cycle as an open cycle has been reported as a feasible option for the waste energy management. In such processes the exhaust gases of the power plants are directed to similar absorbers, where the latent heat of its water vapor is caught by the hygroscopic solution. The heat of absorption is utilized in different process configurations [133,134].

Although the suggested process design lacks to an experimental demonstration, it rests on two well established technologies, the separation by pervaporation and the absorption refrigeration. The presented process is a combination of both processes in a new configuration. The process evaluation and the feasibility study will encourage to proceed with experimental investigations. The most important point that has to be investigated experimentally is to quantify the effect of the membrane selectivity (i.e. the presence of the organic compound) on the process as stated in 4.2. Moreover, test runs and parametric studies on a pilot scale unit would be necessary to give more comprehension and to adjust the suggested process to guarantee a reliable design and operation.

***Concluding this illustration:*** A novel process configuration for pervaporation and vapor permeation is presented. In this process the permeation driving force is realized by absorbing the permeate vapor into a suitable solution with a very low vapor pressure. The refrigeration needed for condensation in the conventional process can be overcome and cost savings could be achieved. Very low vacuum pressures can be reached without any permeate freezing limitations. Preliminary simulations and feasibility studies for the suggested process are presented. The presented results should be considered qualitatively rather than quantitatively as the utility costs are unique for each industry and in each plant. The presented process could be considered as an additional optional process scheme for chemical plants that are going to run membrane dehydration units.

## 8 Conclusion

The aim of this work is achieving technical and economic refinements in pervaporation and vapor permeation processes through systematic process design investigations. Strong emphasis is done on the dehydration processes of organic solvents. The main objectives are the optimization of the process parameters including those of the membranes and of the peripheral equipment, and the investigation of feasible areas for process development and improvement.

The first step during this study was the development of a computer program for the simulation of the membrane process. A simplified transport model has been implemented within this program, it can be extended to make use of different rigorous thermodynamic and diffusion models. By using simplified modeling the membrane transport properties could be easily varied during the simulation. Thus different membranes could be compared for a specific application and the membranes could be tailored for different processes. The membrane program is integrated into the software “Aspen Plus” as a ‘user model’, thus the simulation of the whole unit including condensers, pumps or even in a hybrid combination to distillation columns or reactors has been made possible.

Accordingly, an optimization program is developed to investigate the whole membrane unit with all its periphery equipment. Optimum values for membrane selectivity, condensation temperature and permeate pressure can be determined on an economic basis. Functions for the fixed and variable costs are developed on the basis of offers from different manufacturers and data from large scale chemical companies. This program is implemented to several dehydration applications, and it has been demonstrated that a low membrane selectivity is preferred for applications requiring a high purity retentate. However, using the low selectivity requires a second separation step for the purification of the permeate. Such two stage processes are presented and heat integration measures are studied using the pinch technology.

In another part of this study, the condensation technology for the permeate removal is carefully reviewed looking for improvements and refinements. Beside the high refrigeration costs at low temperatures, it is demonstrated that the condensation temperature and hence the permeate pressure cannot be arbitrary decreased in order to increase the driving force for

permeation. The freezing point of the permeate mixture sets the lowest temperature limit in the condenser to avoid solids accumulation on the heat transfer area. One alternative process which is demonstrated within this thesis is the use of steam jet ejectors for vacuum production. The resulting low pressure steam can then be used for heating tasks inside the process. Applications within the scope of hybrid combinations to distillation and chemical reactors are suggested to be potential areas for implementing this technique. An economic study is carried out to demonstrate the range of permeate pressure feasible for such application.

Yet another process alternative to the condensation technology is introduced in the last part of the present work. Within this alternative the driving force for permeation is enabled by the absorption of the permeate vapor by a suitable solvent with a very low vapor pressure. The refrigeration needed for condensation in the conventional process can be overcome cost savings could be achieved. It is demonstrated that this absorption technology is especially suitable for dehydration applications as it can assist to the commercial scale available absorption refrigerators. If the evaporator of such machines is replaced by a membrane module and the cycle is converted to be an open one, the system could be run as a complete membrane dehydration unit. Preliminary simulations and feasibility investigations show economic and technical advantages over the condensation technology and encourage to proceed with testing this idea on a pilot scale.

## Appendix A: Fixed and variable cost functions

Item	Estimated cost function in €	Nomenclature
Membrane material	80 A	A: Membrane area, m <sup>2</sup>
Membrane modules	250 A	A: Membrane area, m <sup>3</sup>
Vacuum vessels	For $0.8 \text{ m}^3 < V < 4 \text{ m}^3$ 9000 $V^{0.75}$	V: Vessel volume, m <sup>3</sup>
Condensers	$1300Q^{0.7}$	Q: Condenser Duty, KW
Compression refrigeration units	for $25^\circ\text{C} < t < -5^\circ\text{C}$ Fixed cost: $\{1036 + 2870\exp[-(t+25.4)/3.6]\}Q^{(0.97+0.01t)}$ Operating cost/year: $\{149 + 214\exp[-(t+23.6)/19.2]\}Q$	Q: Cooling Duty, (KW) t: refrigerant outlet temp., °C
Liquid pumps	$100 \text{ m}^3/\text{h} < V < 1000 \text{ m}^3/\text{h}$ Fixed cost: $5000 V^{0.2}$ Operating cost/year: $0.5 V \nabla p$ (1 year = 8000 h)	V: Volumetric flow rate, m <sup>3</sup> /h $\nabla p$ : Pressure difference, bar
Vacuum pumps	Fixed cost: $203 V^{0.8}$ Operating cost/year: $9.6 V$ (1 year = 8000 h)	V: Volumetric flow rate, m <sup>3</sup> /h (suction side)
Electricity	0.03 €/kWh	

<b>Item</b>	<b>Estimated cost function in €</b>	<b>Nomenclature</b>
Cooling water	$0.05 \text{ €}/\text{m}^3$ for 25-33°C inlet and outlet temp. 56 Q (per year)	Q: Cooling Duty, (KW)
Steam	1.2 bar: 10.5 t 16 bar: 14 t	t: Tons steam
Jet ejectors	$10 \text{ kg/h} < m_s < 150 \text{ kg/h}$ with 16 bar motive steam $1100 m_s^{0.3}$	$m_s$ : Suction flow rate of water vapor, kg/h
Biological waste water treatment	0.8 k	k: Kg COD
Absorption refrig. unit	$10 < Q < 100$ $15000 + 1035 Q^{0.9}$	Q: Refrigeration duty, KW

### Depreciation period:

Membrane material: 3 years

Process equipment: 10 years

## Appendix B: Material and energy balance for the dehydration process

Material and energy balance data for the dehydration case study of sections 5.1 to 5.3 are presented in more detail in this section. The task is the dehydration of 1000 kg/h ethanol-water mixture from 93 to 99.9 mass% ethanol. Following specifications are considered for the membrane used in this illustration:

Water permeability coefficient: 5E-5 kg/m<sup>2</sup> s Pa

Selectivity (permeability ratio): 30

Permeate Pressure: 800 Pa

Calculated membrane area: 108.2 m<sup>2</sup>.

The flow sheet presented in the next page results from the ‘Aspen Plus’ simulation program that has been used for the investigation of this process. Some additional streams and processes serve for supplying additional data that are used somewhere in the optimization subroutines or to calculate data necessary for the heat integration investigations such as follows:

Required cooling load for condensing the permeate: 62.5 KW

Heating load for an absorption refrigerator (Coefficient of performance 0.65) with the above cooling load: 96.2 KW

Required heat for the reboiler of the distillation column “QR”: 53.8 KW

Total required heating load: (96.2 + 53.8) 150 KW

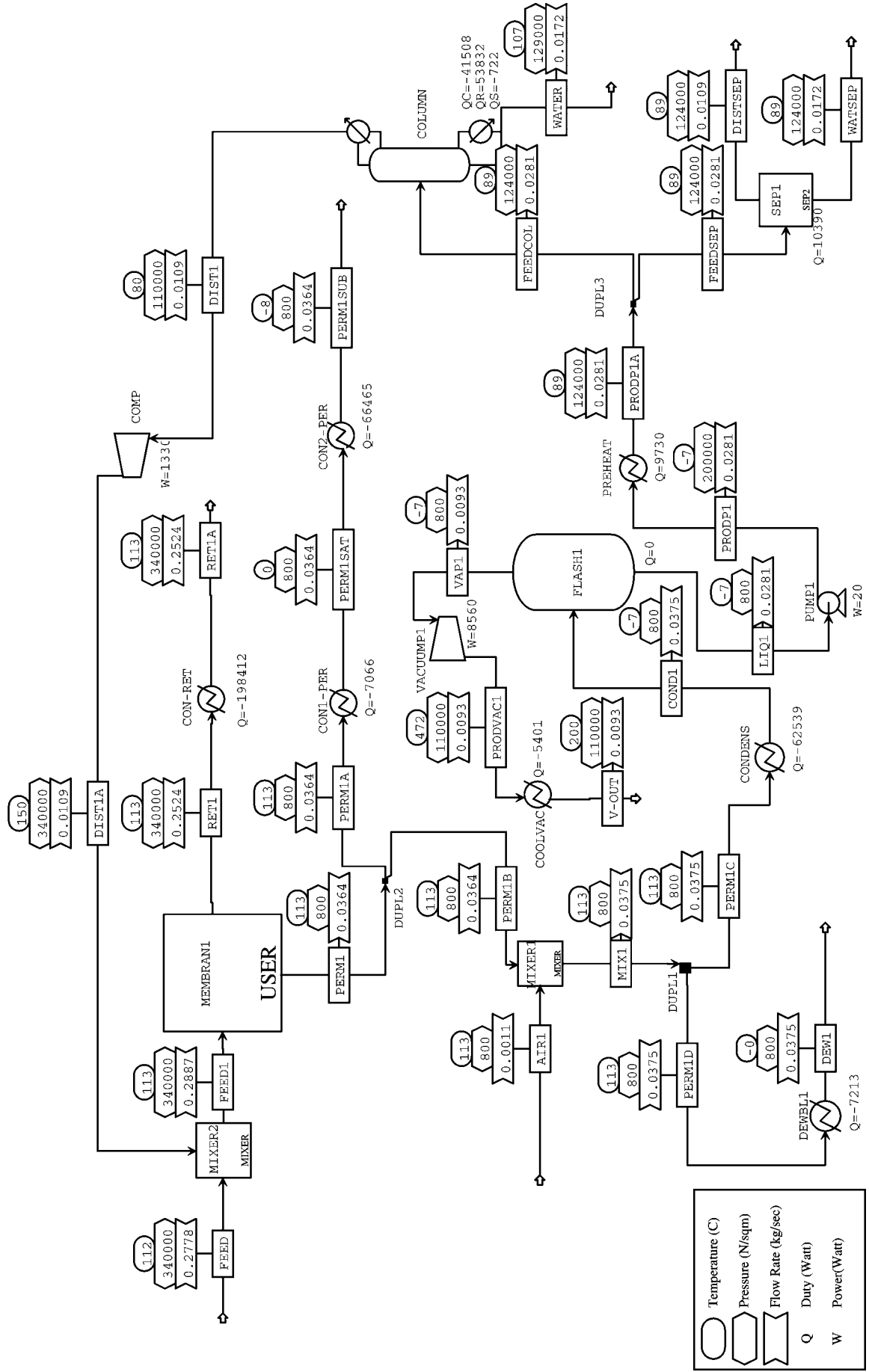
Available latent heat in the retentate stream (duty of “CON-RET”): 198.4 KW

Thus the available latent heat in the retentate is sufficient for running both the absorption refrigeration and the reboiler. Excess heat can be used also elsewhere in the process.

It should be noted that an additional separation unit (SEP1) serves for the precalculation of the material balance around the distillation column that helps in the convergence of the column.

# Flow diagram for the two stage dehydration process

88



## Stream data for the two stage dehydration process

	FEEDSEP	LIQ1	MIX1	PERM1	PERM1A	PERM1B	PERM1C	PERMID	PERMISAT
Mole Flow kmol/sec									
WATER	9.96E-04	9.96E-04	1.11E-03	1.11E-03	1.11E-03	1.11E-03	1.11E-03	1.11E-03	1.11E-03
ETHANOL	2.21E-04	2.21E-04	3.56E-04	3.56E-04	3.56E-04	3.56E-04	3.56E-04	3.56E-04	3.56E-04
AIR	2.96E-09	2.96E-09	3.84E-05	2.96E-09	2.96E-09	2.96E-09	3.84E-05	3.84E-05	2.96E-09
Mass Frac									
WATER	0.6380784	0.6380784	0.5322239	0.5484911	0.5484911	0.5484911	0.5322243	0.5322243	0.5484911
ETHANOL	0.3619185	0.3619185	0.4381164	0.4515066	0.4515066	0.4515066	0.4381161	0.4381161	0.4515066
AIR	3.05E-06	3.05E-06	2.97E-02	2.36E-06	2.36E-06	2.36E-06	2.97E-02	2.97E-02	2.36E-06
Total Flow kmol/sec	1.22E-03	1.22E-03	1.50E-03	1.46E-03	1.46E-03	1.46E-03	1.50E-03	1.50E-03	1.46E-03
Total Flow kg/sec	0.0281261	0.0281261	0.0374649	0.0363538	0.0363538	0.0363538	0.0374649	0.0374649	0.0363538
Total Flow cum/sec	3.36E-05	2.98E-05	6.03E+00	5.878876	5.878876	5.878876	6.033085	6.033085	4.15795
Temperature C	88.80151	-7.149974	113.4641	113.4641	113.4641	113.4641	113.4641	113.4641	0.2903652
Pressure N/sqm	1.24E+05	8.00E+02	800	800	800	800	800	800	800
Vapor Frac	0	0	1	1	1	1	1	1	1
Liquid Frac	1	1	0	0	0	0	0	0	0
Solid Frac	0	0	0	0	0	0	0	0	0
Enthalpy J/kmol	-2.79E+08	-2.87E+08	-2.30E+08	-2.36E+08	-2.36E+08	-2.36E+08	-2.30E+08	-2.30E+08	-2.41E+08
Enthalpy J/kg	-1.21E+07	-1.24E+07	-9.23E+06	-9.51E+06	-9.51E+06	-9.51E+06	-9.23E+06	-9.23E+06	-9.71E+06
Enthalpy Watt	-3.39E+05	3.49E+05	-3.46E+05	-3.46E+05	-3.46E+05	-3.46E+05	-3.46E+05	-3.46E+05	-3.53E+05
Entropy J/kmol-K	-1.78E+05	-2.03E+05	-2.92E+04	-3.2282.31	-3.2282.31	-3.2282.31	-29246.4	-29246.4	-47011.74
Entropy J/kg-K	-7705.655	-8800.317	-1172.12	-1299.254	-1299.254	-1299.254	-1172.12	-1172.12	-1892.063
Density kmol/cum	36.25945	40.7765	2.49E-04	2.49E-04	2.49E-04	2.49E-04	2.49E-04	2.49E-04	3.52E-04
Density kg/cum	837.8876	942.268	6.21E-03	6.18E-03	6.18E-03	6.18E-03	6.21E-03	6.21E-03	8.74E-03
Average MW	23.10811	23.10811	24.95172	24.84681	24.84681	24.84681	24.95171	24.95171	24.84681
Liq Vol 60F cum/sec	3.08E-05	3.08E-05	4.20E-05	4.07E-05	4.07E-05	4.07E-05	4.20E-05	4.20E-05	4.07E-05

## Stream data for the two stage dehydration process, continued

	FEEDSEP	LIQ1	MIX1	PERM1	PERM1A	PERM1B	PERM1C	PERMID	PERMISAT
Mole Flow kmol/sec									
WATER	9.96E-04	9.96E-04	1.11E-03	1.11E-03	1.11E-03	1.11E-03	1.11E-03	1.11E-03	1.11E-03
ETHANOL	2.21E-04	2.21E-04	3.56E-04	3.56E-04	3.56E-04	3.56E-04	3.56E-04	3.56E-04	3.56E-04
AIR	2.96E-09	2.96E-09	3.84E-05	2.96E-09	2.96E-09	2.96E-09	3.84E-05	3.84E-05	2.96E-09
Mass Frac									
WATER	0.6380784	0.6380784	0.5322239	0.5484911	0.5484911	0.5484911	0.5322243	0.5322243	0.5484911
ETHANOL	0.3619185	0.3619185	0.4381164	0.4515066	0.4515066	0.4515066	0.4381161	0.4381161	0.4515066
AIR	3.05E-06	3.05E-06	2.97E-02	2.36E-06	2.36E-06	2.36E-06	2.97E-02	2.97E-02	2.36E-06
Total Flow kmol/sec	1.22E-03	1.22E-03	1.50E-03	1.46E-03	1.46E-03	1.46E-03	1.50E-03	1.50E-03	1.46E-03
Total Flow kg/sec	0.0281261	0.0281261	0.0374649	0.0363538	0.0363538	0.0363538	0.0374649	0.0374649	0.0363538
Total Flow cum/sec	3.36E-05	2.98E-05	6.03E+00	5.878876	5.878876	5.878876	6.033085	6.033085	4.15795
Temperature C	88.80151	-7.149974	113.4641	113.4641	113.4641	113.4641	113.4641	113.4641	0.2903652
Pressure N/sqm	1.24E+05	8.00E+02	800	800	800	800	800	800	800
Vapor Frac	0	0	1	1	1	1	1	1	1
Liquid Frac	1	1	0	0	0	0	0	0	0
Solid Frac	0	0	0	0	0	0	0	0	0
Enthalpy J/kmol	-2.79E+08	-2.87E+08	-2.30E+08	-2.36E+08	-2.36E+08	-2.36E+08	-2.30E+08	-2.30E+08	-2.41E+08
Enthalpy J/kg	-1.21E+07	-1.24E+07	-9.23E+06	-9.51E+06	-9.51E+06	-9.51E+06	-9.23E+06	-9.23E+06	-9.71E+06
Enthalpy Watt	-3.39E+05	3.49E+05	-3.46E+05	-3.46E+05	-3.46E+05	-3.46E+05	-3.46E+05	-3.46E+05	-3.53E+05
Entropy J/kmol-K	-1.78E+05	-2.03E+05	-2.92E+04	-3.2282.31	-3.2282.31	-3.2282.31	-29246.4	-29246.4	-47011.74
Entropy J/kg-K	-7705.655	-8800.317	-1172.12	-1299.254	-1299.254	-1299.254	-1172.12	-1172.12	-1892.063
Density kmol/cum	36.25945	40.7765	2.49E-04	2.49E-04	2.49E-04	2.49E-04	2.49E-04	2.49E-04	3.52E-04
Density kg/cum	837.8876	942.268	6.21E-03	6.18E-03	6.18E-03	6.18E-03	6.21E-03	6.21E-03	8.74E-03
Average MW	23.10811	23.10811	24.95172	24.84681	24.84681	24.84681	24.95171	24.95171	24.84681
Liq Vol 60F cum/sec	3.08E-05	3.08E-05	4.20E-05	4.07E-05	4.07E-05	4.07E-05	4.20E-05	4.20E-05	4.07E-05

## Stream data for the two stage dehydration process, continued

	FEEDSEP	LIQ1	MIX1	PERM1	PERM1A	PERM1B	PERM1C	PERMID	PERMISAT
Mole Flow kmol/sec									
WATER	9.96E-04	9.96E-04	1.11E-03	1.11E-03	1.11E-03	1.11E-03	1.11E-03	1.11E-03	1.11E-03
ETHANOL	2.21E-04	2.21E-04	3.56E-04	3.56E-04	3.56E-04	3.56E-04	3.56E-04	3.56E-04	3.56E-04
AIR	2.96E-09	2.96E-09	3.84E-05	2.96E-09	2.96E-09	2.96E-09	3.84E-05	3.84E-05	2.96E-09
Mass Frac									
WATER	0.6380784	0.6380784	0.5322239	0.5484911	0.5484911	0.5322243	0.5322243	0.5484911	0.5484911
ETHANOL	0.3619185	0.3619185	0.4381164	0.4515066	0.4515066	0.4515066	0.4515066	0.4515066	0.4515066
AIR	3.05E-06	3.05E-06	2.97E-02	2.36E-06	2.36E-06	2.36E-06	2.36E-06	2.36E-06	2.36E-06
Total Flow kmol/sec	1.22E-03	1.22E-03	1.50E-03	1.46E-03	1.46E-03	1.46E-03	1.50E-03	1.50E-03	1.46E-03
Total Flow kg/sec	0.0281261	0.0281261	0.0374649	0.0363538	0.0363538	0.0363538	0.0374649	0.0374649	0.0363538
Total Flow cum/sec	3.36E-05	2.98E-05	6.03E+00	5.878876	5.878876	5.878876	6.033085	6.033085	4.15795
Temperature C	88.80151	-7.149974	113.4641	113.4641	113.4641	113.4641	113.4641	113.4641	0.2903652
Pressure N/sqm	1.24E+05	8.00E+02	800	800	800	800	800	800	800
Vapor Frac	0	0	1	1	1	1	1	1	1
Liquid Frac	1	1	0	0	0	0	0	0	0
Solid Frac	0	0	0	0	0	0	0	0	0
Enthalpy J/kmol	-2.79E+08	-2.87E+08	-2.30E+08	-2.36E+08	-2.36E+08	-2.36E+08	-2.36E+08	-2.36E+08	-2.41E+08
Enthalpy J/kg	-1.21E+07	-1.24E+07	-9.23E+06	-9.51E+06	-9.51E+06	-9.51E+06	-9.23E+06	-9.23E+06	-9.71E+06
Enthalpy Watt	-3.39E+05	-3.49E+05	-3.46E+05	-3.46E+05	-3.46E+05	-3.46E+05	-3.46E+05	-3.46E+05	-3.53E+05
Entropy J/kmol-K	-1.78E+05	-2.03E+05	-2.92E+04	-3.2282.31	-3.2282.31	-3.2282.31	-3.2282.31	-3.2282.31	-29246.4
Entropy J/kg-K	-7705.655	-8800.317	-1172.12	-1299.254	-1299.254	-1299.254	-1299.254	-1299.254	-1172.12
Density kmol/cum	36.25945	40.7765	2.49E-04	2.49E-04	2.49E-04	2.49E-04	2.49E-04	2.49E-04	3.52E-04
Density kg/cum	837.8876	942.268	6.21E-03	6.18E-03	6.18E-03	6.18E-03	6.21E-03	6.21E-03	8.74E-03
Average MW	23.10811	23.10811	24.95172	24.84681	24.84681	24.84681	24.95171	24.95171	24.84681
Liq Vol 60F cum/sec	3.08E-05	3.08E-05	4.20E-05	4.07E-05	4.07E-05	4.07E-05	4.20E-05	4.20E-05	4.07E-05

## References

- 1 S. Loeb, S. Sourirajan: Sea water demineralization by means of an osmotic membrane; *Adv. Chem. Ser.* 38 (1962) 117-132
- 2 H.K. Lonsdale: The growth of membrane technology; *J. Membrane Sci.* 10 (1982) 81-181
- 3 H. Strathmann: Membrane separation processes: current relevance and future opportunities; *AIChE J.* 47 (2001) 1077-1087
- 4 L. Kahlenberg: On the nature of the process of osmosis and osmotic pressure with observations concerning dialysis; *J. Phys. Chem.* 10 (1906) 141-209
- 5 P. Kober: Pervaporation, perstillation and percrystallization; *J. Am. Chem. Soc.* 39 (1917) 944-950.
- 6 Y. Schwob: Sur l'hémipermeabilité à l'eau, des membranes de cellulose régénérée. Ph.D. thesis, Toulouse (France) 23 Mai (1949)
- 7 R. Fries, J. Néel: Transferts sélectifs à travers des membranes actives, *J. Chem. Phys.* 62 (1965) 494-503
- 8 P. Aptel, N. Challard, J. Cuny, J. Néel: Application of the pervaporation process to the separation of azeotropic mixtures, *J. Membrane Sci.* 1 (1976) 271-287
- 9 H. Brüsck, W. Schneider, G. Tusel: Pervaporation membranes for the separation of water and oxygen-containing simple organic solvents; European Workshop on Pervaporation. Nancy, France, Sept. 21-22, 1982
- 10 J. Neel, Q.T. Nguyen, R. Clement, L. Le Blanc: Fractionation of a binary liquid mixture by continuous pervaporation, *J. Membrane Sci.* 15 (1983) 43-62
- 11 M. Goldblatt, C. Godding: An engineering analysis of membrane-aided distillation; *AIChE Symp. Ser.* No. 248 82 (1986) 51-69
- 12 P. Cogat: Dehydration of ethanol, pervaporation compared with azeotropic distillation; Proc. of 3<sup>rd</sup> Int. Conf. on Pervap. Proc. in the Chem. Ind., Nancy, France, Sept. 19-22 (1988), 305-316
- 13 J. Bitter: Evaluation of membrane technology for separation of dilute alcohol solutions; Proc. of 3<sup>rd</sup> Int. Conf. on Pervap. Proc. in the Chem. Ind., Nancy, France, Sept. 19-22 (1988), 476-485
- 14 U. Sander, P.B. Soukup: Design and operation of a pervaporation plant for ethanol dehydration; *J. Membrane Sci.* 36 (1988) 463-475

- 15 J.L. Rapin: The Betheniville pervaporation unit. The first large scale productive plant for the dehydration of ethanol; Proc. of 3<sup>rd</sup> Int. Conf. on Pervap. Proc. in the Chem. Ind., Nancy, France, Sept. 19-22 (1988), 364-378
- 16 T. Asada: Dehydration of organic solvents. Some actual results of pervaporation plants in Japan; Proc. of 3<sup>rd</sup> Int. Conf. on Pervap. Proc. in the Chem. Ind., Nancy, France, Sept. 19-22, 1988,
- 17 R. Rautenbach, U. Meyer-Blumenruth: Module and process design for vapor permeation; Desalination 77 (1990) 295-322
- 18 U. Sander, H. Jansen: Industrial application of vapour permeation; J. Membrane Sci. 61 (1991) 113-129
- 19 U. Hömmerich: Pervaporation und Dampfpermeation mit Zeolitmembranen – Einsatzpotential und Verfahrensintegration, Ph.D. thesis, RWTH Aachen, 6. Nov. 1998
- 20 F. Lipnizki, R. Field: Integration of vacuum and sweep gas pervaporation to recover organic compounds from waste water; Separ. Purif. Technol. 22-23 (2001) 347-360
- 21 H. Brüschke, A. Schneider: Membranverfahren zur Trennung Fluiden Gemische, Germ. Patent , DE 44-10-243-C1, 1995
- 22 H. Brüschke: Multilayer membrane and its use in the separation of liquids by pervaporation. EP 096 339, Dec.21, 1983
- 23 M. Yamamoto, I. Sakata, M. Hirai: Plasma-polymerized membranes and gas permeability; J. Appl. Polym. Sci. 29 (1984) 2981- 2987
- 24 Ebert, K.; Fritsch, D.; Stange, O.; Wenzlaff, A. Hydrophile Kompositmembran zur Entwässerung organischer Lösungen, DE 199-25-475.3.
- 25 K. Okamoto; N. Tanihara; H. Watanabe; K. Tanaka; H. Kita; A. Nakamura; Y. Kusuki; K. Nakagawa: Vapor Permeation and Pervaporation Separation of Water-Ethanol Mixtures through Polyimide Membranes, J. Membrane Sci. 68 (1992) 53-63.
- 26 J.-H. Kim, K.-H Lee, S. Kim: Pervaporation separation of water from ethanol through polyimide composite membranes; J. Membrane Sci. 169 (2000) 81-93
- 27 R. Huang, R. Pal, G. Moon: Crosslinked chitosan composite membrane for the pervaporation dehydration of alcohol mixtures and enhancement of structural stability of chitosan/polysulfone composite membranes; J. Membrane Sci. 160 (1999) 17-30
- 28 A. Chanachai, R. Jiraratananon, D. Uttapap, G. Moon, W. Anderson, R. Huang: Pervaporation with chitosan/hydroxyethylcellulose (CS/HEC) blended membranes; J. Membrane Sci. 166 (2000) 271-280
- 29 T. Kataoka, T. Tsuru, S. Nakao, S. Kimura: Membrane transport properties of pervaporation and vapor permeation in ethanol-water system using polyacrylonitrile and cellulose acetate membranes; J. Chem. Eng. Jap. 24 (1991) 334-339

- 30 X.-P Wang: Modified alginate composite membranes for the dehydration of acetic acid; *J. Membrane Sci.* 170 (2000) 71-79
- 31 R. Huang, R. Pal, G. Moon: Pervaporation dehydration of aqueous ethanol and isopropanol mixtures through alginate/chitosan two ply composite membrane supported by poly(vinylidene fluoride) porous membrane; *J. Membrane Sci.* 167 (2000) 275-289
- 32 W. Wenzlaff, K. Böddeker, K. Hattenbach: Pervaporation of water-ethanol through ion exchange membranes; *J. Membrane Sci.* 22 (1985) 333-344
- 33 H.-H. Schwarz, N. Scharnagl, R.-D. Behling, M. Aderhold, R. Apostel, G. Frigge, D. Paul, K.-V. Peinemann, K. Richau: Polyelektrolyt-Komposit-Membran, EP 0 587 071 A1, 3.9.1993
- 34 N. Scharnagl, K.-V. Peinemann, A. Wenzlaff; H.-H. Schwarz; R.-D Behling: Dehydration of organic compounds with SYMPLEX composite membranes, *J. Membrane Sci.* 113 (1996) 1-5
- 35 J. Meier-Haack, W. Lenk, D. Lehmann, K. Lunkwitz: Pervaporation separation of water/alcohol mixtures using composite membranes based on polyelectrolyte multilayer assemblies; *J. Membrane Sci.* 184 (2001) 233-243
- 36 S. Doguparthy: Pervaporation of aqueous alcohol mixtures through a photopolymerized composite membrane; *J. Membrane Sci.* 185 (2001) 201-205
- 37 Y. Lee, S. Nam, S. Ha: Pervaporation of water/isopropanol mixtures through polyaniline membranes doped with poly(acrylic acid); *J. Membrane Sci.* 159 (1999) 41-46
- 38 W. Chan,, C. Ng, S. Lam-Leung, X. He: Water-alcohol separation by pervaporation through chemically modified poly(amidesulfonamide)s; *J. Membrane Sci.* 160 (1999) 77-86
- 39 K. Lee, M. Teng, H. Lee, J. Lai: Dehydration of ethanol/water mixtures by pervaporation with composite membranes of polyacrylic acid and plasma-treated polycarbonate; *J. Membrane Sci.* 164 (2000) 13-23
- 40 K. Lee, M. Teng, T. Hsu, J. Lai: A study on pervaporation of aqueous ethanol solution by modified polyurethane membrane; *J. Membrane Sci.* 162 (1999) 173-180
- 41 S. Chen, K. Yu, S. Lin, D. Chang, R. Liou: Pervaporation separation of water/ethanol mixture by sulfonated polysulfone membrane; *J. Membrane Sci.* 183 (2001) 29-36
- 42 P. Ten, R. Field: Organophilic pervaporation: an engineering science analysis of component transport and the classification of behavior with reference to the effect of permeate pressure; *Chem. Eng. Sci.* 55 (2000) 1425-1445
- 43 C. Streicher, P. Kremer, V. Thomas, A. Hübner, G. Ellinghorst: Development of new pervaporation membranes, systems and processes to separate alcohols/ ethers/

- hydrocarbon mixtures; Proceedings of Fifth International Conference on Pervaporation Processes in the Chemical Industry, Reno, 1995, 297-309
- 44 H. Brüschke: State-of-art of pervaporation processes in the chemical industry; in 'Membrane Technology in the chemical industry' (ed. by S. Nunes and K.-V. Peinemann), WILEY-VCH, Weinheim, Germany, (2001) 127-172
  - 45 M. Tsuyumoto, A. Teramoto, P. Meares: Dehydration of ethanol on a pilot-plant scale, using a new type of hollow-fiber membrane; *J. Membrane Sci.* 133 (1997) 83-94
  - 46 S. Zhang, E. Drioli: Pervaporation membranes; *Separ. Sci. Technol.* 30 (1995) 1-31
  - 47 X. Feng, R. Huang: Liquid separation by membrane pervaporation: a review; *Ind. Eng. Chem. Res.* 36 (1997) 1048-1066
  - 48 F. Lipnizki, R. Field; P.-K. Ten: Pervaporation-based hybrid process: a review of process design, applications and economics. *J. Membrane Sci.* 153 (1999) 183-210.
  - 49 K. Okamoto, H. Kita, k. Horii, K. Tanaka, M. Kondo: Zeolite NaA membrane: preparation, single gas permeation, and pervaporation and vapor permeation of water/organic liquid mixtures; *Ind. Eng. Chem. Res.* 40 (2001) 163-175
  - 50 M. Noack, P. Kölsch, J. Caro, M. Schneider, P. Toussaint, I. Sieber: MFI membranes for different Si/Al ratios for pervaporation and steam permeation; *Microp. Mesop. Mat.* 35-36 (2000) 253-265
  - 51 R. de Vos, H. Verweij: High -selectivity, high-flux silica membranes for gas separation; *Sience* 279 (1998) 1710-1711
  - 52 M. Naito, k. Nakahira, Y. Fukuda, H. Mori, J. Tsubaki: Process conditions on the preparation of supported microporous SiO<sub>2</sub> membranes by sol-gel modification techniques; *J. Membrane Sci.* 129 (1997) 263-269
  - 53 K. Kuraoka, Z. Shugen, K. Okita, T. Kakitani, T. Yazawa: Permeation of methanol vapor through silica membranes prepared by the CVD method with the aid of evacuation; *J. Membrane Sci.* 160 (1999) 31-39
  - 54 A. Nijmeijer, B. Bladergroen, H. Verweij: Low-temperature CVI modification of  $\gamma$ -alumina membranes; *Microp. Mesop. Mat.* 25 (1998) 179-184
  - 55 J. Caro, M. Noack, P. Kölsch: Chemically modified ceramic membranes; *Microp. Mesop. Mat.* 22 (1998) 321-332
  - 56 M. Noack, P. Kölsch, R. Schäfer, P. Toussaint, J. Caro: Molekularsieb-Membranen für industrielle Anwendungen – Probleme, Fortschritte, Lösungen; *Chem.-Ing.-Tech.* 73 (2001) 958-967
  - 57 J. Caro, M. Noack, P. Kölsch, R. Schäfer: Zeolite membranes – state of their development and perspective; *Microp. Mesop. Mat.* 38 (2000) 3-24

- 58 J. Coronas , J. Santamaria: Separations using zeolite membranes; *Separ. Purif. Methods* 28 (1999) 127-177
- 59 K. Jansen, T. Maschmeyer: Progress in zeolitic membranes; *Topics in Catalysis* 9 (1999) 113-122
- 60 A. Tavolaro, E. Orioli: Zeolite membranes; *Adv. Mater.* 11 (1999) 975-996
- 61 Y. Lin: Microporous and dense inorganic membranes: current status and prospective; *Separ. Purif. Technol.* 25 (2001) 39-55
- 62 T. Pressly, K. Ng: A Break-even Analysis of Distillation-Membrane Hybrids; *AIChE J.* 44 (1998) 93-105
- 63 T. Pettersen, K. Lien: Design of Hybrid Distillation and Vapor Permeation Processes; *J. Membrane Sci.* 102 (1995) 21-30
- 64 T. Pettersen, A. Argo, R. Noble, C. Koval: Design of Combined Membrane and Distillation Processes; *Separ. Technol.* 6 (1996) 175-187
- 65 Rautenbach, R.; Knauf, R.; Struck, A.; Vier, J. Simulation and Design of Membrane Plants with AspenPlus; *Chem. Eng. Technol.* 19 (1996) 391-397
- 66 U. Hömmerich, R. Rautenbach: Design and optimization of combined pervaporation-distillation processes for the production of MTBE; *J. Membrane Sci.* 146 (1998) 53-64
- 67 F.-F. Kuppinger, R. Meier and R. Düssel: Hybridverfahren zur Zerlegung azeotroper Mehrkomponentengemische durch Rektifikationskolonnen mit Seitenstrom; *Chem.-Ing.-Tech.* 72 (2000) 333-338
- 68 R. Waldberger, F. Widmer: Membrane reactors in chemical production processes and the application to the pervaporation-assisted-esterification; *Chem. Eng. Technol.* 19 (1996) 117-126
- 69 M. Kemmere, J. Keurentjes: Industrial membrane reactors; in ‘Membrane Technology in the chemical industry’ (ed. by S. Nunes and K.-V. Peinemann), WILEY-VCH, Weinheim, Germany, (2001) 191-221
- 70 H. Brüsck, W. Schneider: Optimierung einer Kopplung Pervaporation und Reaktion zur Esterherstellung; *Preprints 5. Aachener Membrankolloquium* (1995) 207-222
- 71 S. Blum, B. Gutsche, W. Barlage: Membranunterstützte Batchreaktionen – Konzepte und Scale-up; *Preprints 6. Aachener Membrankolloquium* (1997) 161-178
- 72 S. Klatt: Zum Einsatz der Pervaporation im Umfeld der chemischen Industrie; Ph.D. Thesis, RWTH Aachen, 30. April 1993
- 73 T. Sherwood, R. Pigford, C. Wilke: Mass Transfer; (1975), McGraw-Hill, 153

- 74 V. Gekas, B. Hallstörm: Mass transfer in the membrane concentration polarization layer under turbulent cross flow. I. Critical literature review and adaptation of existing Sherwood correlations to membrane operations; *J. Membrane Sci.* 30 (1987) 153-170
- 75 I. Langmuir: The adsorption of gases on plane surfaces of glass, mica and platinum; *J. Am. Chem. Soc.* 40 (1918) 1361-1403
- 76 W. Vieth, H. Howell, J. Hsieh: Dual sorption theory; *J. Membrane Sci.* 1 (1976) 177-220
- 77 E. Favre, Q. Nguyen, R. Clement, J. Neel: The engaged species induced clustering (ENSIC) model: a unified mechanistic approach of sorption phenomena in polymers; *J. Membrane Sci.* 117 (1996) 227-236
- 78 C. Bokis, H. Orbey: Properly model polymer processes; *Chem. Eng. Prog.* 95 (1999) 39-52
- 79 H. Orbey, C. Bokis, C-C. Chen: Polymer-solvent vapor-liquid equilibrium: Equation of state versus activity models; *Ind. Eng. Chem. Res.* 37 (1998) 1567-1573
- 80 P. Flory: Thermodynamics of high polymer solutions; *J. Chem. Phys.* 10 (1942) 51-61
- 81 M. Huggins: Thermodynamic properties of solutions of long-chain compounds; *Ann. N.Y. Acad. Sci.* 43 (1942) 1-32
- 82 D. Abrams, J. Prausnitz, Statistical thermodynamics of liquid mixtures: A new expression for the excess Gibbs energy of partly or completely miscible mixtures; *AIChE J.* 21 (1975) 116-128
- 83 J. Prausnitz, R. Lichtenthaler, E. de Azevedo: *Molecular Thermodynamics of Fluid Phase Equilibria*, 2nd ed., Prentice-Hall, Englewood Cliffs, NJ, 1986
- 84 A. Jonquieres, L. Perrin, S. Arnold, P. Lochon: Comparison of UNIQUAC with related models for modeling vapor sorption in polar materials; *J. Membrane Sci.* 150 (1998) 125-141
- 85 A. Heinz, W. Stephan: A generalized solution-diffusion model of the pervaporation process through composite membranes. Part I. Prediction of mixture solubilities in the dense active layer using the UNIQUAC model; *J. Membrane Sci.* 89 (1994) 143-151
- 86 D. Ruthven, S. Farooq, K. Knaebel: Fundamentals of adsorption; Chapter 2 in 'Pressure Swing Adsorption', VCH Publishers, New York (1994) 11-65
- 87 A. Kapoor, R. Yang: Correlation of equilibrium adsorption data of condensable vapours on porous adsorbents; *Gas separation and purification* 3 (1989) 187-192
- 88 S. Scholl, M. Schacht, W. Sievers, P. Schweighart, A. Mersman: Calculation methods for multicomponent adsorption equilibria; *Chem. Eng. Technol.* 14 (1991) 311-324
- 89 H. Fujita: Diffusion in polymer-diluent systems; *Fortschr. Hochpolym.-Forsch.* 3 (1961) 1-47

- 90 J. Vrentas, J. Duda: Molecular diffusion in polymer solutions; AIChE J. 25 (1979) 1-24
- 91 W. Koros, T. Chern, V. Stannett, H. Hopfenberg: A model for permeation of mixed gases and vapors in glassy polymers; J. Polym. Sci. 19 (1981) 1513-1530
- 92 N. Peppas, H. Moynihan: Solute diffusion in swollen membranes. IV. Theories for moderately swollen networks; J. Appl. Polym. Sci. 30 (1985) 2589-2606
- 93 F. Müller-Plathe: Diffusion of water in swollen poly(vinyl alcohol) membranes studied by molecular dynamics simulation; J. Membrane Sci. 141 (1998) 147-154
- 94 D. Hofmann, L. Fritz, D. Paul: Molecular modelling of pervaporation separation of binary mixtures with polymeric membranes; J. Membrane Sci. 144 (1998) 145-159
- 95 R. Taylor, R. Krishna: Multicomponent mass transfer, Wiley, New York (1993)
- 96 A. Heinz, W. Stephan: A generalized solution-diffusion model of the pervaporation process through composite membranes. Part II. Concentration polarization, coupled diffusion and the influence of the porous support layer; J. Membrane Sci. 89 (1994) 153-169
- 97 J. Bausa, W. Marquardt: Detailed modeling of stationary and transient mass transfer across pervaporation membranes; AIChE J. 47 (2001) 1318-1332
- 98 E. Mason, A. Malinauskas: Gas transport in porous media: the dusty-gas model; Chemical Engineering Monographs 17, Elsevier, Amsterdam (1983)
- 99 A. Kapoor, R. Yang, C. Wong: Surface diffusion; Catal. Rev.—Sci. Eng. 31 (1989) 129-214
- 100 R. Uhlhorn, K. Keizer, A. Burggraaf: Gas transport and separation with ceramic membranes. Part I. Multilayer diffusion and capillary condensation; J. Membrane Sci. 66 (1992) 259-269
- 101 A. Shelekhin, A. Dixon, Y. Ma: Theory of gas diffusion and permeation in inorganic molecular-sieve membranes; AIChE J. 41 (1995) 58-67
- 102 Y. Seo, G. Kum, N. Seaton: Monte Carlo simulation of transport diffusion in nanoporous carbon membranes; J. Membrane Sci. 195 (2002) 65-73
- 103 F. Kapteijn, W. Bakker, G. Zheng, J. Poppe, J. Moulijn: Permeation and separation of light hydrocarbons through a silicalite-1 membrane. Application of the generalized Maxwell-Stefan equations; Chem. Eng. J. 57 (1995) 145-153
- 104 R. Krishna, D. Paschek: Separation of hydrocarbon mixtures using zeolite membranes: a modeling approach combining molecular simulations with the Maxwell-Stefan theory; Separ. Purif. Technol. 21 (2000) 111-136
- 105 J. Veldsink, G. Versteeg, W. van Swaaij: An experimental study of diffusion and convection of multicomponent gases through catalytic and noncatalytic membranes; J. Membrane Sci. 92 (1994) 275-291

- 106 U. Beuscher, C. Gooding: The permeation of binary gas mixtures through support structures of composite membranes; *J. Membrane Sci.* 150 (1998) 57-73
- 107 J. Neto, M. Pinho: Mass transfer modeling for solvent dehydration by pervaporation; *Separ. Purif. Technol.* 18 (2000) 151-161
- 108 O. Stange: Stofftransport durch eine hydrophile Polymermembran am Beispiel der Dampfpermeation; Ph.D. Dissertation, University of Hannover, (April 2001)
- 109 K. Ebert, D. Fritsch, O. Stange, A. Wenzlaff: Hydrophile Kompositmembran zur Entwässerung organischer Lösungen, DE 199 25 475 (1999)
- 110 K. Ebert, O. Stange, K. Ohlrogge: Dehydration of organic solutions by vapor permeation with temperature stable polymeric membranes; 6th World Congress of Chemical Engineering, Melbourne (2001)
- 111 R. Naylor, P. Backer: Enrichment calculations in gaseous diffusion: Large separation factor; *AIChE J.* 1 (1955) 95-99
- 112 M. Collura, W. Luyben: Energy-saving distillation designs in ethanol production; *Ind. Eng. Chem. Res.* 27 (1988) 1686-1696
- 113 R. Huang, J. Rhim: Separation characteristics of pervaporation membrane separation processes; in R. Huang (Ed.), *Pervaporation Membrane Separation Processes*, Elsevier, Amsterdam (1991) 111-180
- 114 P. Rony: The extent of separation; *AIChE Symp. Series* 120, vol. 68, New York, (1972) 89-104
- 115 K. Sirkar: On the Composite Nature of the Extent of Separation; *Separ. Sci.* 12 (1977) 211-229
- 116 F. McCandless: Stage extent of separation in ideal countercurrent recycle membrane cascades; *J. Membrane Sci.* 154 (1999) 15-23
- 117 Y. Kao, M. Qiu, S. Hwang: Critical evaluation of two membrane gas permeator designs: Continuous membrane column and two strippers in series, *Ind. Eng. Chem. Res.* 28 (1989) 1514-1520
- 118 A. Baudot, M. Marin: Improved recovery of an ester compound by pervaporation coupled with a flash condensation; *Ind. Eng. Chem. Res.* 38 (1999) 4458-4469
- 119 B. Linnhoff: A user guide on process integration for the efficient use of energy; The Institution of Chemical Engineers, Rugby (1982)
- 120 D. Arnold: Optimierungsstrategien zur Einbindung von Pervaporationsanlagen bei der Entwässerung von Lösungsmittelgemischen, Dissertation, RWTH Aachen, (1995)
- 121 P.G. Hill, Incompressible Jet Mixing in Converging-Diverging Axisymmetric Ducts, *J. Basic Eng., Trans. ASME*, March (1967) 210-220

- 122 E. Razinky, J.A. Brighton: A theoretical model for nonseparated mixing of a confined jet, J. Basic Eng., Trans. ASME, September (1972) 551-558
- 123 R.B. Power: Steam jet ejectors for the process industries, McGraw-Hill, USA, (1994)
- 124 Standards for Steam Jet Ejectors, Heat Exchange Institute, New York, (1967)
- 125 J.L. Ryans, D.L. Roper: Process vacuum system design and operation, McGraw-Hill, USA, (1986)
- 126 M. Heckmann: Die Verbesserung der Destillation durch hybride Systeme; Vakuum in Forschung und Praxis 2 (2000) 108-111
- 127 K. Herold, R. Radermacher, S. Klein: Absorption chillers and heat pumps, 1<sup>st</sup> Edition, CRC Press, Inc. (1996)
- 128 Y. Park, J.-S. Kim, H. Lee: Physical properties of the lithium bromide + 1,3- propandiol + water system, Int. J. Refrig. 20 (1997) 319-325
- 129 P. Glugla, S. Sax: Vapor liquid equilibrium for salt-containing systems: A correlation of vapor pressure depression and a prediction of multicomponent systems, AIChE J. 31 (1985) 1911-1914
- 130 J. Fu: Salt containing model for simulation of salt-containing extractive distillation, AIChE J. 42 (1996) 3364-3372
- 131 D. Meranda, W. Furter, Vapor-Liquid Equilibrium in Alcohol-Water Systems Containing Dissolved Halide Salts and Salt Mixutes, AIChE J. 18 (1972) 111-116
- 132 D. Jaques, W. Furter: Salt effects in vapor-liquid equilibrium: Testing the thermodynamic consistency of ethanol-water saturated with inorganic salts, AIChE J. 18 (1972) 343-346
- 133 P. Bittrich, D. Hebecker: Abluft- und Brüdenwärmennutzung mit Sorptionskreisläufen, Chem.-Ing.-Tech. 67 (1995) 766-770
- 134 W. Fratzscher, K. Stephan: Regionale Objektbereiche und Entwicklungsstrategien; chapter (4) in Strategien zur Abfallenergieverwertung, 1st Edition, Friedr. Vieweg Verlag, (2000) 165-295

## Lebenslauf

### **Persönliche Daten**

Name: Fahmy  
 Vorname: Alaa  
 Geburtsdatum: 2. Dezember 1972  
 Geburtsort: Kairo  
 Familienstand: verheiratet, ein Sohn  
 Nationalität: ägyptisch

### **Schulbildung:**

1977 - 81	Dar-Elmoalem Grundschule, Kairo
1981 - 89	Deutsche Evangelische Oberschule, Kairo

### **Studium:**

10/89 - 07/94	Bachelor-Studiengang Chemical Engineering, Universität Kairo Abschluss: Bachelor of Science
10/94 - 07/97	Master-Studiengang Chemical Engineering, Universität Kairo Abschluss: Master of Engineering

### **Berufliche Tätigkeiten:**

10/94 - 09/98	Wissenschaftlicher Mitarbeiter am „Department of Chemical Engineering“ der Universität Kairo
Seit 10/98	Wissenschaftlicher Mitarbeiter am Institut für Verfahrenstechnik der Universität Hannover

### **Nebenberufliche Tätigkeiten:**

07/94 - 11/94	Teilzeit-Mitarbeiter, Fa. ETMAM, Kairo, Industrial Consulting
01/95 - 06/95	Teilzeit-Mitarbeiter, National Research Center, Kairo, Environmental Consulting
07/95 - 07/96	Teilzeit-Mitarbeiter, Fa. Catalyst, Kairo, Anlagenbau
07/96 - 12/96	Teilzeit-Mitarbeiter, Development Research and Technological Planning Center, Kairo, Industrial Audits, Pollution Prevention Consulting
09/97 - 09/98	Teilzeit-Mitarbeiter, Fa. Mass for Trading and Industries, Kairo, Produktentwicklung im Bereich der Farben und Bauchemikalien

Hannover, im Juni 2002